TECHNICAL REPORT

Report No.: ESSO-INCOIS-OMDA-TR-04(2025)

An interim report on the projected climate change induced extreme sea levels and coastal vulnerability along the Indian coasts

by

Nidheesh A G, Archit Wadalkar, Abhisek Chatterjee*, Aneesh Lotliker, Mahendra R S, Mohanty P C, Ch Lakshmi Sravani, Padmanabham J, Francis P A, Srinivasa Kumar T, Balakrishnan Nair T M & M Ravichandran

Indian National Centre for Ocean Information Services (INCOIS)
Ministry of Earth Sciences, Hyderabad-500090.

*This interim report is an outcome of Vertical 2 of the Deep Ocean Mission. Any correspondence on this report may be directed to Dr. Abhisek Chatterjee (abhisek.c@incois.gov.in). The report should be cited as follows:

Nidheesh A G, Archit Wadalkar, Abhisek Chatterjee, Aneesh Lotliker, Mahendra R S, Mohanty P C, Ch Lakshmi Sravani, Padmanabham J, Francis P A, Srinivasa Kumar T, Balakrishnan Nair T M and Ravichandran M. An interim report on the projected climate change induced Extreme Sea Levels and coastal vulnerability along the Indian coasts. INCOIS Technical Report No. ESSO-INCOIS-OMDA-TR-04(2025).

DOCUMENT CONTROL SHEET

Earth System Science Organization (ESSO)

Ministry of Earth Sciences (MoES)

Indian National Centre for Ocean Information Services (INCOIS)

ESSO Document Number: ESSO-INCOIS-OMDA-TR-04(2025)

Title of the report:

"An interim report on the projected climate change induced Extreme Sea Levels and coastal vulnerability along the Indian coasts"

Author(s):
Nidheesh A G, Archit Wadalkar, Abhisek Chatterjee, Aneesh Lotliker, Mahendra R S, Mohanti P C, Ch Lakshmi Sravani, Padmanabham J, Francis P A, Srinivasa Kumar T, Balakrishnan Nair T M & M Ravichandran

Originating unit: OMDA, Ocean Modeling, Applied Research & Services (OMARS) Group, INCOIS

Type of Document: Technical Report (TR)
Number of pages and figures: 65, 43
Number of references: 44
Keywords: Mean Sea Level, Tide, Storm surge, Extreme Waves, Inundation, Coastal Vulnerability.
Security classification: Open
Distribution: Open
Date of publication: 25 July 2025

Abstract (148 words):

This is an interim report on the "Projected Changes in Extreme Sea Levels and Coastal Vulnerability along the Indian Coasts" as part of the Deep Ocean Mission. It presents a comprehensive assessment of future sea-level rise and its implications for coastal India and the associated vulnerable maps for the 11 selected locations along the Indian coast. Using global climate models and probabilistic methods, the report projects that relative mean sea levels (RMSL) along the Indian coastline could rise by 0.62 m (Visakhapatnam) to 0.87 m (Bhavnagar) under SSP5-8.5 (high emission scenario) by 2100, whereas extreme sea levels along the Indian coasts and islands are projected to rise between 0.68 m (Chennai) and 1.12 m (Bhavnagar). Further, Indian coastal regions north of 13^{o}N are seen as more vulnerable to extreme sea-level change, with the Gulf regions off Gujarat and the northern coasts of the Bay of Bengal experiencing the largest changes in tidal maxima and climate extremes.

Executive summary:

The increase in the concentration of greenhouse gases (GHGs), especially anthropogenic CO2, causes Earth's climate to warm continuously, melting land ice (ice sheets and mountain glaciers) and seawater thermal expansion. This results in an increase in ocean volume and mean sea-level rise over most of the global oceans. According to the latest IPCC (6^{th} assessment report of the Intergovernmental Panel on Climate Change) reports, the global mean sea level has been rising over the last century at a rate of 1.8 mm/yr. The satellite observations over the previous few decades indicate an increase in the global mean sea level (GMSL) rise rate of ~3.2 mm/yr, suggesting an acceleration in the sea level rise in the early part of the 21st century.

The regional sea-level rise often deviates from the global mean sea-level rise rate primarily due to ocean circulation and local vertical land motion (VLM). The coastal sea levels are further affected by several processes like tides, waves, and storm surges, thus making deterministic predictions of extreme coastal sea-level changes complex. The relative mean sea level (RMSL) around coastal India is projected to rise by 0.5 – 1 meter by the end of the century, and our findings suggest that the RMSL change is the main contributor to the extreme sea-level rise along the Indian coastlines in this century. Our findings also suggest that climate change-induced hazards (storm surges and waves) and tides may significantly contribute to end-of-century Extreme Sea Level (ESL) at specific locations around coastal India. For instance, while ESLs over the coastal zones of the Gulf region of Gujrat are largely affected by changes in tidal amplitude, changes in climate extremes would become an important source of ESL change at Visakhapatnam. Our findings are based solely on various available global model simulations. Further, this report highlights various sources of uncertainties and the potential way forward to reduce those uncertainties.

The ESL rise poses a significant risk for India owing to its long-stretched coastline of over 11098.81 km (including Andaman, Nicobar, and Lakshadweep Islands) with several low-lying areas that lie well within five meters of mean sea level (e.g. the deltaic regions in the northern Bay of Bengal and parts of Lakshadweep Islands, expansive intertidal regions in Gujarat, and many). The rising sea levels cause beach retreat and erosion, permanent flooding of coastal areas, and loss of marine biodiversity. Moreover, because a large fraction of the Indian population (more than 350 million) lives near the coastline and is primarily dependent on the marine economy, a wide range of marine activities dominate the maritime zone of India.

Therefore, there is an urgent need to assess the projected changes in extreme sea levels along the Indian coasts, which will facilitate better coastal zone management and policy making.

Here, we have used currently available information on the projected changes in the relative mean sea level, tides, and climate extremes to assess the projected changes in extreme sea levels for the end of this 21st Century (year 2100) along the Indian subcontinents and Indian islands under the SSP2-4.5 (A scenario representing the medium challenges to mitigation and adaptation to the radiative forcing reaching up to 4.5 W/m^2) and SSP5-8.5 (Fossil-fuelled based Development: high challenges to mitigation, low challenges to adaptation with the radiative forcing reaching up to 8.5 W/m^2) climate scenarios. The key findings are summarised below:

- Global mean sea level (GMSL) has increased by 0.2 [0.15 – 0.25] m between 1901 and 2018 and is projected to reach 0.5 – 1 m very likely by 2100.

- Future projections of relative mean sea level (with respect to 1995 – 2014) indicate a rise all along the Indian coasts ranging from 0.62 m (Visakhapatnam) to 0.87 m (Bhavnagar) under SSP5-8.5 (high emission scenario) by 2100, whereas it varies from 0.40 m (Vishakhapatnam) to 0.63 m (Bhavanagar) by 2100 under SSP2-4.5 (mid-emission scenario).

- Present-day extreme sea levels along the Indian coasts and islands are projected to rise between (Chennai) 0.68 [0.53 – 0.9] m and (Bhavnagar) 1.12 [0.96 – 1.28] m under high emission scenario by 2100, and between (Mumbai) 0.38 [0.32 - 0.47] m and (Bhavnagar) 0.87 [0.70 - 1.01] m under mid emission scenario by 2100.

- Relative mean sea-level rise is the major contributor to extreme sea-level change along the Indian coasts, with additional contributions from tidal maximum (largest tidal amplitude increase of ~ 0.16 m at Bhavnagar, Gujarat) and climate extremes (largest change of ~ 0.09 m at Visakhapatnam).

- Indian coastal regions north of 13^{o}N are seen as more vulnerable to extreme sea-level change, with the Gulf regions off Gujarat and the northern coasts of the Bay of Bengal experiencing the largest changes in tidal maxima and climate extremes.

- Global projections of extreme sea levels and their components still come with large uncertainties. Process modelling based on regional-specific models with sustained observations may potentially reduce the uncertainty bounds of the climate projections.

1. Introduction

Global mean sea-level rise is one of the major consequences of global climate warming, potentially impacting coastal communities worldwide. Over the past century, the global sea level has risen by an average rate of 1.8 mm per year. This rate is expected to increase in the coming decades due to the increased mass loss of ice sheets and glaciers and the thermal expansion of ocean waters (Fig. 1; IPCC Climate Assessment Report – Phase 6, Fox-Kemper et al., 2021). Indian subcontinent and other Southeast Asian countries are particularly vulnerable to sea-level rise due to the large population living in low-lying coastal areas (Nicholls and Cazenave, 2010; Nicholls et al. 2021). However, making robust estimates of sea-level rise and its coastal impacts has been challenging in the past for many regions, including the Indian coasts. The difficulty was mainly due to sparse and weak coastal sea-level observations and other monitoring systems for the oceanographic and climatic features of the region. However, the situation has changed remarkably today as dense coastal observations (tide-gauges, buoys, gliders, and many others) are in place, supported by new high-precision satellite-based coastal monitoring systems (e.g. The Surface Water and Ocean Topography – SWOT). Nevertheless, understanding and predicting climate-change-driven coastal sea-level changes requires sufficiently long-period observations and well-trained physical models, and it is no wonder why IPCC climate change projections heavily rely on global climate models.

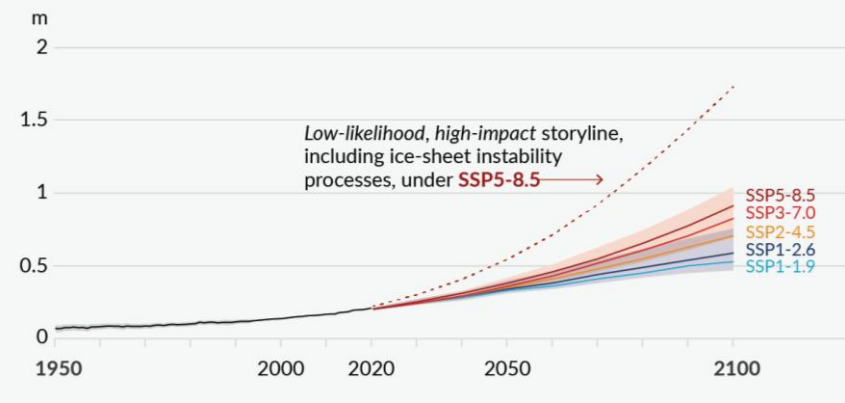

Figure 1: **Global-mean sea-level change** (in meters) relative to 1900. The historical changes are observed (from tide gauges before 1992 and altimeters afterwards), and the future changes are assessed consistently with observational constraints based on the emulation of CMIP, ice sheet, and glacier models. Likely ranges are shown for SSP1-2.6 and SSP3-7.0. Only likely ranges are assessed for sea level changes due to difficulties in estimating the distribution of deeply uncertain processes. The dashed curve indicates the potential impact of these deeply uncertain processes. It shows the 83rd percentile of SSP5-8.5 projections, including low-likelihood, high-impact ice-sheet processes that cannot be ruled out. (**Source:** IPCC, 2023: SPM)

Additionally, owing to the expansion of the tropics, potentially driven by anthropogenic global warming, there has been a poleward shift in the tropical cyclone tracks from their climatology over the past decades (e.g., Kossin et al. 2016). This phenomenon has profound impacts on the coastal regions of the north Indian Ocean as the seas (the Arabian Sea and the Bay of Bengal) are landlocked immediately to the north. Historical data suggests that (very likely) there is an increase in the tropical cyclone intensity globally, reaching at least Category 3 intensity over the past four decades (Kossin et al. 2020Th). This has strong implications for extreme sea levels along the tropical basins as extreme weather phenomena like storms and cyclones primarily cause it. By analysing historical tide-gauge sea-level records in the north Indian Ocean, Sreeraj et al. (2022) showed that extreme sea levels have become more frequent, longer-lasting, and intense along the Indian Ocean coastlines over the past few decades.

As noted above, the global-scale changes in climate extremes and extreme sea levels are not necessarily projected to occur in every oceanic basin – but they may vary in their characteristics regionally. The extreme sea level (or extreme coastal water level) changes are essentially a local phenomenon driven by local weather extremes, tides and waves. Consequently, projections of extreme sea-level change demand dynamic modelling at regional scales, which can resolve the local oceanographic features, weather, and climate of the region. At present, the utility of such regional downscaled models (mean sea level, storm surge, and wave models) to project extreme sea levels is still in the developmental phase, and global projections (though coarse and relying on global-model-based inputs) are in place for regional comparisons (e.g. Muis et al. 2016). This report provides details of projected changes in extreme sea levels along the Indian Ocean coastlines by synthesising available data from these existing global model projections and a few regional studies.

2. Processes contributing to extreme sea-level change

The occurrence of an exceptionally high or low local sea surface height is called extreme sea level (ESL), sometimes extreme coastal water levels. ESLs are primarily driven by meteorological conditions – such as surges and waves generated during a storm passing, often in combination with low or high tide levels (Woodworth et al., 2004; Pugh et al., 2014). On decadal to longer time scales, relative mean sea-level (RSL) change is indicated as the primary factor that drives a change in the amplitude and frequency of ESL occurrence around the globe (Lowe et al., 2010; Church et al., 2013; Vousdoukas et al., 2018; Sreeraj et al., 2022). Hence, the classical definition of ESL goes as follows:

Extreme Sea Level = (Relative) Mean Sea Level + Tide + Storm surge + Wave (1)

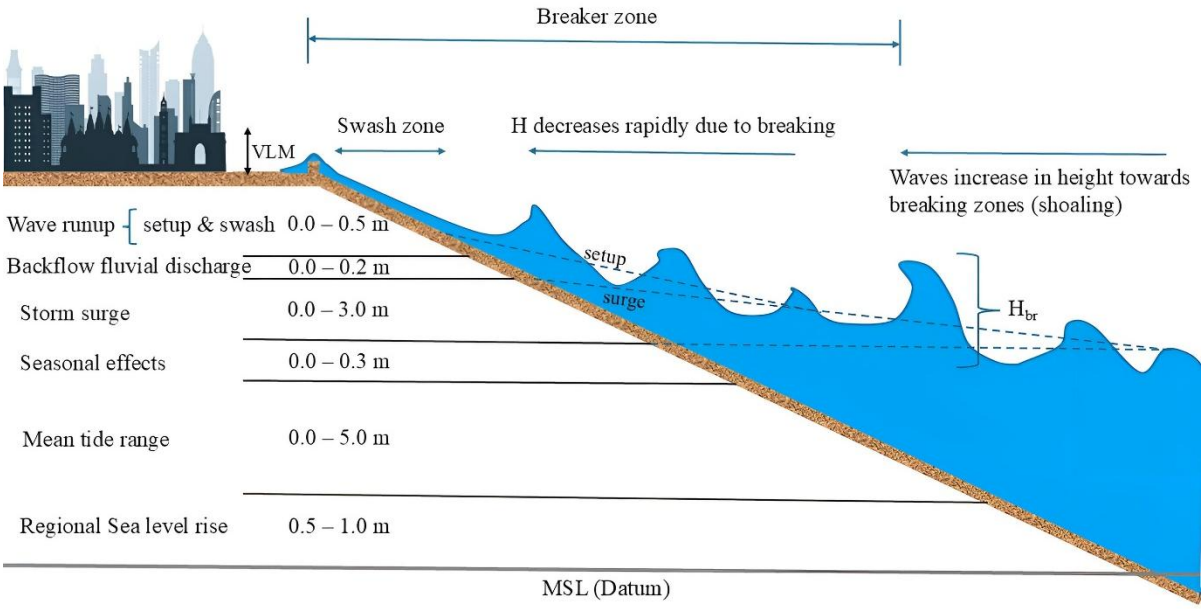

Figure 2: An illustration of processes and water level components shaping the extreme sea-level (total water level) changes. The range of values is based on historical observations and modelling-based literature for the coastal region of Mumbai (73E, 19N) on the west coast of India. (H = wave height, Hbr = breaking wave height). The total water-level change at the coast is a combined effect of regional mean sea-level rise and other coastal phenomena (e.g. tides, storm surges, seasonal effects, and waves) as illustrated. The projected ESL change off Mumbai is discussed in the report.

Relative Mean Sea Level

The relative mean sea level[1], which is the mean sea level related to a local reference datum, varies under processes acting over global to local scales (e.g. land ice melting, ocean thermal expansion, and regional ocean dynamics), and the coastal water levels are further modified by several coastal phenomena as illustrated in Figure 2. Over the past decades, global warming has driven and will continue to drive an unabated rise of GMSL via ocean thermal expansion and land-ice melting (Fox-Kemper et al., 2021). Locally, the regional mean sea-level change rate deviates from the GMSL change rate – mainly due to ocean circulation and vertical land movements. For instance, the deltaic regions in the northern Bay of Bengal experience relative mean sea-level rise rates nearly twice the GMSL rise rate due to land subsidence (e.g., Unnikrishnan et al., 2007, 2015). Consequently, the ESL change in such regions (where relative sea-level rise is high) is expected to be prominent, and a few recent studies that addressed the

[1] **Mean Sea Level** always refers to **Relative** Mean Sea Level throughout this report.

extreme sea-level changes along the Indian coasts support this notion (e.g. Unnikrishnan et al., 2004; Sindhu et al., 2011; Antony et al., 2016; Sreeraj et al., 2022; Unnikrishnan et al., 2022). However, projections of the relative mean sea level for this century mainly rely on CMIP, ice sheet, and glacier models (Fox-Kemper et al., 2021), which inherently hold large uncertainties arising from process modelling. This is particularly true for the Indian Ocean because the ocean circulation is complex, and coastal zones experience substantial vertical land movements.

Tides, Storm Surges, and Waves

North Indian Ocean is predicted to be one of the hotbeds of tropical cyclone genesis in the world (Unnikrishan et al., 2004; Bhatia et al., 2018; Knutson et al., 2020; Knutson et al., 2021; Singh et al., 2022; Murty et al., 2023), making the rim of the north Indian Ocean highly vulnerable to storm surges and waves. This is particularly true for the Bay of Bengal coastlines, where the deadliest tropical cyclones developed in the reported history (Sindhu et al., 2011; Antony et al., 2016). A storm surge is defined as the elevation (or depression) of the sea surface with respect to the predicted tide during a storm. Alternatively, the observed sea level is a combined response to surge (including wave and pressure effects) and tide – indicating that highest sea surface height occurs when the storm surge coincides with the high tide (keeping nonlinear interactions aside). The definition of storm surge also indicates that accurate information of storm falling the land is crucial in predicting total water level change, as it (timing) determines the phase of the predicted tide at that location.

Even though most of the past literature suggests that the long-term changes in extreme sea levels are driven mainly by mean sea-level rise, a few region-specific modelling studies indicate a rise with increasing storminess (e.g. Antony et al. 2016). A recent modelling study by Ramakrishnan et al. (2022) showed that the wave setup induced by wind waves caused substantial flooding in southwest India during a storm passing. Even though the prediction of astronomical tides, in principle, attained complete skill, the inclusion of tides in storm surge or wave models is often absent due to the computational requirements.

3. Extreme sea-level prediction

Equation (1) is a good approximation for determining the total water level at the coasts during a storm passage (Vousdoukas et al., 2018). Probability distributions of change in mean sea level, tide, and storm surges are usually derived either from direct observations (e.g. tide-gauge sea-level data, see Sreeraj et al., 2022) or from estimates obtained from physical models (global climate models, storm surge/tide model; see Vousdoukas et al., 2018). Generalised extreme

value (GEV) analysis has been popularly employed to obtain return levels and periods. Most recently, more advanced statistical techniques (Monte Carlo simulation, for instance) have been used to improve ESL estimates and to derive the associated confidence levels (Church et al., 2013; Vousdoukas et al., 2018; Palmer et al., 2020; Harrison et al., 2021; Hermans et al., 2021; Fox-Kemper et al., 2021; Jevrejeva et al., 2023).

In this report, we estimate the probabilistic 100-year return ESLs along the coasts of the Indian subcontinent – including a few island stations (65°-95°E, 0°-25°N) for the moderate emission-mitigation (SSP245) and high emission, business-as-usual (SSP585) scenarios. Projections of mean sea level (η_{msl}), high-tide water level (η_{tide}), and water level (variations due to extreme events such as storm surges and wave setup (a function of significant wave height, H_s) collectively referred to climate extremes[2], η_{CE} in this report) at the end of the 21st Century is used. Based on these estimates, coastal vulnerability maps are generated at selected 11 tide-gauge stations along the Indian coasts and are provided in Appendix B.

The aim is to estimate the change in ESLs and their driving components with corresponding uncertainties, which would potentially assist in making a first-line assessment of coastal vulnerability to future ESL hazards along the coasts of the Indian subcontinent. A detailed description of various datasets and the methodology is given in Appendix A.

4. Projected Change in Extreme Sea Level and its components

In the following sections, we provide details of projected changes in ESL, its components, and their corresponding uncertainties at selected tide-gauge stations along the Indian coasts. Following (1), the ESL is estimated from the probabilistic distribution of mean sea level, tidal maximum, and climate extremes (storm surges and waves; see Appendix A). Hence, we first discuss the ESL components and then the combined effect (ESL changes) in the following sections for the two different climate change scenarios (SSP2 4.5 and SSP5 8.5). To efficiently assess the ESL change with respect to the baseline values over coastal locations and island stations, we provide baseline and projected values of ESL change and its components at 11 selected cities along the Indian coasts (in the vicinity of 11 tide-gauge stations) in Tables 1 - 3. A summary of the results, based on 11 coastal stations along the Indian subcontinent, and the perspectives are also provided at the end.

[2] Climate Extreme may include meteorological events such as extreme rain, heat waves, etc. Further, extreme oceanic conditions from geological events such as Tsunamis can also contribute to the sea level extremes. However, in this study, "Climate Extreme" refers to contribution from storm surges and wave setup.

4.1 Mean Sea Level (MSL)

Fig. 3 shows the projected mean sea level at the end of 21st Century along the Indian coasts with respect to the present-day mean sea level (considered as the year 2020) for the two SSPs. Since the MSL is referenced to the 1995 – 2014 period, the present-day MSL is well below 10 cm with minimum uncertainty (Fig. 3a, d). In general, the MSL projections along the Indian coasts are rather uniform and vary from 0.4 – 0.6 m (SSP2 4.5) and by 0.6 – 1 m (SSP5 8.5) with similar ranges of uncertainty (Fig. 3). However, the projected values are slightly different from these ranges at certain tide-gauge locations (Tables 2 and 3). As the present-day MSL is close to zero (Fig. 3a), the values of projected MSL change (Fig. 4) with respect to the baseline are similar to the projected MSL itself (Fig. 3) for both emission scenarios.

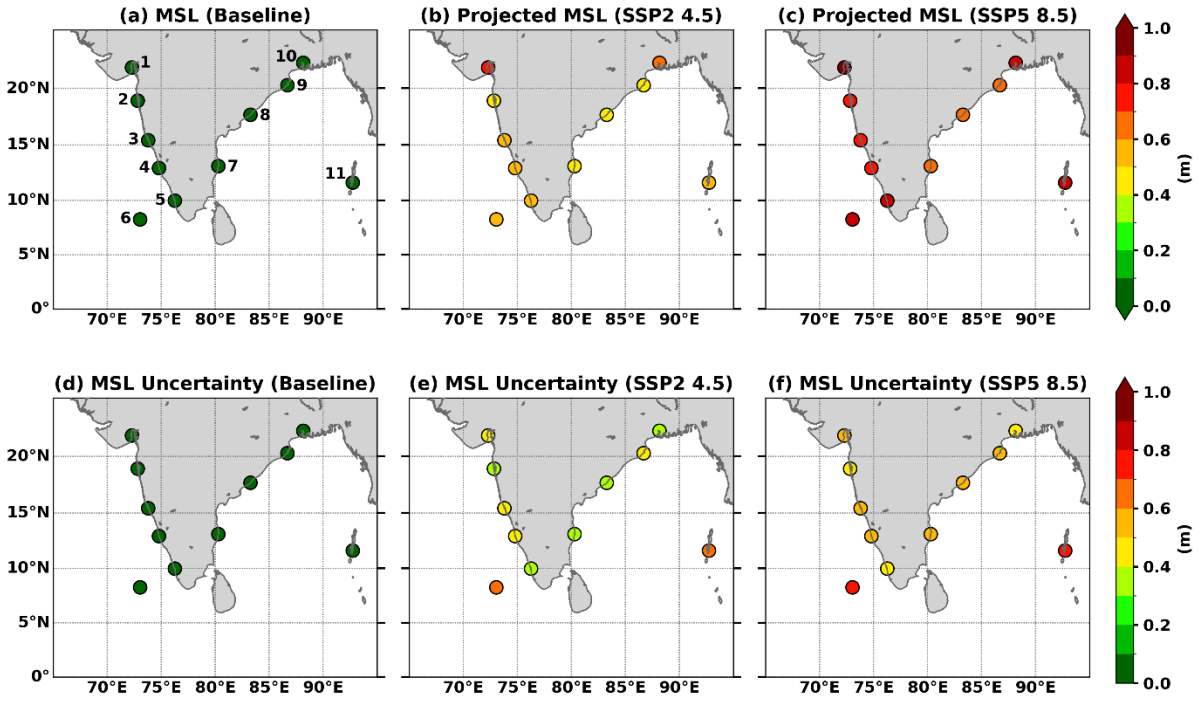

Figure 3: **The present-day and projected mean sea level (MSL)**: median of (a) present-day (baseline) and projected mean sea level for (b) SSP2-4.5, (c) SSP5-8.5 scenarios. The 1-sigma uncertainty of the median for baseline and two future scenarios is also given in panels (d), (e), and (f), respectively. Units are in meters. The baseline period of MSL is 1995 – 2014, and the projections are estimated for 2080 – 2100. The location of tide-gauge stations (selected coastal cities) and the ESL projections are provided in Tables 1, 2, and 3.

The inputs to MSL projections are essentially based on various process models, including models of the ice sheet and glacier changes and Earth system models (see Fox-Kemper et al. 2021). Further, the spatial distribution of the projections also considers observationally

constrained vertical land movements (VLM; see Kopp et al. 2023) for the relative sea-level projections. All these components, especially the ice sheet contributions during the second half of the century, bring large uncertainties, which are eventually propagated into the final total uncertainties in RSL projections, as shown in Figs. 3 and 4, leading to high uncertainties for both the SSPs.

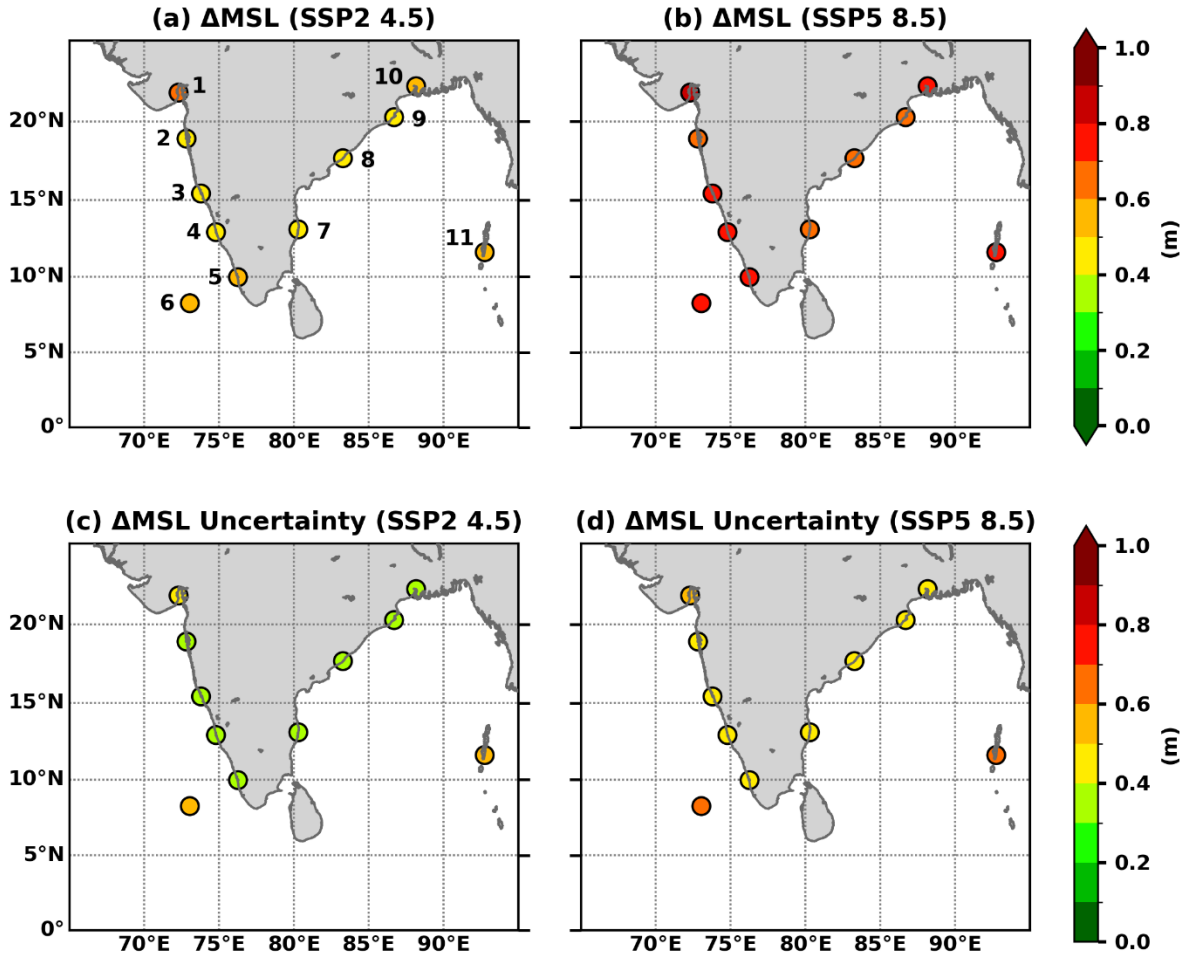

Figure 4: **The projected change in mean sea level**: Median of projected mean sea-level change and the corresponding 1-sigma uncertainty for (a, c) SSP2-4.5 and (b, d) SSP5-8.5 scenarios. Units are in meters. The baseline period is 1995 – 2014, and the projections are for 2080 – 2100.

As shown in Table 3b, the MSL change varies between 66 cm (Chennai) and 87 cm (Bhavnagar) for the high-emission scenario. The MSL change varies between 0.41 cm (Visakhapatnam) and 63 cm (Bhavnagar) for SSP2 4.5 (Table 3a). The projected rise in MSL in the island stations (Minicoy and Port Blair) is notably high (78.6 and 76 cm, respectively) for the high emission scenario, indicating the islands' vulnerability to ESL-driven hazards.

Table 1: The present-day values (baseline) of extreme sea levels and their components at selected coastal cities along the Indian coasts. The geographic locations of the selected tide gauges are shown in Fig. 3.

Sr. No.	City Name	Lat (°N)	Lon (°E)	*MSL* (m)	η_{tide} (m)	η_{CE} (m)	*ESL* (m)
1	Bhavnagar (Gujarat)	21.8	72.3	0.08 (0.05-0.12)	5.22 (5.06-5.46)	1.56 (1.52-1.62)	6.88 (6.71-7.11)
2	Mumbai (Maharashtra)	18.9	72.8	0.04 (0.01-0.06)	2.64 (2.59-2.68)	1.54 (1.5-1.59)	4.22 (4.15-4.29)
3	Mormugao (Goa)	15.4	73.8	0.04 (0.02-0.07)	1.11 (1.09-1.13)	1.53 (1.49-1.59)	2.68 (2.63-2.75)
4	Mangalore (Karnataka)	12.9	74.8	0.04 (0.02-0.07)	1.78 (1.73-1.82)	1.22 (1.18-1.26)	3.04 (2.98-3.11)
5	Cochin (Kerala)	10.0	76.3	0.05 (0.03-0.08)	0.54 (0.53-0.55)	1.06 (1.02- 1.1)	1.65 (1.61-1.7)
6	Minicoy (Lakshadweep)	8.3	73.1	0.05 (0.01-0.10)	0.59 (0.58-0.6)	0.97 (0.94- 1.01)	1.62 (1.56-1.68)
7	Chennai (Tamil Nadu)	13.1	80.3	0.03 (0.01-0.06)	0.69 (0.66-0.71)	0.83 (0.81-0.87)	1.56 (1.51-1.6)
8	Vishakhapatnam (Andhra Pradesh)	17.7	83.3	0.03 (0.01-0.06)	0.91 (0.9-0.92)	1.23 (1.20-1.28)	2.18 (2.13-2.23)
9	Paradip (Odisha)	20.3	86.7	0.03 (0.01-0.06)	1.21 (1.18-1.24)	1.37 (1.33-1.42)	2.62 (2.57-2.68)
10	Diamond Harbour (West Bengal)	22.2	88.2	0.06 (0.04-0.08)	2.57 (2.48-2.65)	1.16 (1.13-1.20)	3.79 (3.7-3.89)
11	Port Blair (Andaman and Nicobar Islands)	11.6	92.7	0.05 (0.01-0.1)	1.19 (1.17-1.21)	0.64 (0.62-0.67)	1.88 (1.82-1.94)

4.2 Tidal maximum (η_{tide})

As described in Appendix A of this report, the projected tidal maximum along the Indian coasts (including the island stations) comes from a global hydrodynamic model that incorporates the projected mean sea-level rise in its tidal simulations for the two emission scenarios (Vousdoukas et al., 2018). As the baseline tidal ranges are underestimated in the global model, we estimated the tidal maxima at the 11 stations using harmonic analysis on observed tide-gauge data at these stations. Then we applied a quantile mapping procedure to obtain a revised set of tidal maximum projections using the observed (baseline) and projected (from the global model) tidal maximum. The present-day and the projected distribution of tidal maximum (median) and the corresponding uncertainties are shown in Fig. 5, for moderate and high emission scenarios.

The present-day tidal maximum along the Indian coast ranges between 0.5 – 2 meters in general (Bhavnagar is an exception where the tidal maximum is about 5 meters), with the tidal amplitude (maximum) increasing from south to north (Fig. 4a). The northward increase of tidal

ranges along the Indian coastlines is reported in the past (e.g. Sindhu et al. 2013). The projected tidal maxima also display a similar spatial distribution with higher amplitudes found north of 13°N for both scenarios. The tidal maximum is highest in the Gulf regions off Gujrat and in the deltaic regions of the northern Bay of Bengal (> 2 m; Fig. b, c). The spatial pattern of uncertainty in the tidal maximum also exhibits a similar structure with large uncertainties existing in regions where tidal maxima are higher (Fig. 5d-f).

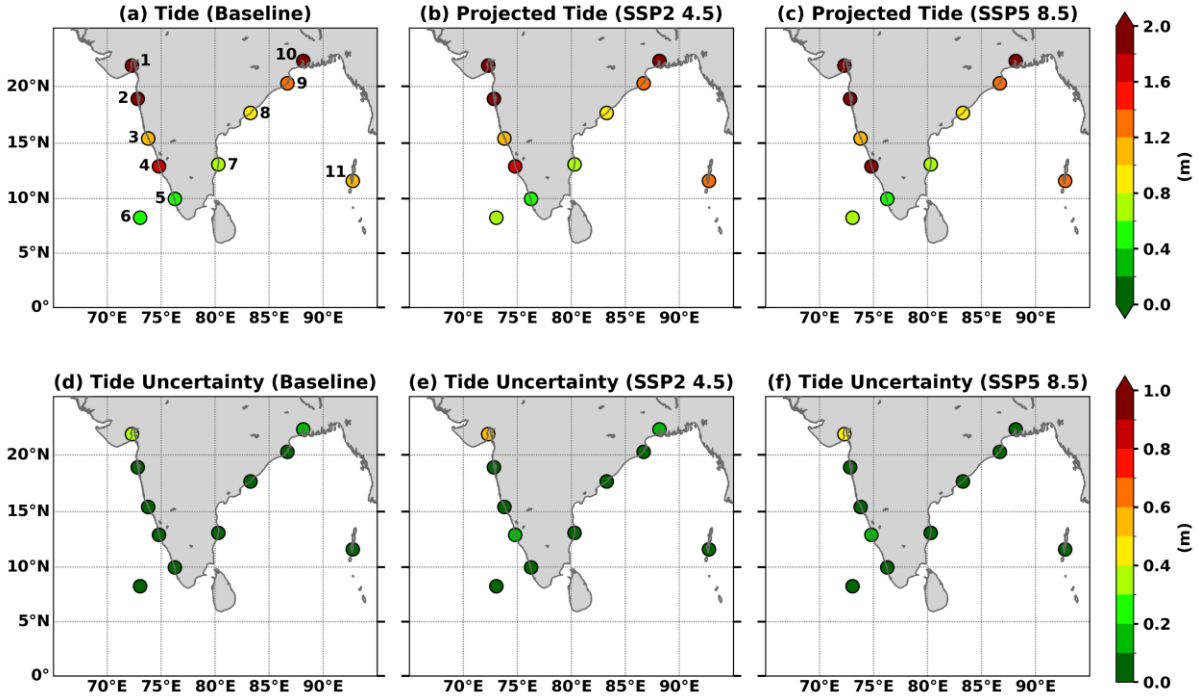

Figure 5: **The present-day and projected tidal maximum (η_{tide})**: Median of (a) present-day (baseline) and projected tidal maximum for (b) SSP2-4.5, (c) SSP5-8.5 scenarios. The 1-sigma uncertainty of the median for baseline and two future scenarios is also given in panels (d), (e), and (f), respectively. Units are in meters. The baseline period is 1980 – 2014, and the projections are estimated for 2100. The ESL projections are tabulated and provided in Tables 1, 2, and 3.

The change in tidal maximum by the end of this century ranges between a few centimetres, with maximum change observed in Bhavnagar (~ 20 cm increase) for both SSP2 and SSP5. Minimal tidal maximum changes are observed for a few stations – Cochin (0.5 cm), Mormugao (1.7 cm), and Port Blair (0.8 cm). The tidal changes are moderate but negative – indicating a decrease in the tidal maximum – in Diamond Harbour (~ -11 cm for SSP5 8.5). Generally, a decrease in tidal maximum (~ by 5 – 10 cm) is observed at many locations in the northern Bay of Bengal by the end of the century (Fig. 6a, b). The projections of tidal changes come with a similar range of uncertainty, with larger uncertainties (> 10 cm) found in the northern Bay of Bengal and the northwest coastal regions (off Mumbai and Bhavnagar; see tables 3a, b).

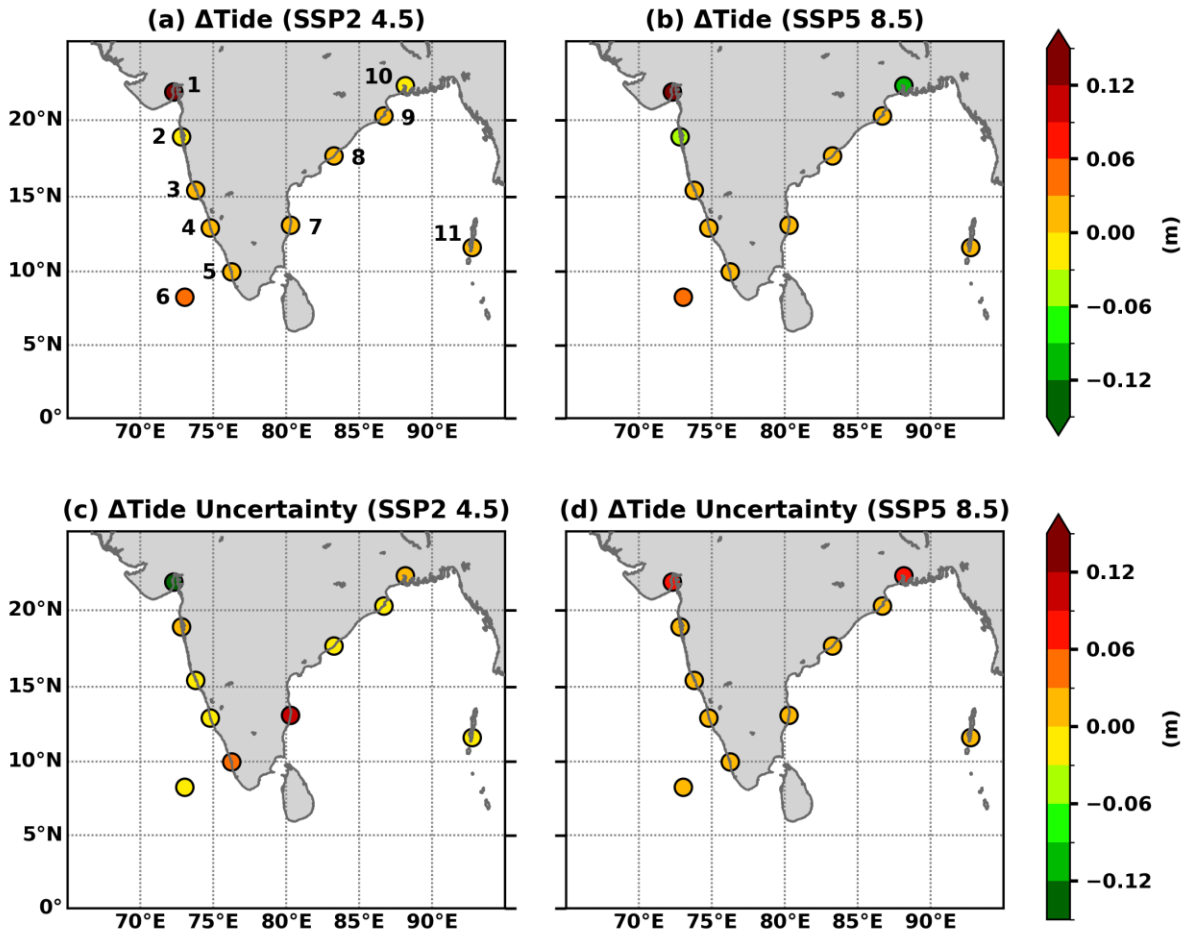

Figure 6: **The projected change in tidal maximum**: Median of projected tidal maximum change and the corresponding 1-sigma uncertainty for (a, c) SSP2-4.5 and (b, d) SSP5-8.5 scenarios. Units are in meters. The baseline period is 1980 – 2014, and the projections are for 2100.

4.3 Climate extremes (storm surges and waves)

The wave projections used in this report come from a global model (WAVEWATCH III), and the wave setup is approximated through an empirical formula counting the significant wave height (Appendix A). The storm surge projections are also attained using a global model (DEFLOW-FM), with the flexible mesh incorporating the cyclone tracks from various sources (Vousdoukas et al., 2018).

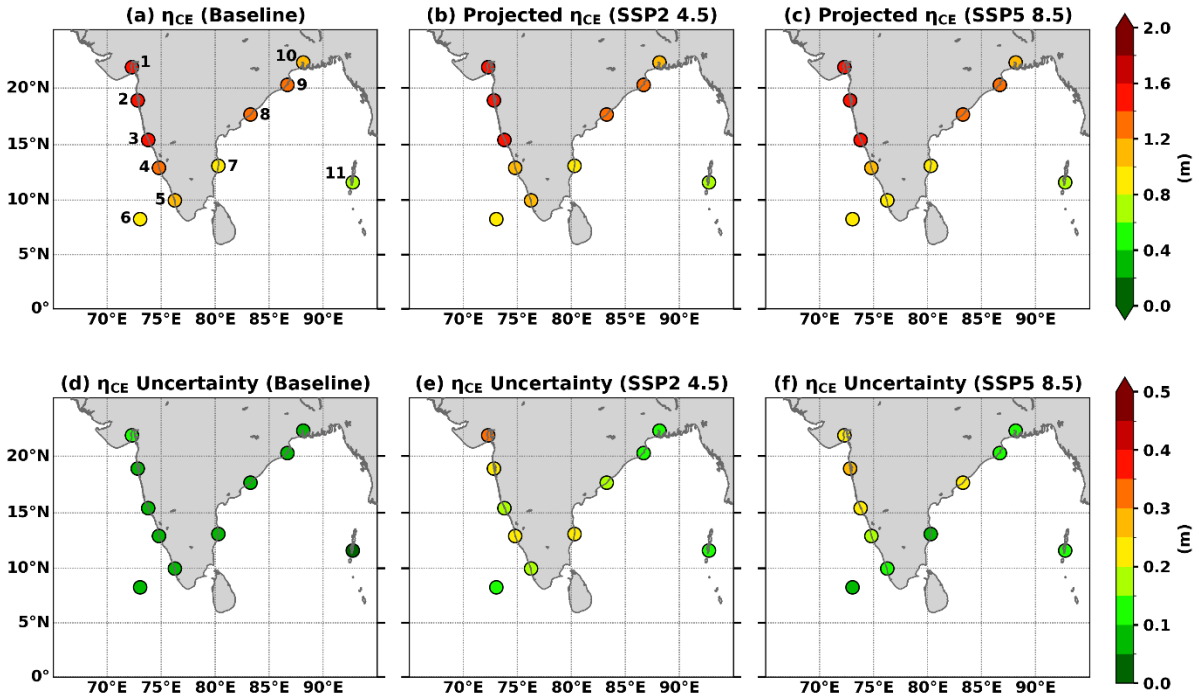

Figure 7: **The present-day and projected climate extremes (**storm surges + waves**)**: Median of (a) present-day (baseline) and projected climate extremes for (b) SSP2-4.5, (c) SSP5-8.5 scenarios. The 1-sigma uncertainty of the median for baseline and two future scenarios is also given in panels (d), (e), and (f), respectively. Units are in meters. The baseline period is 1980 – 2014, and the projections are estimated at 2100.

Fig. 7 & 8 suggest that the projections of climate extremes have more spatial variations than any other components of ESL, as discussed in this report. The highest present-day values are observed along the coasts of Bangladesh and Myanmar. However, the projected changes in climate extremes by the end of this century indicate that the changes are indeed negative ($\Delta\eta CE < 0$) over coastal zones south of 13°N, for both scenarios (Fig. 8a, b). The projected change in climate extremes across Mormugao, Mangalore, Cochin, Chennai, and Minicoy varies between -10 cm and -1 cm (i.e., a decreasing trend for these stations) considering the two emission scenarios (Table 3). On the other hand, the projected climate extremes at 2100 show the most considerable changes along the northern Bay of Bengal coasts for SSP5 8.5 (especially along the coasts of West Bengal in India and off Bangladesh and Myanmar). There is a remarkable increase in climate extremes (~ 10 cm) along the coast of Andhra Pradesh by the end of this century (Fig. 8b). The projected rise in climate-extreme-driven sea level at Vishakhapatnam is 9.1 cm (Table 3b).

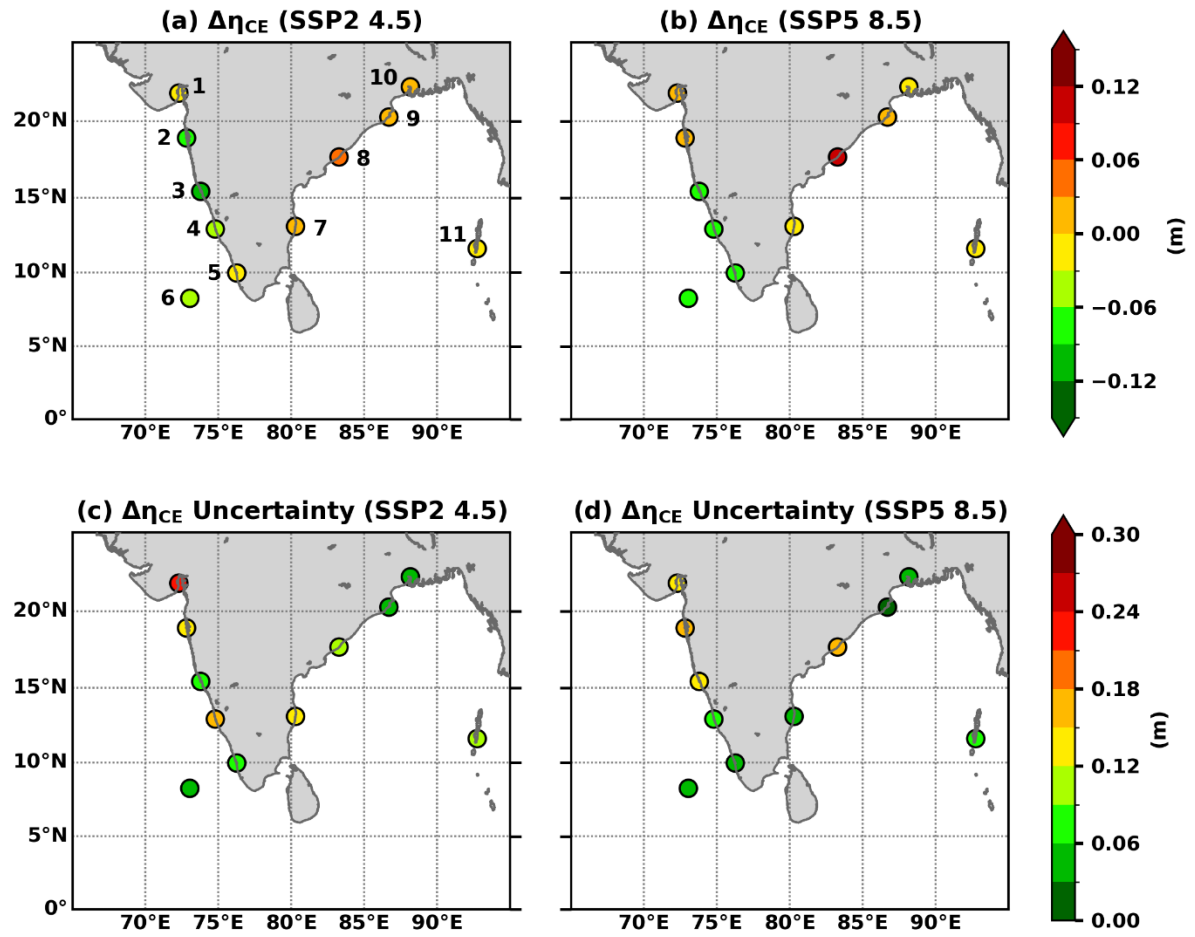

Figure 8: **The projected change in climate extremes**: Median of projected climate extremes change and the corresponding 1-sigma uncertainty for (a, c) SSP2-4.5 and (b, d) SSP5-8.5 scenarios. Units are in meters. The baseline period is 1980 – 2014, and the projections are for 2100.

4.4 Extreme Sea Level (ESL)

Through a random sampling of the probability density functions of ESL components (MSL, tide, and climate extremes) and adding them linearly following (1), we could generate ESL sample values followed by GEV analysis for obtaining the parameters (see Appendix A). The salient features of the projected ESL changes along the Indian coasts are discussed below.

The distribution of ESL along the Indian coastlines at the present period (1995 – 2014), in general, indicates a gradual increase in ESL from south to north (Fig. 9a). Present-day ESL values are typically about 1 meter along the coastlines of the southern peninsula (Karnataka, Kerala, Tamil Nadu coasts) gradually increasing values up to 4 meters along the northern Bay of Bengal and Gujarat coasts. The ESL values range between 1 – 2 meters across the island regions in the north Indian Ocean (Fig. 9a). The characteristic feature of northward increase in ESL along the coasts. As shown in section 4.2, the tidal amplitudes are maximum (> 2 meters) along the Gujrat coasts (Gulf of Khambhat for instance) and along the coasts of northern Bay

(Sundarbans). Present-day climate extremes (i.e., storm surges + waves) have higher values (typically 1.5 – 2 meters) along the west coast of India (about 13°N – 23°N) and in the coastal regions of the northeastern Bay of Bengal (Fig. 7a). These factors are indeed reflected in the present-day ESL distribution along the Indian coasts (Fig. 9a). For instance, the high ESL values in the Gujarat coasts and northern Bay of Bengal are explained mainly by the occurrence of high values of tidal maximum and climate extremes in these regions. It is to be noted that, however, both regions show considerable uncertainty in the present-day tidal maximum, which is seen in present-day ESLs as well (Fig. 9d).

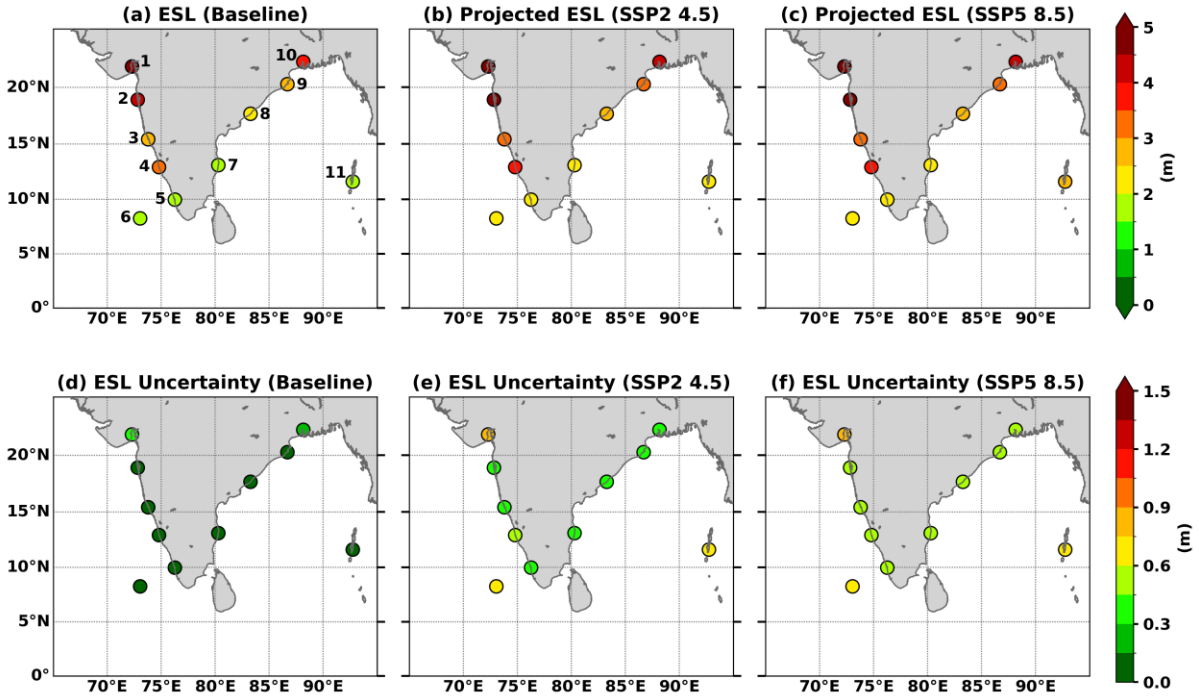

Figure 9: **The present-day and projected extreme sea level (ESL)**: Median of (a) present-day (baseline) and projected ESLs for (b) SSP2-4.5, (c) SSP5-8.5 scenarios. The 1-sigma uncertainty of the median for baseline and two future scenarios is also given in panels (d), (e), and (f), respectively. Units are in meters. The baseline period is 1980 – 2014; the projections are estimated at 2100.

The projected ESLs vary significantly along the coasts (ranging from 1 – 6 meters; Fig. 9b, c) for both scenarios and as shown for the present-day distribution (Fig. 9a), this non-uniform distribution originates from the fact that the contributing components (tides and storm surges) vary significantly along the coasts in the future as well (Figs. 5, 7). The projected changes of ESL and its components at the 11 selected stations are provided in Tables 2 and 3. As seen in Table 2, the projected ESLs are more prominent towards the northern coasts (e.g. the Gulf of Gujrat and the rim of northern Bay), where the tidal ranges are getting maximum (Table 2). Similarly, the projected ESLs are minimal (ranging from 1 to 3 meters) along the low-latitude island stations where tidal maximum and storm surges are also weak compared to the northern

coasts. The uncertainty of the projected ESLs is large for both emission scenarios (~ up to 1 m) and mainly comes from uncertainties associated with the MSL projections (Figs. 3e, f).

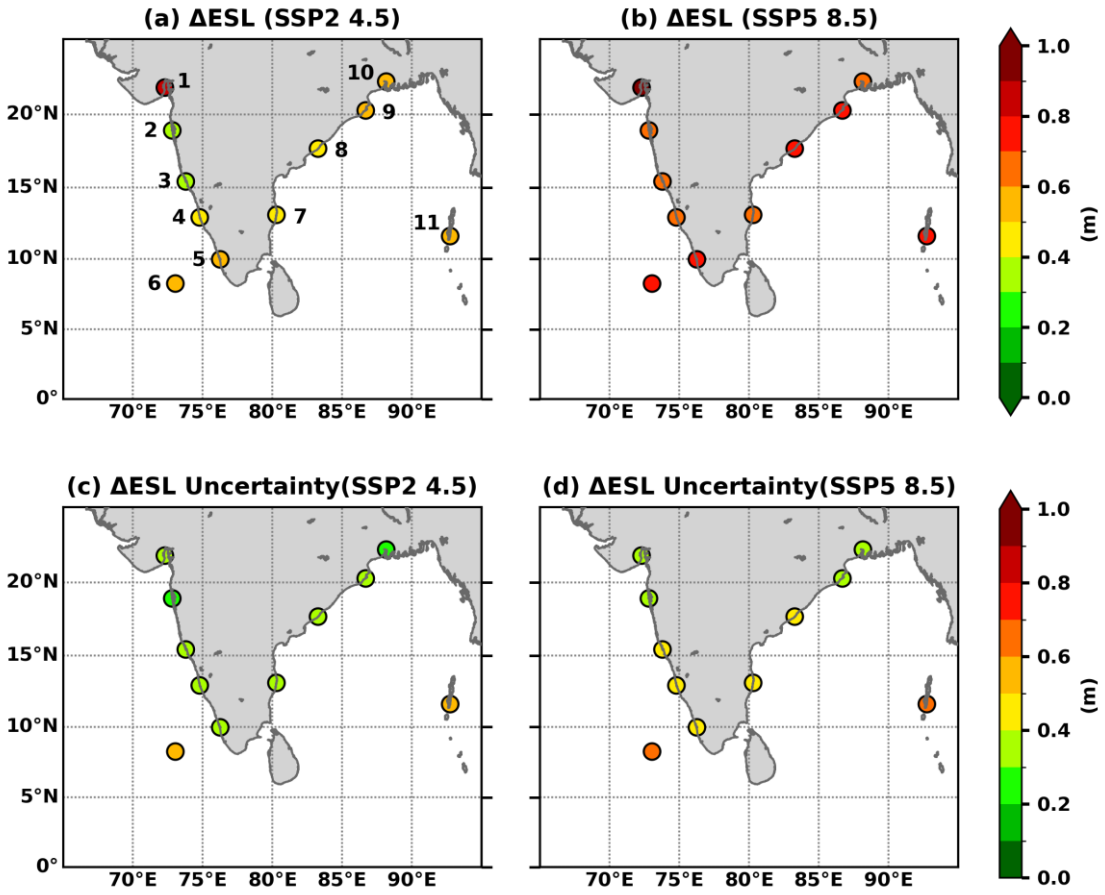

Figure 10: **The projected change in extreme sea level (ESL)**: Median of projected climate extremes change and the corresponding 1-sigma uncertainty for (a, c) SSP2-4.5 and (b, d) SSP5-8.5 scenarios. Units are in meters. The baseline period is 1980 – 2014 and the projections are for 2100.

Table 2 a): Projected highest water levels at selected coastal cities along the Indian coasts in 2100 under the SSP2 - 4.5 scenario.

Sr. No.	City Name	Lat (°N)	Lon (°E)	*MSL* (m)	η_{tide} (m)	η_{CE} (m)	*ESL* (m)
1	Bhavnagar (Gujarat)	21.8	72.3	0.71 (0.50-0.97)	5.42 (5.18-5.7)	1.56 (1.42-1.75)	7.74 (7.38-8.15)
2	Mumbai (Maharashtra)	18.9	72.8	0.46 (0.32-0.68)	2.61 (2.59-2.66)	1.47 (1.37-1.60)	4.59 (4.40-4.83)
3	Mormugao (Goa)	15.4	73.8	0.51 (0.34-0.75)	1.11 (1.09-1.13)	1.42 (1.35-1.53)	3.06 (2.87-3.31)
4	Mangalore (Karnataka)	12.9	74.8	0.52 (0.23-0.71)	1.8 (1.75-1.85)	1.17 (1.07-1.30)	3.52 (3.29-3.79)
5	Cochin (Kerala)	10.0	76.3	0.58 (0.43-0.82)	0.54 (0.53-0.55)	1.04 (0.97- 1.13)	2.18 (2.0-2.41)
6	Minicoy (Lakshadweep)	8.3	73.1	0.60 (0.28-0.97)	0.63 (0.6-0.65)	0.94 (0.89-1.00)	2.17 (1.85-2.53)
7	Chennai (Tamil Nadu)	13.1	80.3	0.45 (0.30-0.69)	0.71 (0.67-0.73)	0.86 (0.78-0.98)	2.04 (1.86-2.29)
8	Vishakhapatnam (Andhra Pradesh)	17.7	83.3	0.43 (0.27-0.66)	0.93 (0.91-0.95)	1.27 (1.19-1.38)	2.66 (2.47-2.9)

9	Paradip (Odisha)	20.3	86.7	0.47 (0.30-0.71)	1.24 (1.20-1.28)	1.39 (1.34-1.48)	3.12 (2.93-3.37)
10	Diamond Harbour (West Bengal)	22.2	88.2	0.64 (0.48-0.86)	2.54 (2.44-2.58)	1.17 (1.12-1.24)	4.34 (4.14-4.57)
11	Port Blair (Andaman and Nicobar Islands)	11.6	92.7	0.58 (0.26-0.94)	1.2 (1.18-1.22)	0.62 (0.56-0.71)	2.41 (2.09-2.77)

Table 2 b): Projected highest water levels at selected coastal cities along the Indian coasts in 2100 under the SSP5 - 8.5 scenario.

Sr. No.	City Name	Lat (°N)	Lon (°E)	*MSL* (m)	η_{tide} (m)	η_{CE} (m)	*ESL* (m)
1	Bhavnagar (Gujarat)	21.8	72.3	0.95 (0.71-1.27)	5.39 (5.19-5.68)	1.58 (1.48-1.72)	7.99 (7.64-8.43)
2	Mumbai (Maharashtra)	18.9	72.8	0.70 (0.51-0.99)	2.61 (2.57-2.63)	1.54 (1.43-1.70)	4.88 (4.64-5.19)
3	Mormugao (Goa)	15.4	73.8	0.75 (0.54-1.05)	1.12 (1.10-1.15)	1.47 (1.37-1.60)	3.37 (3.13-3.68)
4	Mangalore (Karnataka)	12.9	74.8	0.75 (0.44-1.0)	1.81 (1.75-1.86)	1.14 (1.07-1.23)	3.73 (3.49-4.04)
5	Cochin (Kerala)	10.0	76.3	0.82 (0.63-1.12)	0.54 (0.53-0.55)	0.98 (0.93- 1.05)	2.36 (2.16-2.65)
6	Micoy (Lakshadweep)	8.3	73.1	0.84 (0.5-1.25)	0.63 (0.61-0.65)	0.89 (0.85-0.95)	2.37 (2.04-2.77)
7	Chennai (Tamil Nadu)	13.1	80.3	0.69 (0.49-1.0)	0.71 (0.67-0.73)	0.82 (0.78-0.88)	2.23 (2.01-2.52)
8	Vishakhapatnam (Andhra Pradesh)	17.7	83.3	0.65 (0.44-0.96)	0.93 (0.91-0.95)	1.33 (1.22-1.47)	2.94 (2.7-3.26)
9	Paradip (Odisha)	20.3	86.7	0.69 (0.49-0.99)	1.24 (1.2-1.28)	1.39 (1.34-1.46)	3.34 (3.12-3.63)
10	Diamond Harbour (West Bengal)	22.2	88.2	0.86 (0.66-1.14)	2.45 (2.38-2.48)	1.16 (1.11-1.23)	4.46 (4.25-4.74)
11	Port Blair (Andaman and Nicobar Islands)	11.6	92.7	0.81 (0.46-1.22)	1.2 (1.18-1.22)	0.63 (0.59-0.69)	2.65 (2.31-3.05)

The changes in ESL by the end of this century vary significantly between the two SSPs, as shown in Fig. 10a, b. While SSP2-4.5 indicates a change that broadly varies between 0.4 – 0.6 m, the ESL change for SSP5-8.5 varies between 0.6 – 0.8 m. Bhavnagar (Gujarat) shows the largest change (1.1 m), followed by Port Blair (Andaman and Nicobar Islands, 0.79 m), as shown in Table 3b. The MSL change by the end of this century (which roughly varies from 0.4 to 0.8 m depending on location and scenario; see tables 3a, b) contributes mainly to the ESL change. However, for a few stations (Mormugao, Mangalore, Cochin, and Minicoy), a decrease in climate extremes (Table 3b) offset the contribution from MSL change, leading to a slight reduction in ESL change (Table 3b). For instance, the high ESL change at Port Blair results from the MSL rise, and the change in tidal maximum and climate extreme is negligible for this island station.

The uncertainty of ESL change also mainly stems from uncertainties in MSL projections. In fact, the uncertainties of tides and climate extremes are not so significant in magnitude in most regions except for those hotspot locations observed in present-day and projection maps. For instance, the uncertainty in projected tidal maximum is most prominent in the Gulf of Khambhat and along the coasts of the northern Bay of Bengal (~10 - 20 cm; Fig. 6d). The uncertainty of projected climate extremes is prominent along the northeastern coast of the Bay of Bengal, along the coast of Myanmar, Bangladesh and west Bengal (20 – 30 cm; Fig. 8d).

As mentioned in the introduction, the results presented in this report come from global physical models, which have several limitations in accurately predicting the processes and corresponding changes. A few such caveats are discussed in the following section, along with our perspective on improving the ESL projections discussed in the present report.

Table 3a): Projected changes in ESL and the contributing components at selected coastal cities along the Indian coasts under the SSP2 - 4.5 scenario.

Sr. No.	City Name	Lat (°N)	Lon (°E)	ΔMSL (cm)	$\Delta\eta_{tide}$ (cm)	$\Delta\eta_{CE}$ (cm)	ΔESL (cm)
1	Bhavnagar (Gujarat)	21.8	72.3	62.9 (45.1-86.0)	20.0 (11.7-23.9)	-0.2 (-9.9-13.4)	86.1 (66.8-104.0)
2	Mumbai (Maharashtra)	18.9	72.8	42.4 (30.8-62.0)	-2.6 (-5.1 - -2.1)	-6.8 (-12.1-0.6)	37.1 (24.9-53.9)
3	Mormugao (Goa)	15.4	73.8	46.4 (32.1-67.6)	0.4 (0.2-0.8)	-10.7 (-14.1- -6.1)	38 (23.7-56.5)
4	Mangalore (Karnataka)	12.9	74.8	47.2 (23.2-64.2)	2.0 (1.4-2.8)	-4.3 (-10.6- 4.4)	47.2 (31.0-67.7)
5	Cochin (Kerala)	10.0	76.3	52.9 (39.8-74.0)	0.2 (0.1-0.3)	-1.8 (-5.1- 2.9)	53.1 (39.4-71.9)
6	Minicoy (Lakshadweep)	8.3	73.1	54.4 (26.7-86.5)	3.4 (2.5-4.7)	-3.3 (-5.4- -0.4)	55.5 (28.9-85.1)
7	Chennai (Tamil Nadu)	13.1	80.3	42.2 (29.8-62.5)	1.6 (1.1-2.3)	2.7 (-3.3-11.0)	49.0 (34.4-68.5)
8	Vishakhapatnam (Andhra Pradesh)	17.7	83.3	40.1 (27.4-60.1)	2.0 (1.3-2.9)	3.6 (-1.1-10.0)	47.9 (33.8-66.5)
9	Paradip (Odisha)	20.3	86.7	43.8 (29.3-65.1)	2.4 (1.5-3.7)	2.2 (0.0-5.3)	50.2 (36.4-68.0)
10	Diamond Harbour (West Bengal)	22.2	88.2	57.6 (44.2-78.1)	-3.0 (-4.5-1.0)	1.0 (-0.9-3.7)	54.5 (44.1-68.4)
11	Port Blair (Andaman and Nicobar Islands)	11.6	92.7	52.8 (25.5-84.4)	0.9 (0.6-1.2)	-1.4 (-5.4-4.0)	53.6 (26.7-83.3)

Table 3b): Projected changes in ESL and the contributing components at selected coastal cities along the Indian coasts under the SSP5-8.5 scenario.

Sr. No.	City Name	Lat (°N)	Lon (°E)	ΔMSL (cm)	$\Delta\eta_{tide}$ (cm)	$\Delta\eta_{CE}$ (cm)	ΔESL (cm)
1	Bhavnagar (Gujarat)	21.8	72.3	87 (65.5-115.7)	16.4 (12.8-21.6)	2.8 (-2.8-10.6)	111.7 (92.8-131.4)
2	Mumbai (Maharashtra)	18.9	72.8	66.6 (49.8-93)	-3.4 (-4.5 - -2.0)	0.8 (-6-10.3)	66.8 (49.9-89.8)

3	Mormugao (Goa)	15.4	73.8	70.6 (52.4-98.2)	1.7 (1.3-2.2)	-6 (-11.5- -1.7)	68.8 (49.9-93.5)
4	Mangalore (Karnataka)	12.9	74.8	71 (52.2-99.2)	3.0 (2.2-4.0)	-7.2 (-10.9- -2.0)	68.9 (50.8-93.0)
5	Cochin (Kerala)	10.0	76.3	76.9 (59.7-104.3)	0.5 (0.4-0.6)	-7.3 (-9.5- -4.2)	71.5 (54.7-95.4)
6	Minicoy (Lakshadweep)	8.3	73.1	78.6 (48.8-115.2)	3.6 (2.7-4.9)	-7.8 (-9.2- -6)	75.4 (47.0-108.9)
7	Chennai (Tamil Nadu)	13.1	80.3	66 (47.9-93.8)	1.6 (1.1-2.3)	-1.1 (-2.8-1.1)	67.7 (50.4-91.9)
8	Vishakhapatnam (Andhra Pradesh)	17.7	83.3	62.7 (44.2-90.4)	2.0 (1.4-2.9)	9.1 (2.4-18.5)	76.6 (56.4-102.7)
9	Paradip (Odisha)	20.3	86.7	66.1 (47.7-93.4)	2.6 (1.7-3.8)	1.8 (0.7-3.4)	71.9 (55.1-94.7)
10	Diamond Harbour (West Bengal)	22.2	88.2	79.8 (62.6-106.1)	-11.6 (-17.2- -10.4)	-0.3 (-2.1-2.2)	67.0 (54.5-85.3)
11	Port Blair (Andaman and Nicobar Islands)	11.6	92.7	76 (46.1-112.5)	0.9 (0.6-1.3)	-0.6 (-3.1-2.9)	77.4 (48.5-111.3)

5. Caveats and Perspectives

The most significant contributor to end-century ESL change is the mean sea level (MSL) rise. However, the MSL change by 2100 along the Indian coasts (ranges between 0.5 and 1 meter) comes with a similar range of uncertainty. The uncertainty in MSL comes from uncertainties of its contributing components (processes). In the long term (after 2050), for instance, ice loss from Antarctica becomes the main source of uncertainty, contributing 50% of the total uncertainty in projected MSL by the end of the century (Palmer and Weeks, 2024). On the other hand, in a short-term period (before 2030), ocean dynamic sea-level rise is the main source of uncertainty (Vousdoukas et al. 2018). The regional dynamic sea-level projections come from coarse global climate models that cannot properly resolve coastal currents and sea levels. Dynamical ocean downscaling at regional scales using high-resolution ocean general circulation models is suggested to solve this problem largely (see Tinker et al. 2020). Similarly, regions with large vertical land motion (VLM, e.g., deltaic regions of the northern Bay of Bengal) are shown to experience large ESL more frequently (Unnikrishnan and Antony, 2022) owing to the higher relative mean sea-level rise. Hence, the lack of VLM observations at coastal locations can also bring large uncertainties in RSL projections, as seen in this report. Downscaled dynamic sea-level projections and revised projections with updated local VLM information would potentially narrow down the large uncertainties in regional MSL projections – that we keep as a perspective.

For moderate emission scenarios, climate extremes (storm surges and wave setup) remain the main source of uncertainty over most of the century towards ESL prediction (Vousdoukas et al. 2018). The uncertainty can largely be related to the predictive skill of the corresponding model

(storm surge/wave models). Both storm surges and waves discussed in this report have been taken from global models that may not adequately capture the regional climate. More importantly, the wave setup projections used in this report are approximated through an empirical formula and do not consider resolving the full coastal dynamics (for example, the effect of bottom slope on wave setup). This is also the case for projections for tidal maxima, which again employ a global tide model. Past literature suggests that the tides are significantly modified by (coastal fine scale) bathymetry and bottom slope, and the global model solutions may not accurately predict the tide, especially over wide, shallow shelf regions (e.g. Testut and Unnikrishnan, 2016). For example, Mitra et al. (2020) showed that the global tidal models have underestimated the tidal amplitude in the Gulf regions off Gujarat, and such an underestimation is also present in the tidal maximum presented in this report. Further, the negative trend in tidal maxima observed in the northern Bay, however small, is significant since it negates the impact of sea level rise. This makes it all the more important for us to simulate tides in a climate change scenario accurately. The best practice for overcoming these caveats is to develop regional model configurations for tides and climate-extreme variables (waves and storm surges), with adequately resolved coastal bathymetry and observed or bias-corrected wind forcing. In other words, developing high-resolution regional models for dynamic sea levels, storm surges, waves, and tides would greatly reduce the current range of uncertainties reported in this document. INCOIS has already taken such initiatives under the Deep Ocean Mission programme, and the regional downscaled simulations based on high-resolution models are expected to provide better extreme sea-level projections with reduced uncertainty along the coast of India.

The results presented in this report exclude a few of the potential nonlinear interactions between the ESL components, as these variables are simulated through separate models and then combined offline. Such biases might arise because the nonlinear interactions between sea level, tide, storm surge, and waves are important at the coastal locations; for example, the tide-surge interaction is significant at some locations of the Bay of Bengal (Antony et al., 2013). However, the coupled modelling of ESL components is computationally very expensive (Vousdoukas et al., 2018). Despite that, the 100-year ESLs estimated in this study are consistent with the results reported by Sindhu et al. (2011) at Chennai and Vishakhapatnam based on a regional storm surge model configured for the Bay of Bengal domain using an improved bathymetry (Sindhu et al. (2011) considered atmospheric forcing and tides from global models). In Paradip, the ESL shown in this report is much lower than that of Sindhu et al.

(2011), which indicates an underestimation of ESL in the northern part of the Indian coastal basin presented in this report. These findings indicate that the global-model-based ESL simulations might be more consistent with those derived from observations towards the southern part of the Indian subcontinent (including island stations), but they are likely underestimated towards the north.

Note that this study did not consider other geological causes, such as tsunamis, in the estimates of extreme sea level and in deriving the vulnerability maps. In another study, INCOIS has conducted a multi-hazard assessment to evaluate coastal exposure to oceanic hazards, taking into account sea level rise, coastal erosion, and extreme water levels resulting from storm surges, coastal flooding, and tsunamis (Nayak et al., 2022).

6. Summary

Mean sea-level rise is one of the major consequences of global warming, threatening the existence of many low-lying coastal regions and islands worldwide. At the coasts, the mean sea level will conflate with storm surges and tides to induce substantial changes in the coastal water level (of the order of a few meters) to produce extreme sea levels. Historically, the north Indian Ocean has been a hotbed for tropical cyclones, and the coasts of the Indian subcontinent are prone to storm surges and tidal maxima with a typical range of a few meters. Notably, a large part of the coastal zones of the Indian subcontinent lies well within 5 – 10 meters of mean sea level. Global model projections indicate that, for the business-as-usual emission scenario, the mean sea level off the Indian coasts will experience a rise ranging from 0.62 (Visakhapatnam) to 0.87 meters (Bhavnagar) by the end of this century. To what extent the ESLs would change in response to the MSL rise is unknown. In this report, we examine the distribution of extreme sea levels and their components of the Indian subcontinent by 2100 through synthesising simulations from global climate models and other published literature. The present-day extreme sea-level distribution varies between 1.27 m (Chennai) – 4.37 m (Bhavnagar) along the Indian coasts, with the highest range of contributions coming from tidal maxima (~ 0.3 – 2.7 m) followed by climate extremes (storm surges and waves; 1 – 1.5 m).

The present-day extreme sea levels along the Indian coasts and islands are projected to change from (Chennai) 0.68 [0.53 – 0.9] m to (Bhavnagar) 1.12 [0.96 – 1.28] m by the end of the present century, under SSP5-8.5. The mean sea-level rise (0.63 – 0.87 m) is the main driver of extreme sea-level change along the coasts, with additional contributions from tidal maximum ranges between -0.12 m (Diamond Harbour) and 0.16 m (Bhavnagar) and climate extremes

range between -0.08 m (Minicoy) and 0.09 m (Visakhapatnam). In general, coastal regions north of 13ºN are seen as more vulnerable to extreme sea levels, with the Gulf regions off Gujarat and the northern coasts of the Bay of Bengal experiencing the largest changes in tidal and climate extremes, and the extreme sea levels are slightly decreasing towards low latitude coastal regions, including the island stations. The projected extreme sea levels along the Indian coasts show maximum changes in those regions where present-day extreme sea-level maxima are observed, indicating no extreme sea-level hotspot origin along the Indian coastlines in the future warming scenario. Both extreme sea levels and their components come with a large set of uncertainties mainly originating from uncertainties in process modelling. Also, all the results presented in this report are derived from global models with limitations on coarse resolution and biases originating from many sources. The best practice for overcoming this caveat is to develop better regional ocean model configurations for climate extremes with adequately resolved coastal bathymetry and observed and bias-corrected wind forcing. Simulations from high-resolution regional models with sustained observations (for instance, observations for vertical land movement) may reduce the current range of ESL projection uncertainties reported in this document.

Appendix A

Methods

As briefly discussed in Section 2, Extreme Sea Level (ESL) events are an integrated effect of mean sea level rise, astronomical tides, and climate extremes (storm surges and waves). ESL can be estimated as follows:

$$ESL = \eta_{msl} + \eta_{tide} + \eta_{CE} (2)$$

Where,

$$\eta_{CE} = \eta_{stormsurge} + 0.2H_s (3)$$

Hs is the significant wave height. The last term in equation 3 is a rough approximation to wave setup caused by a wave with significant wave height *Hs*. The details of various data and the methods followed in the computation of ESL are shown further in Figure A1 as a flow chart, which is detailed below.

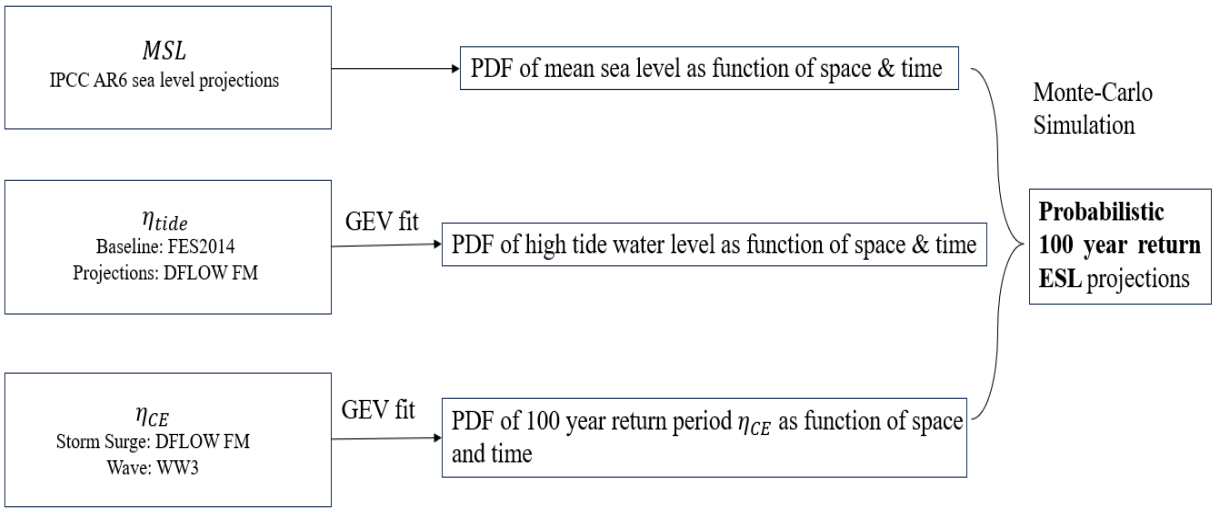

Figure A1: Flow diagram showing the methodology of generating probability distribution of extreme sea level (ESL), updated from Vousdoukas et al. 2018.

Relative mean sea level (η_{msl}): The projections for relative mean sea level (RMSL) along the coasts of the Indian subcontinent are obtained from the IPCC AR6 sea-level projection tool (Fox-Kemper et al., 2021). These projections are simulated at both tide gauges and a global ocean grid. In this report, we consider the SSP5-8.5 scenario (pertaining to high emission, low mitigation, and medium confidence projections) of RMSL projections. The RMSL projections include contributions from several processes as stated before. Note that these projections do not consider the high impact - low likelihood processes like marine ice cliff instability (MICI).

These probabilistic mean sea level projections are generated by simulating a Monte Carlo of driver constituents, contributing to global and regional mean sea levels. The global ocean thermal expansion and ocean dynamic sea level are estimated using the multi-model ensemble CMIP6 output (Kopp et al. 2023). The glacier and ice sheet melting contribution to sea level rise is modelled using the Phase 2 Gaussian process emulator from Glacier Modelling Intercomparison Project (GlacierMIP2) and Ice-sheet Modelling Intercomparison Project (ISMIP6), respectively. We consider projected values in 2020 (referenced to the 1995-2014 period) as a present-day (baseline) estimate of mean sea level (and all other components discussed in this report as well). For end-of-century values, we consider projections in 2100 which are referenced to the baseline period (1995-2014).

High-tide water level (η_{tide}) and coastal water level due to climate extremes (η_{CE}): The baseline high-tide water levels (from a tide model - FES2014) and projections of tidal highs and the fluctuations in water levels due to climate extremes (baseline values and projections) are taken from Vousdoukas et al. (2018). Tidal projections are simulated using the DFLOW FM model, the next version of Delft-3D, where FM stands for Flexible Mesh. The model simulations include mean sea-level rise derived from CMIP5 RCP 8.5 sea-level projections. These baseline and projected tidal datasets pertaining to 5th, 50th, and 95th percentiles are available at the LISCoAsT repository (Large scale Integrated Sea-level and Coastal Assessment Tool, Vousdoukas et al., 2018), by JRC (Joint Research Commission) of the European Commission.

In the climate extremes part, the storm surge is also modelled using a DFLOW-FM setup. It is used because global climate models do not have the needed resolution, while the flexible mesh can trace cyclonic tracks. The waves are simulated using the WaveWatch III model. The models are forced using ERA-Interim reanalysis wind and pressures for the baseline period. The observed cyclone tracks are also considered from various resources (see Vousdoukas et al., 2018 for more details). The wave heights are corrected with Globe Wave altimeter datasets (satellite-derived wind-wave datasets from the European Space Agency). For projections, both models (DFLOW-FM and WaveWatch III) are forced with CMIP5 RCP8.5 wind and mean sea-level pressure projections. The datasets pertaining to the 100-year return period and 5th, 50th, and 95th percentiles are available at the LISCoAsT repository.

Estimation of baseline and projected ESLs: The mean sea-level change probability distributions are readily available from the IPCC AR6 sea-level projections. For η_{tide} and η_{CE}

components, we fit the available percentiles from the datasets at each location (sources are described above) in generalised extreme value (GEV) distribution using the Nelder-Mead algorithm to obtain the distribution parameters (location, scale, and shape), assuming these values follow GEV distribution (Vousdoukas et al., 2018). The algorithm optimises the distribution parameters by minimising the difference between LISCoAsT values and water level values obtained from assumed probability distribution parameters at a given probability percentile. We generate component values from those obtained distribution parameters at each probability quantile for each location to create a probability distribution function (PDF). We randomly draw values from the PDF of each ESL component and linearly add them as shown in ($Eq.2$) to generate ESL sample values, followed by fitting in GEV distribution. We repeat the sampling process a million times until there is satisfactory convergence in GEV parameters (a similar approach can be seen in Vousdoukas et al., 2018). This process is the same for present-day (i.e., for 2020) and projected (in 2100) ESLs. The uncertainty of these projections is estimated using the likely range (17th – 83rd percentile range) of the distribution.

Appendix B

We present the coastal vulnerability maps for the selected cities (in the vicinity of tide-gauge stations), as discussed in this report, under two emission scenarios (SSP2-4.5 and SSP5-8.5). We define coastal vulnerability as those coastal points where the topography is less than or equal to the projected ESL value of the respective emission scenario. We present three maps per station: 1. The original digital elevation map (DEM; generated using ALTM and DEM from Survey of India) showing the coastal topography near the tide-gauge station, 2. The vulnerable area under end-of-century mean sea level (MSL), MSL + Tide, and ESL change under SSP2-4.5, and 3. The vulnerable area under end-of-century mean sea level (MSL), MSL + Tide, and ESL change under SSP5-8.5.

Disclaimer:

Note that the maps below represent the coastal vulnerability due to climate-driven oceanic changes, but **NOT** a flood map under future extreme sea levels. The coastal flooding should be essentially determined from suitable hydrodynamic flood models.

1. Bhavnagar (Gujarat)

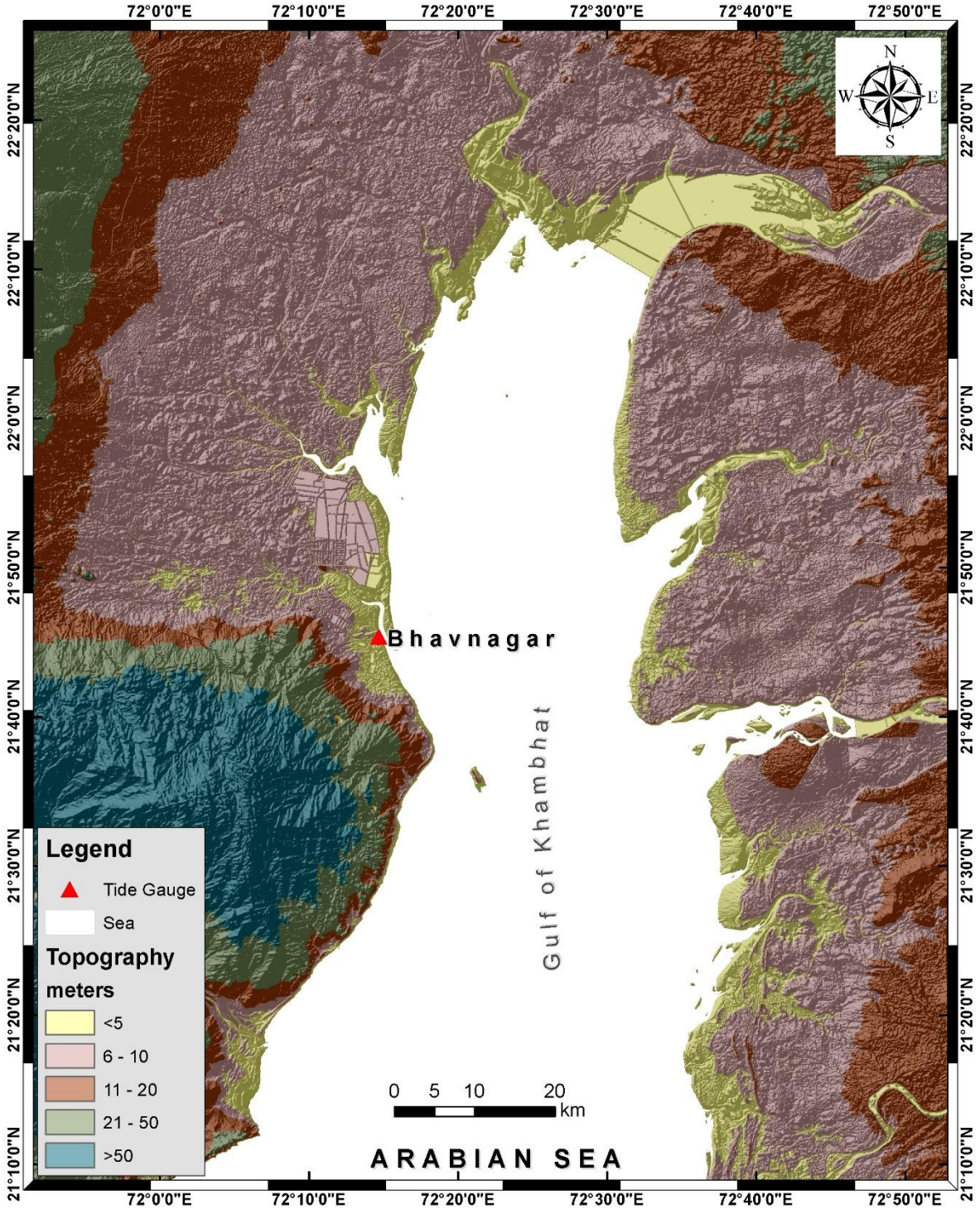

Basemap

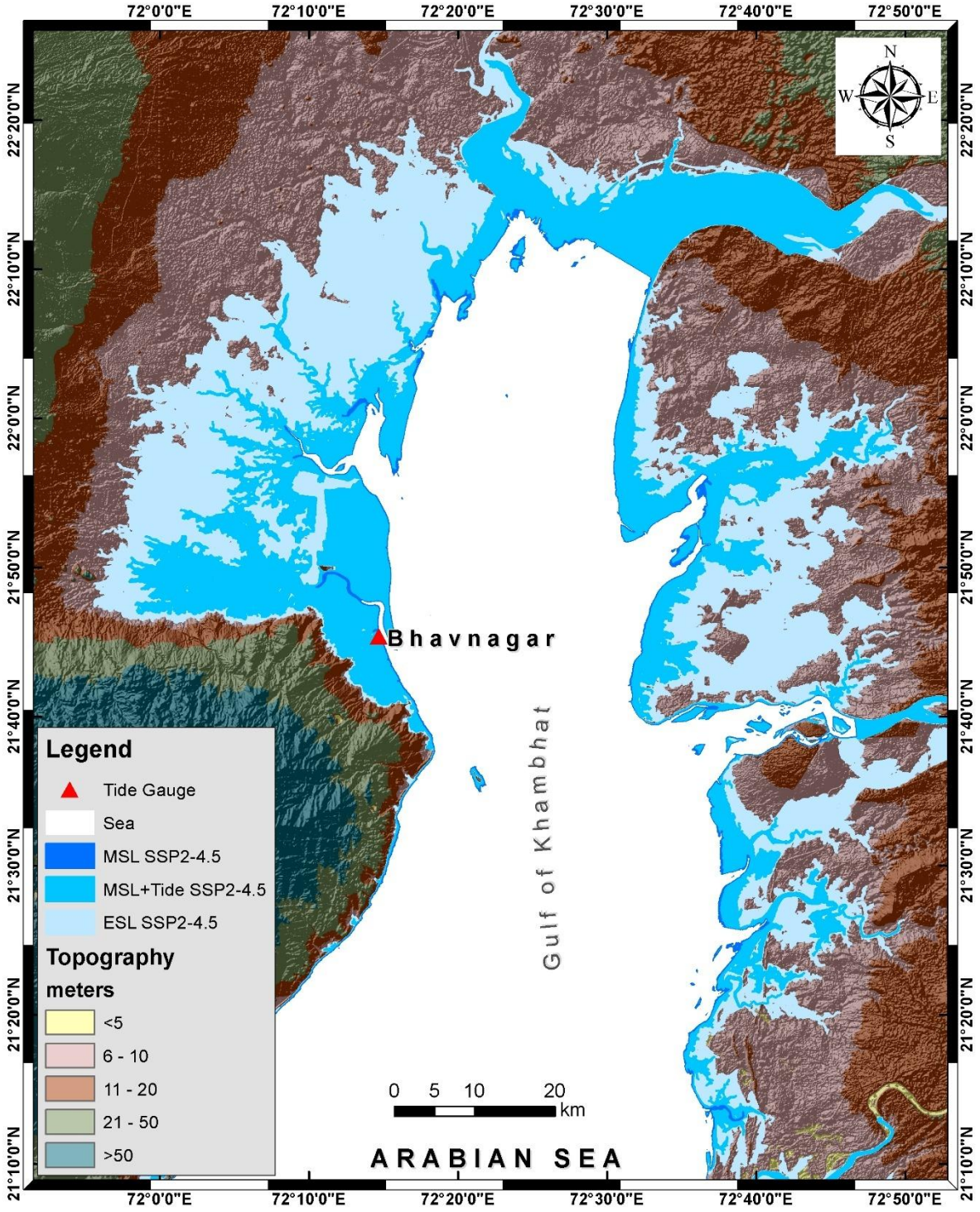
72°0'0"E
72°10'0"E
72°20'0"E
72°30'0"E
72°40'0"E
72°50'0"E
22°20'0"N
22°10'0"N
22°0'0"N
21°50'0"N
21°40'0"N
21°30'0"N
21°20'0"N
21°10'0"N
N
W
E
S
Bhavnagar
Gulf of Khambhat
ARABIAN SEA
0 5 10 20
km
Legend
Tide Gauge
Sea
MSL SSP2-4.5
MSL+Tide SSP2-4.5
ESL SSP2-4.5
Topography
meters
<5
6 - 10
11 - 20
21 - 50
>50

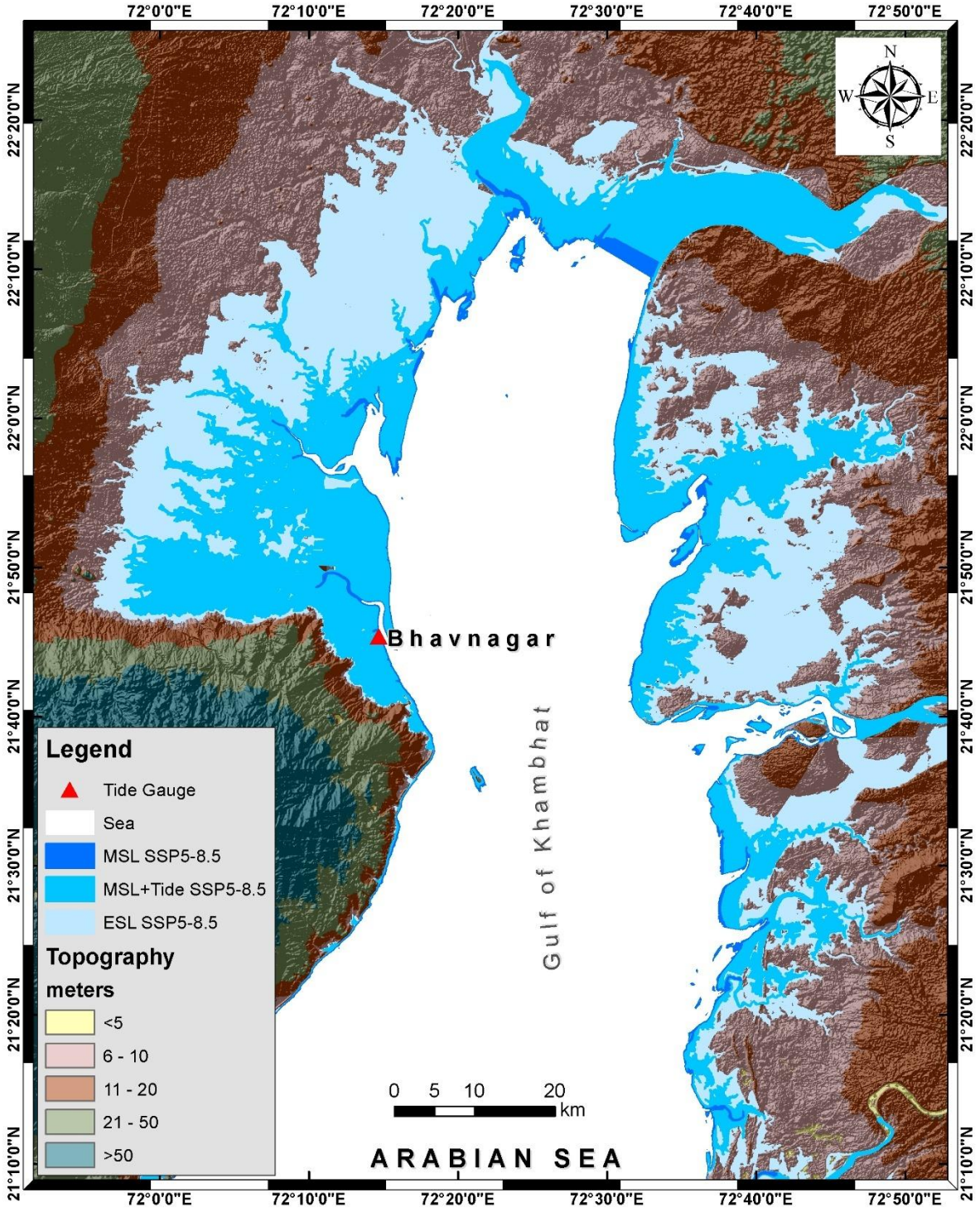
72°0'0"E
72°10'0"E
72°20'0"E
72°30'0"E
72°40'0"E
72°50'0"E
22°20'0"N
22°10'0"N
22°0'0"N
21°50'0"N
21°40'0"N
21°30'0"N
21°20'0"N
21°10'0"N
N
W
E
S
Bhavnagar
Gulf of Khambhat
ARABIAN SEA
0 5 10 20
km
Legend
Tide Gauge
Sea
MSL SSP5-8.5
MSL+Tide SSP5-8.5
ESL SSP5-8.5
Topography
meters
<5
6 - 10
11 - 20
21 - 50
>50

2. **Mumbai (Maharashtra)**

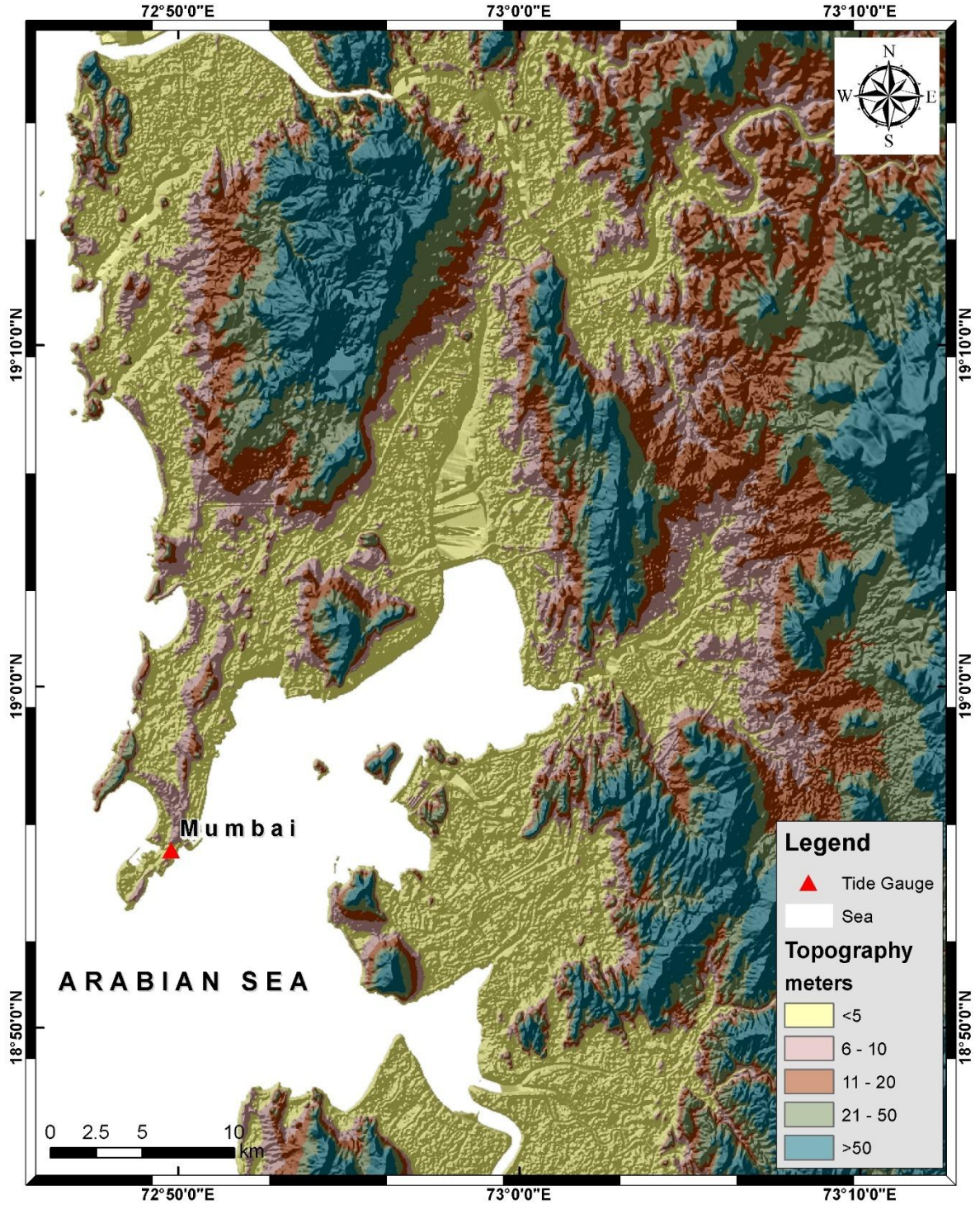

Basemap

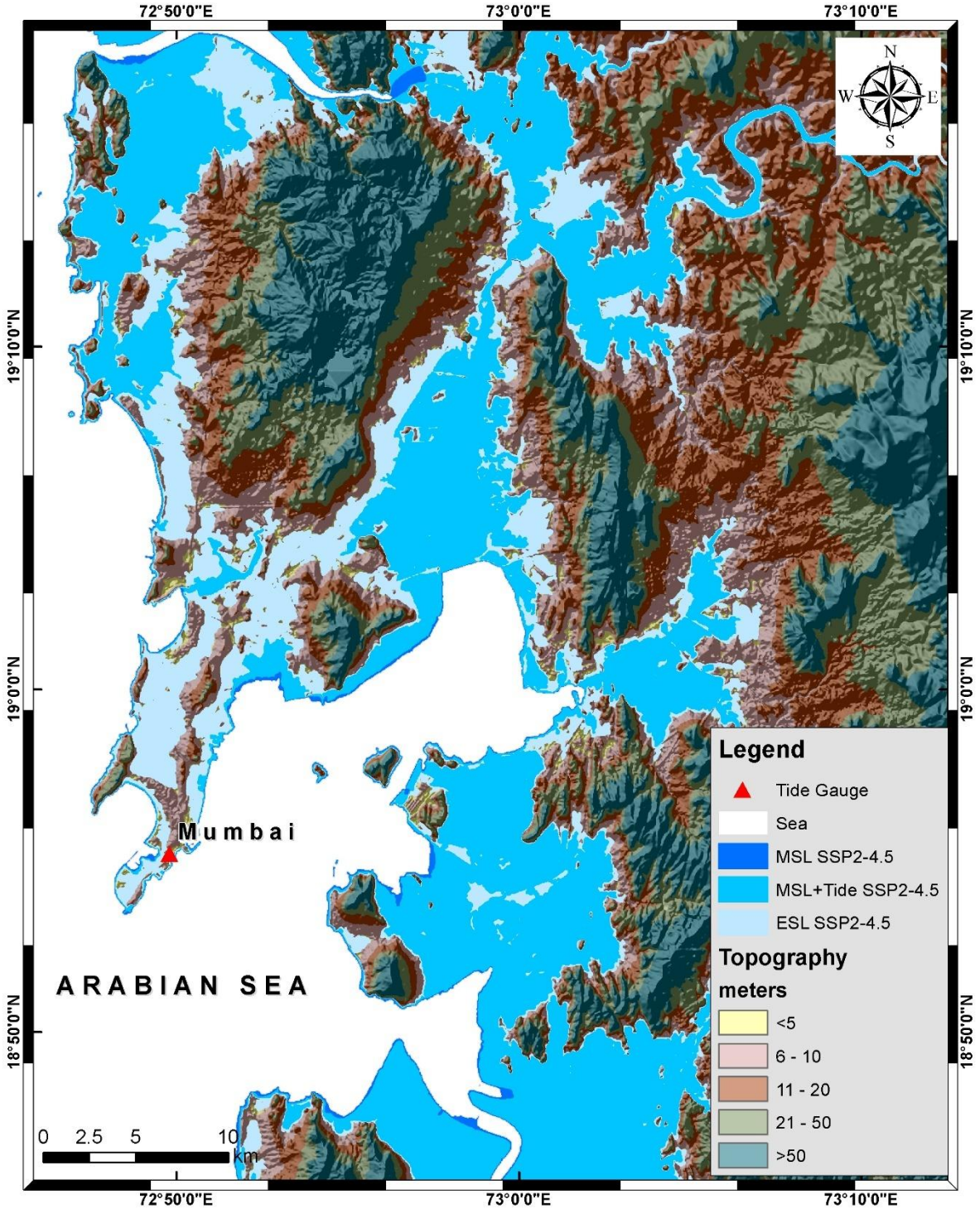
72°50'0"E
73°0'0"E
73°10'0"E
19°10'0"N
19°0'0"N
18°50'0"N
N
W
E
S
Mumbai
ARABIAN SEA
0 2.5 5 10
km
Legend
Tide Gauge
Sea
MSL SSP2-4.5
MSL+Tide SSP2-4.5
ESL SSP2-4.5
Topography
meters
<5
6 - 10
11 - 20
21 - 50
>50

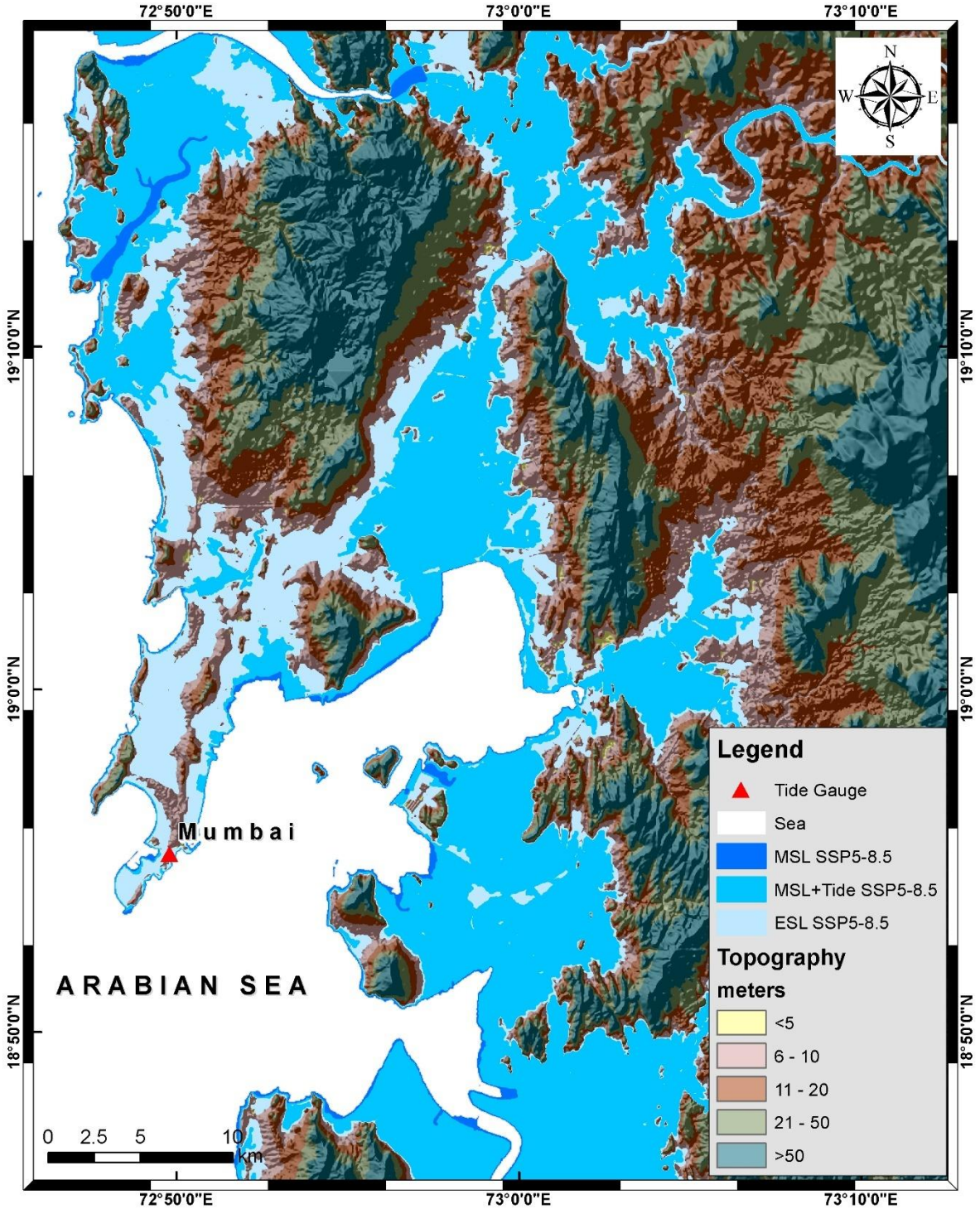
72°50'0"E
73°0'0"E
73°10'0"E
19°10'0"N
19°0'0"N
18°50'0"N
N
W
E
S
Mumbai
ARABIAN SEA
0 2.5 5 10
km
Legend
Tide Gauge
Sea
MSL SSP5-8.5
MSL+Tide SSP5-8.5
ESL SSP5-8.5
Topography
meters
<5
6 - 10
11 - 20
21 - 50
>50

3. Mormugao (Goa)

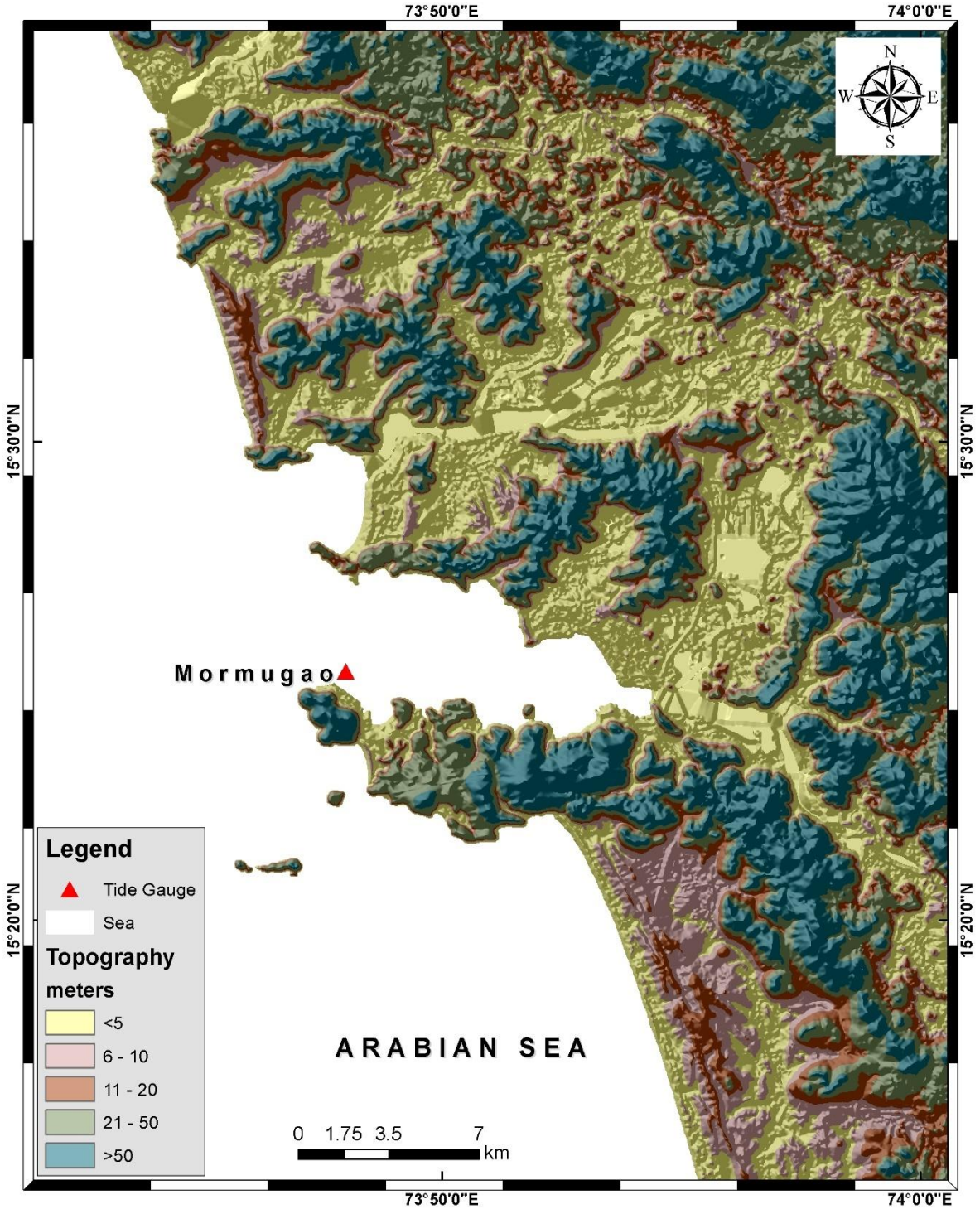

Basemap

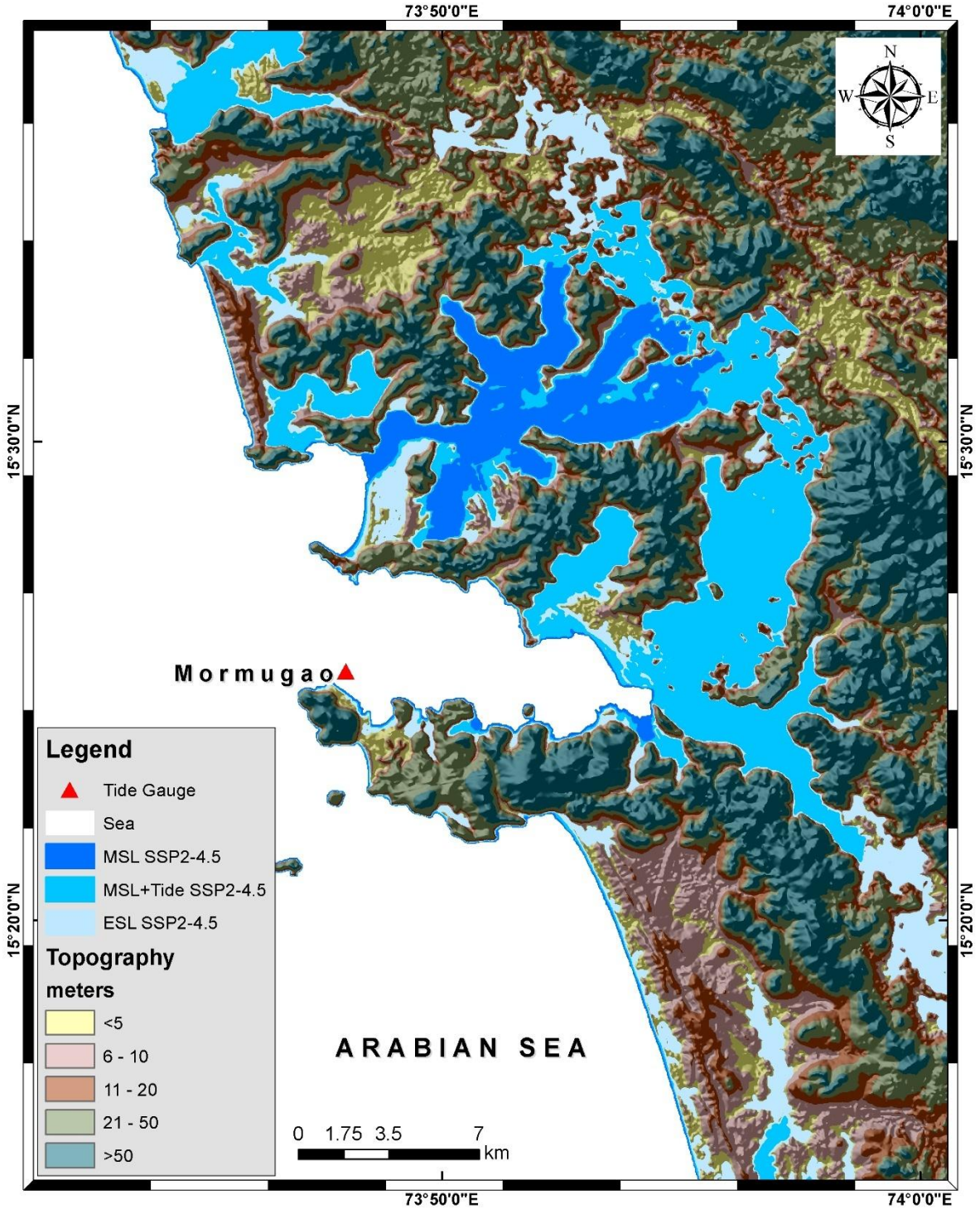
73°50'0"E
74°0'0"E
15°30'0"N
15°20'0"N
N
W
E
S
Mormugao
Legend
Tide Gauge
Sea
MSL SSP2-4.5
MSL+Tide SSP2-4.5
ESL SSP2-4.5
Topography
meters
<5
6 - 10
11 - 20
21 - 50
>50
ARABIAN SEA
0 1.75 3.5 7
km

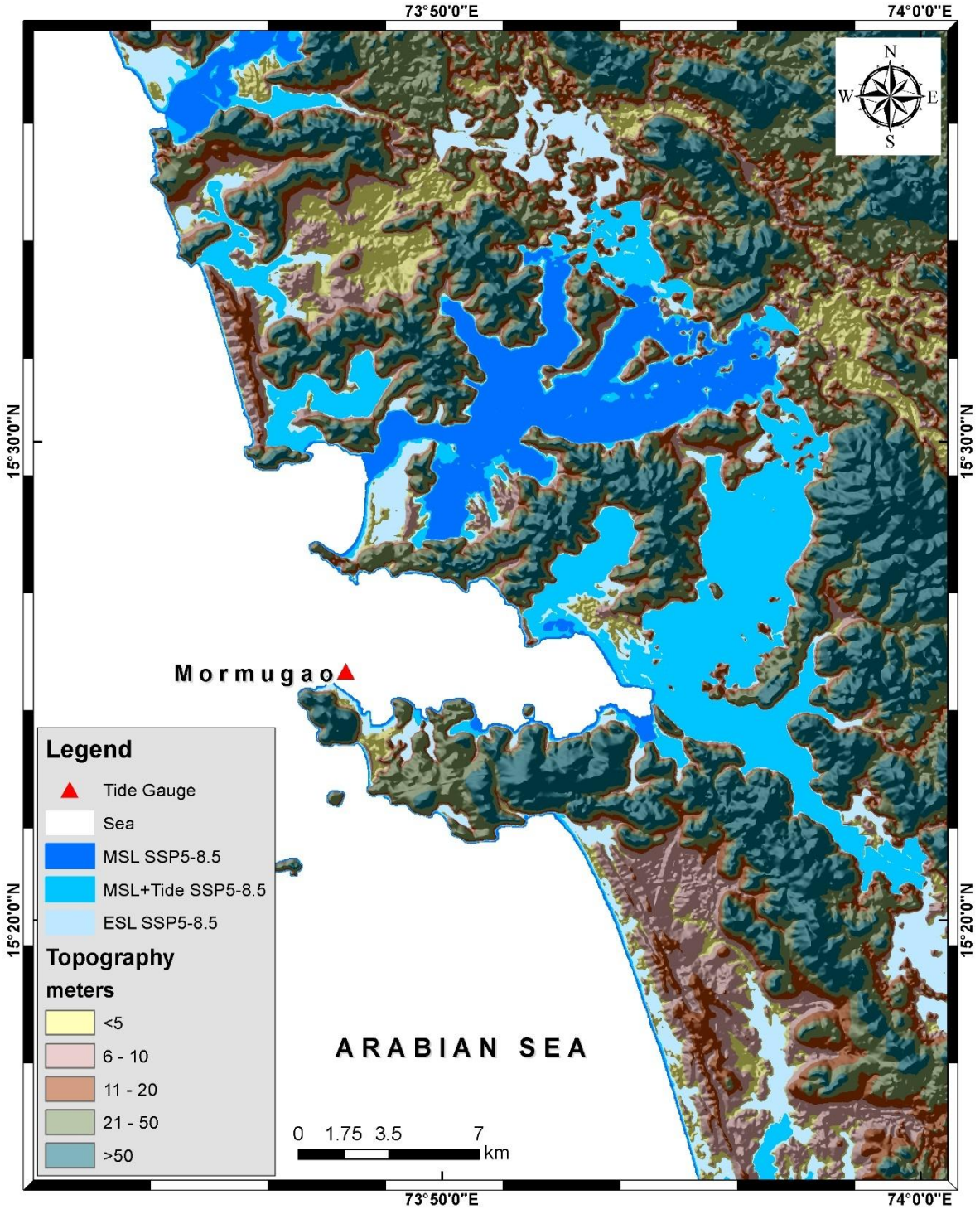
73°50'0"E
74°0'0"E
15°30'0"N
15°20'0"N
N
W
E
S
Mormugao
Legend
Tide Gauge
Sea
MSL SSP5-8.5
MSL+Tide SSP5-8.5
ESL SSP5-8.5
Topography
meters
<5
6 - 10
11 - 20
21 - 50
>50
ARABIAN SEA
0 1.75 3.5 7
km

4. Mangalore (Karnataka)

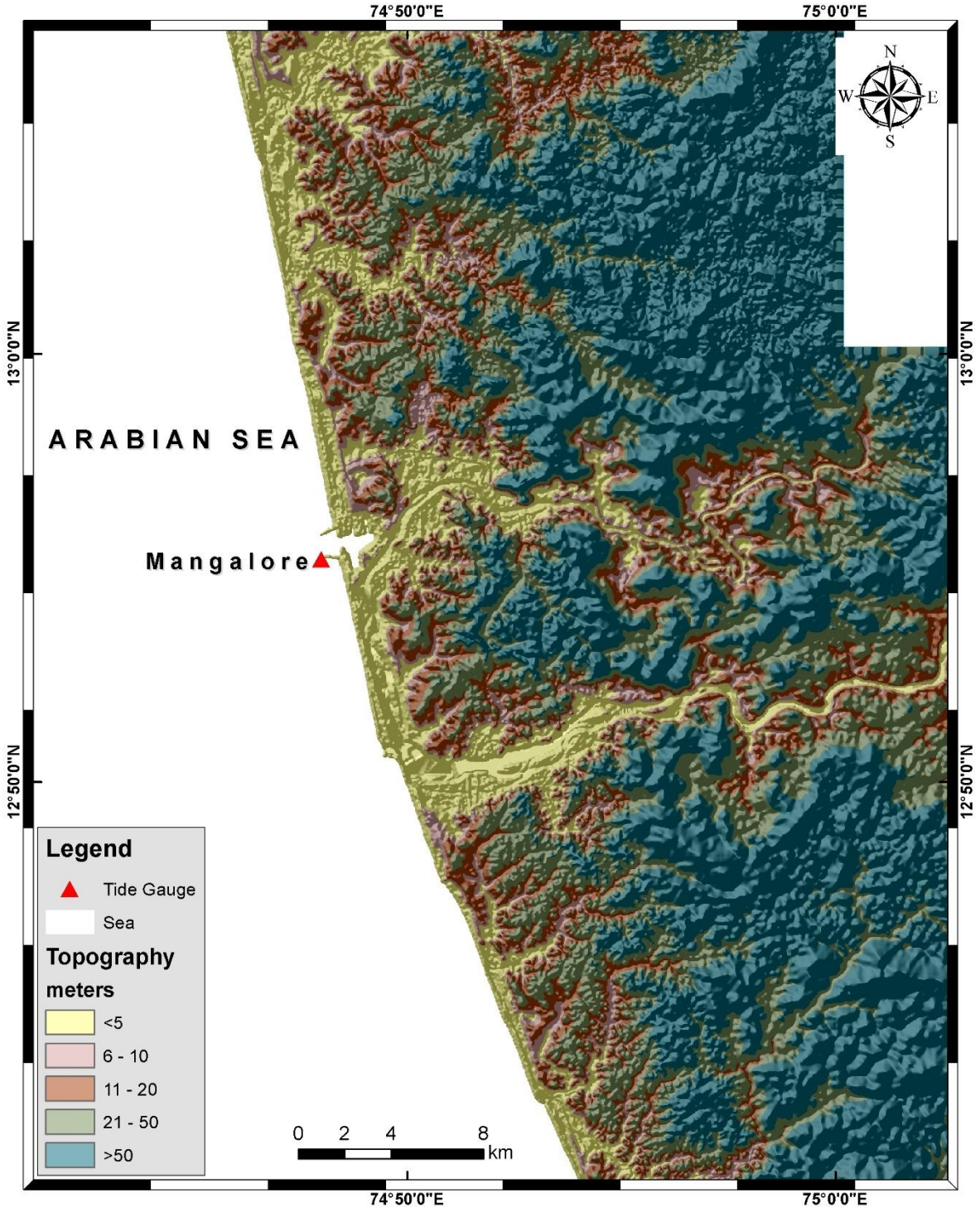

Basemap

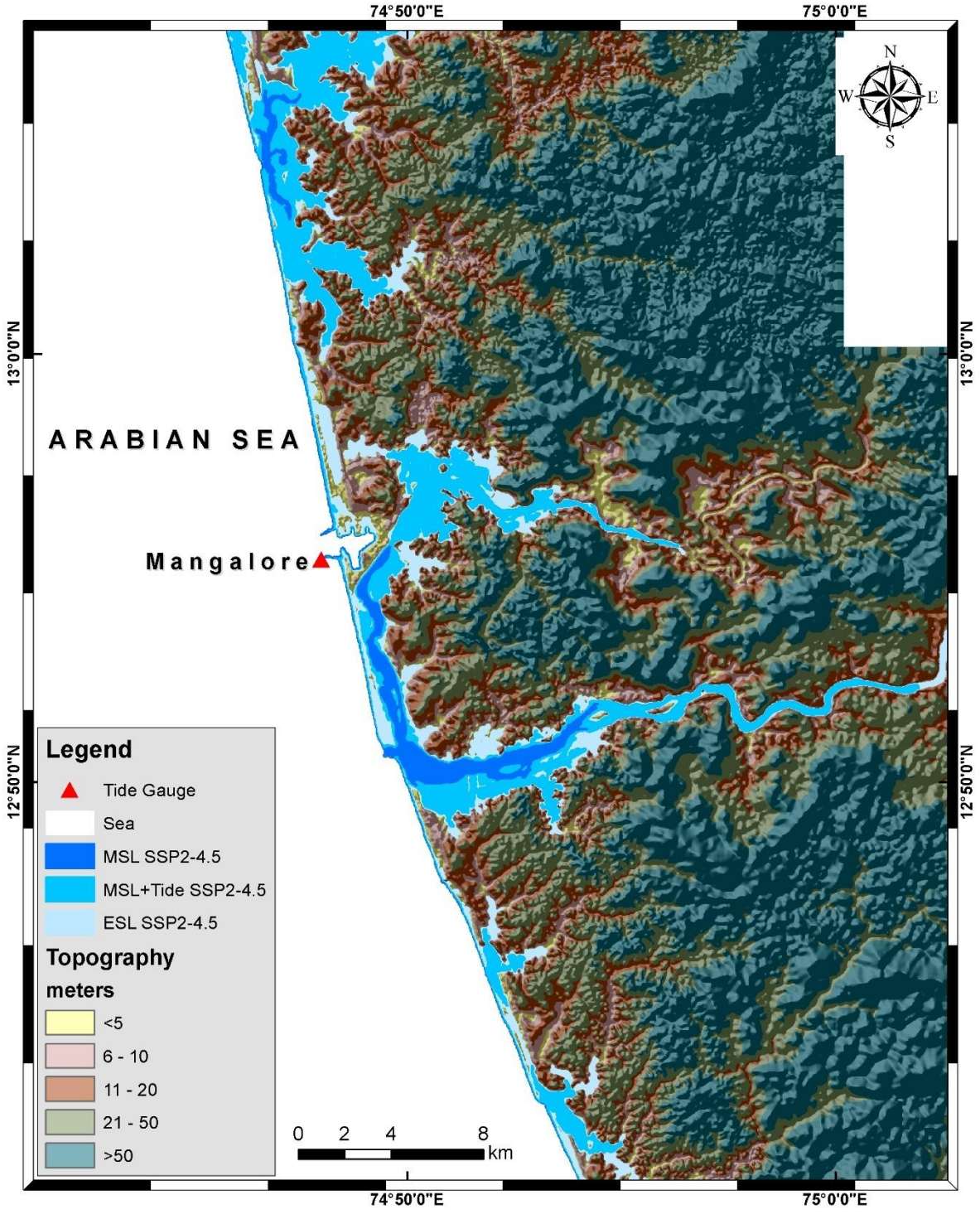
74°50'0"E
75°0'0"E
13°0'0"N
12°50'0"N
N
W
E
S
ARABIAN SEA
Mangalore
Legend
Tide Gauge
Sea
MSL SSP2-4.5
MSL+Tide SSP2-4.5
ESL SSP2-4.5
Topography
meters
<5
6 - 10
11 - 20
21 - 50
>50
0 2 4 8
km

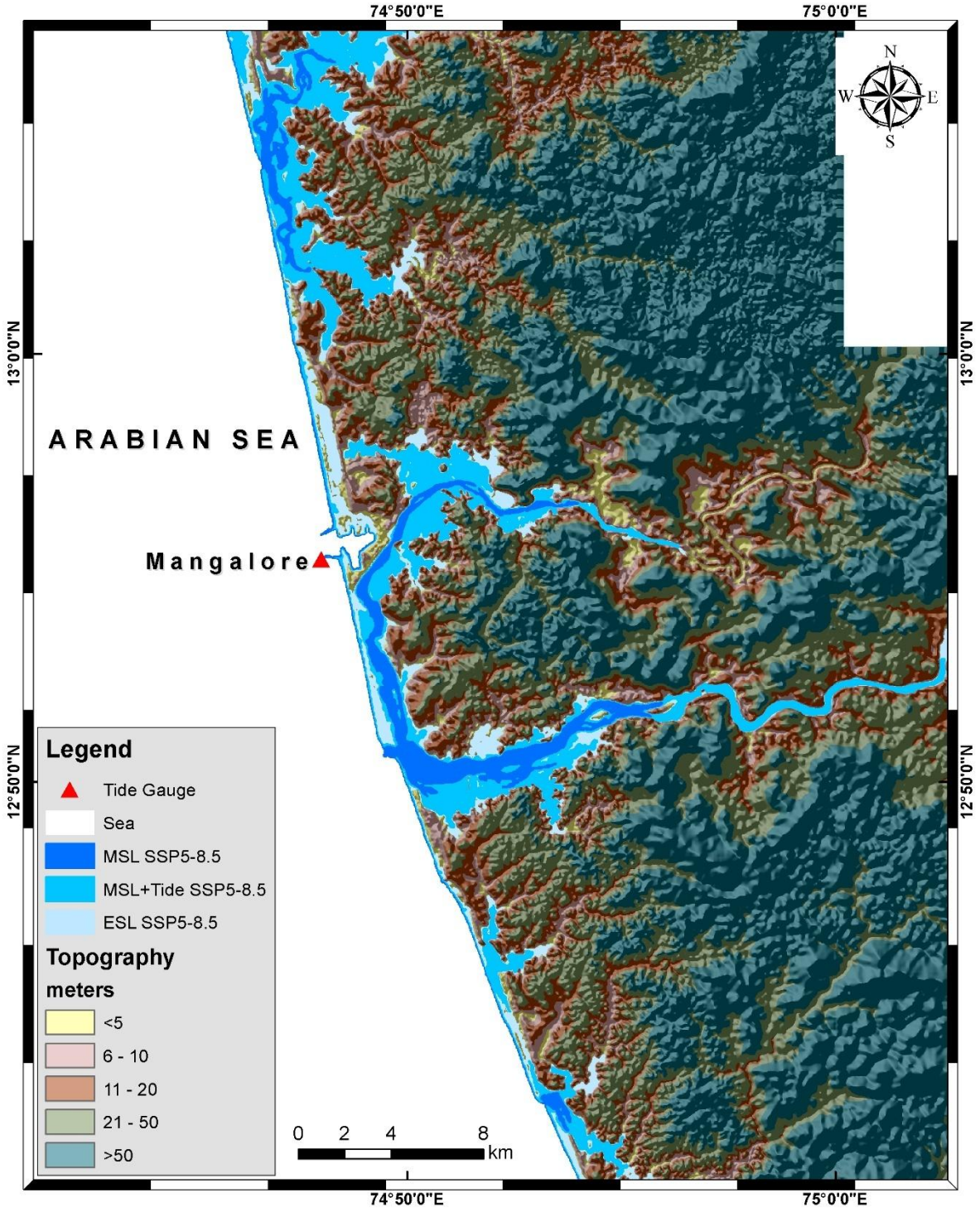
74°50'0"E
75°0'0"E
13°0'0"N
12°50'0"N
N
W
E
S
ARABIAN SEA
Mangalore
Legend
Tide Gauge
Sea
MSL SSP5-8.5
MSL+Tide SSP5-8.5
ESL SSP5-8.5
Topography
meters
<5
6 - 10
11 - 20
21 - 50
>50
0 2 4 8
km

5. Cochin (Kerala)

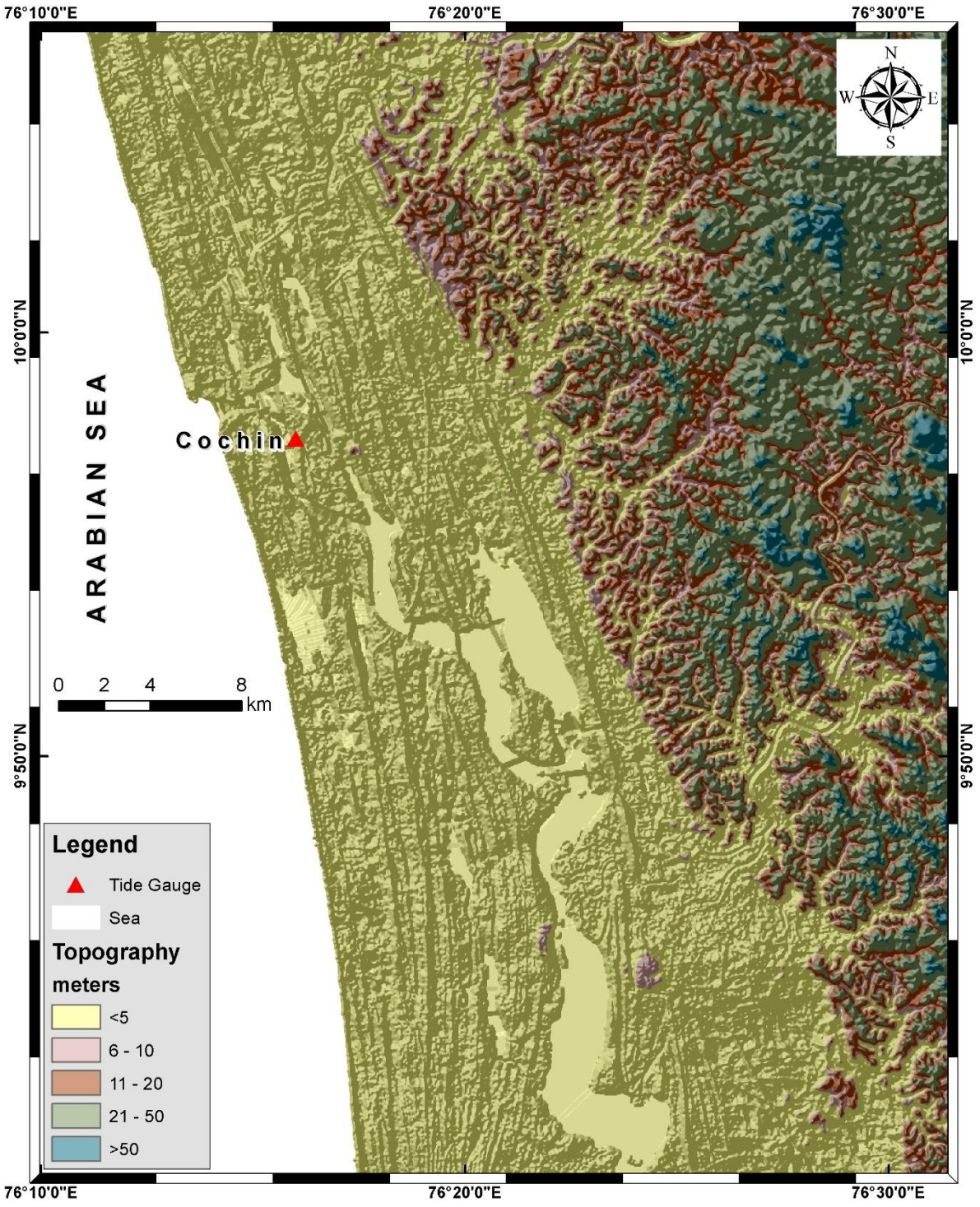

Basemap

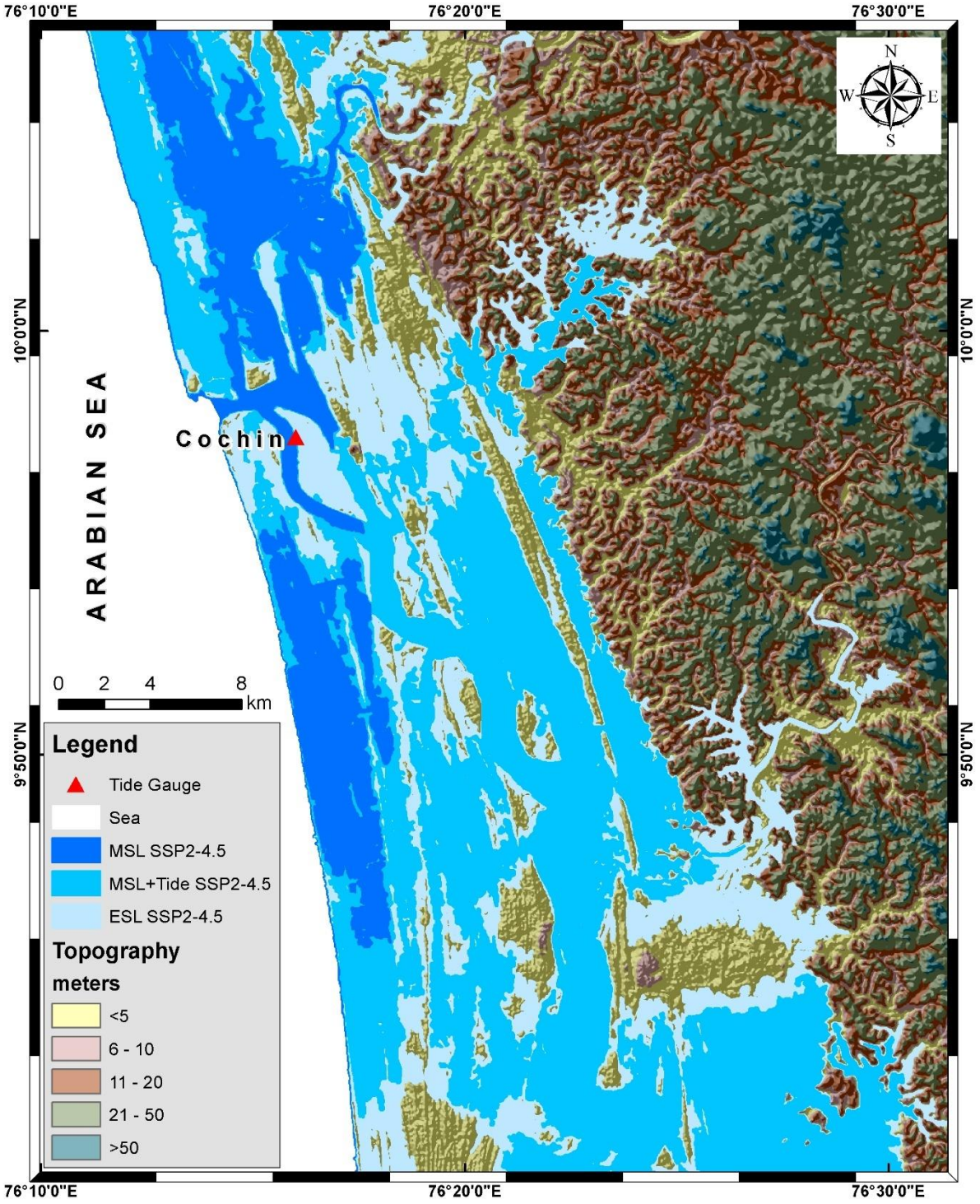
76°10'0"E
76°20'0"E
76°30'0"E
10°0'0"N
9°50'0"N
N
W
E
S
ARABIAN SEA
Cochin
0 2 4 8
km
Legend
Tide Gauge
Sea
MSL SSP2-4.5
MSL+Tide SSP2-4.5
ESL SSP2-4.5
Topography
meters
<5
6 - 10
11 - 20
21 - 50
>50

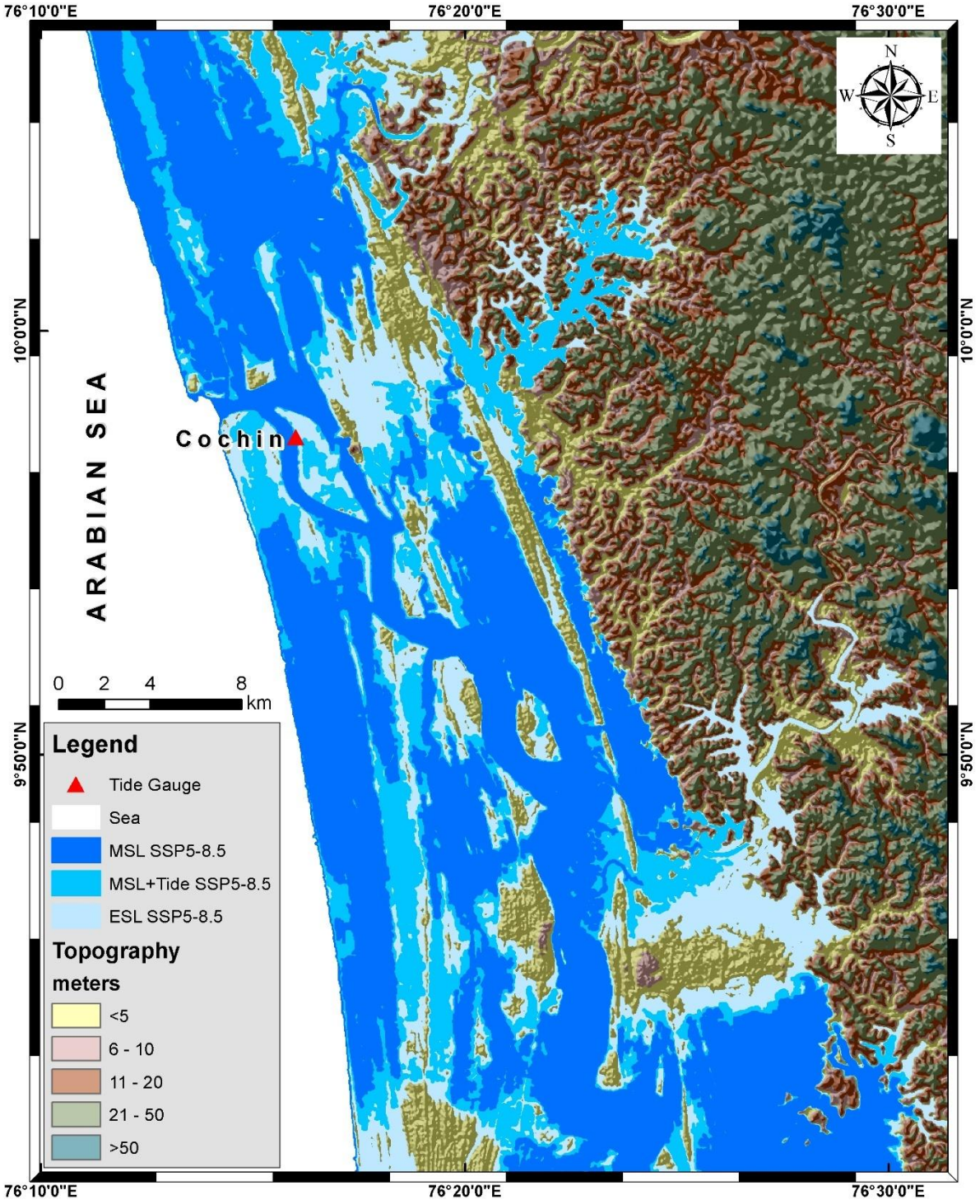
76°10'0"E
76°20'0"E
76°30'0"E
10°0'0"N
9°50'0"N
N
W
E
S
ARABIAN SEA
Cochin
0 2 4 8
km
Legend
Tide Gauge
Sea
MSL SSP5-8.5
MSL+Tide SSP5-8.5
ESL SSP5-8.5
Topography
meters
<5
6 - 10
11 - 20
21 - 50
>50

6. Chennai (Tamil Nadu)

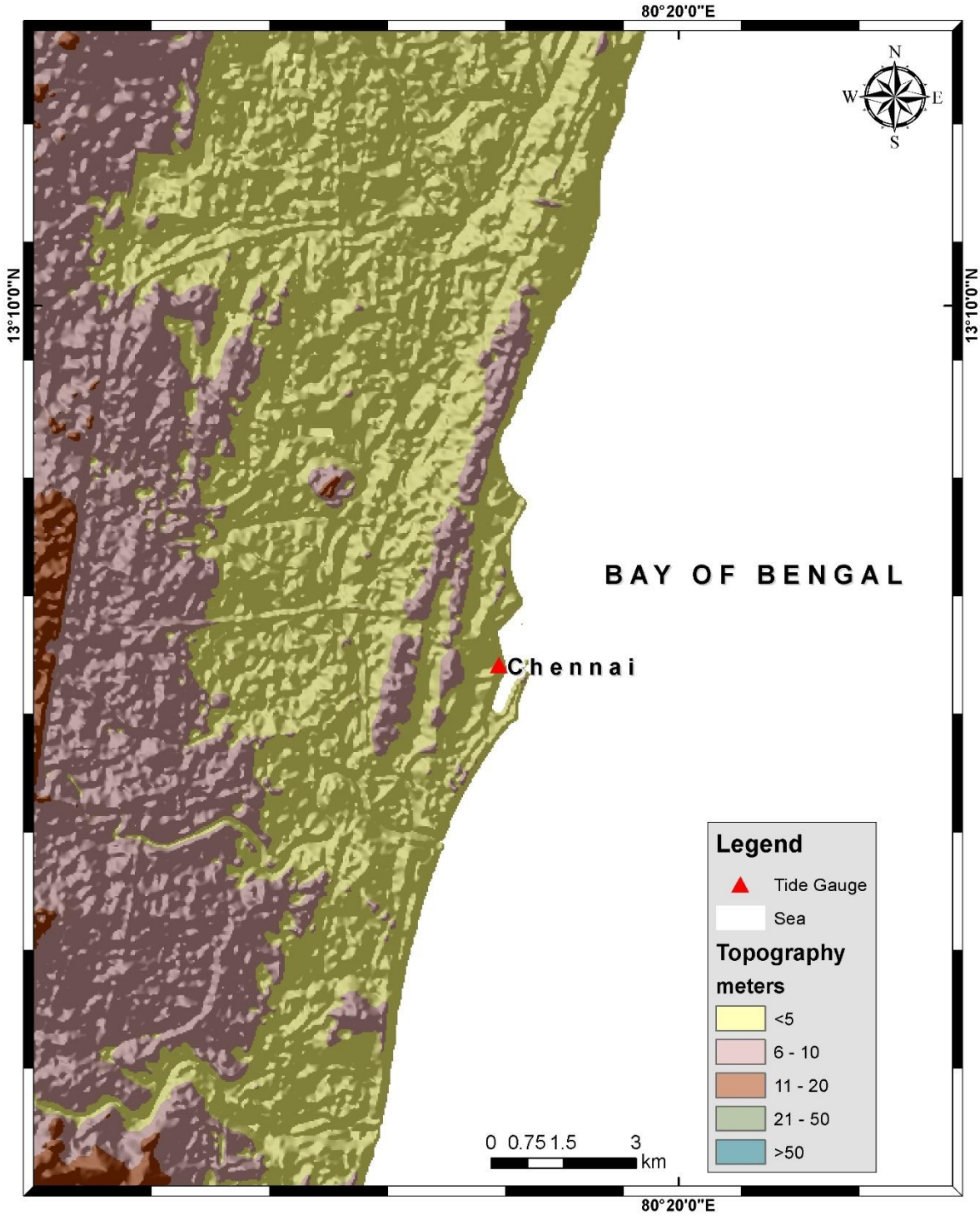

Basemap

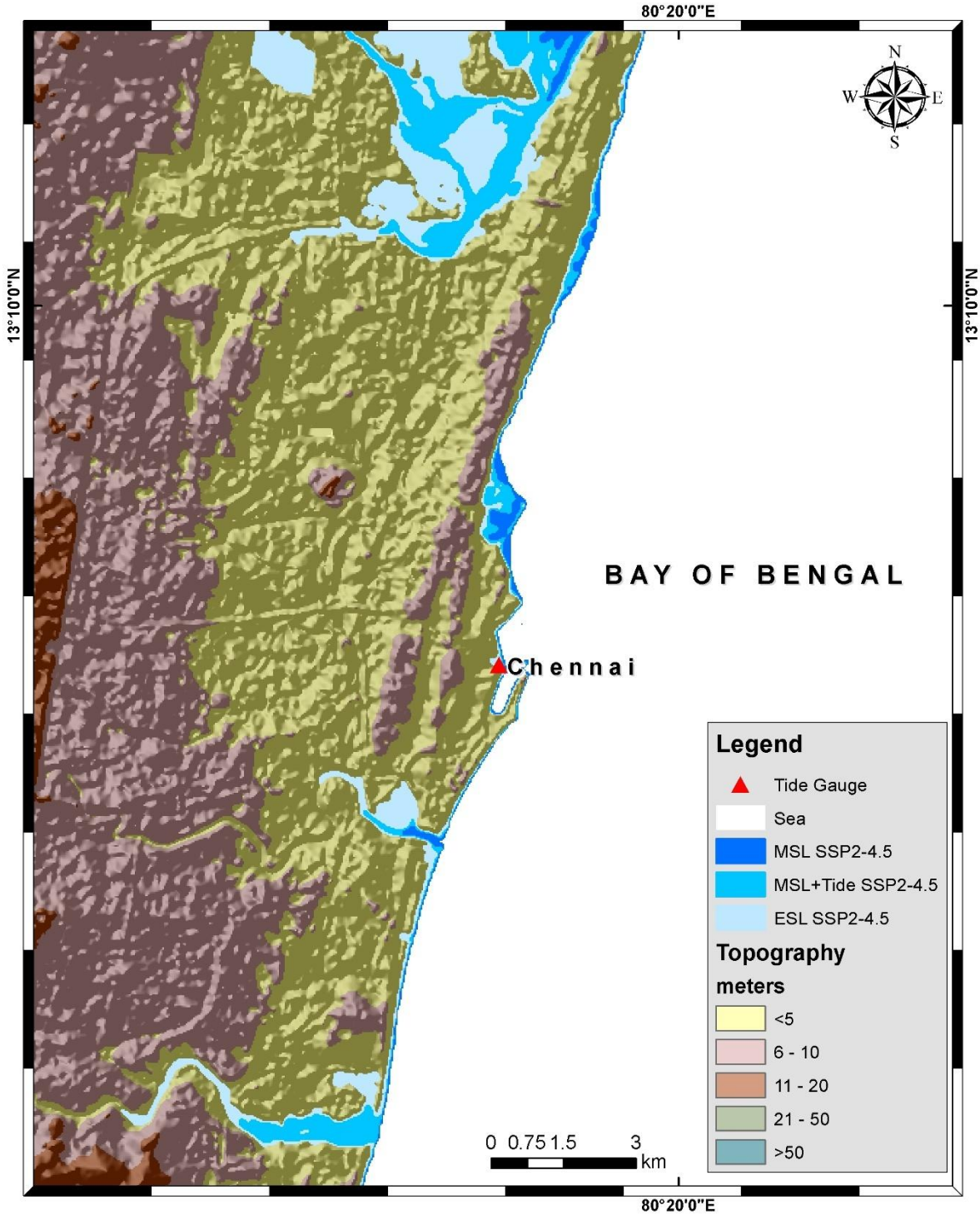
80°20'0"E
13°10'0"N
N
W
E
S
BAY OF BENGAL
Chennai
Legend
Tide Gauge
Sea
MSL SSP2-4.5
MSL+Tide SSP2-4.5
ESL SSP2-4.5
Topography
meters
<5
6 - 10
11 - 20
21 - 50
>50
0 0.75 1.5 3
km
80°20'0"E

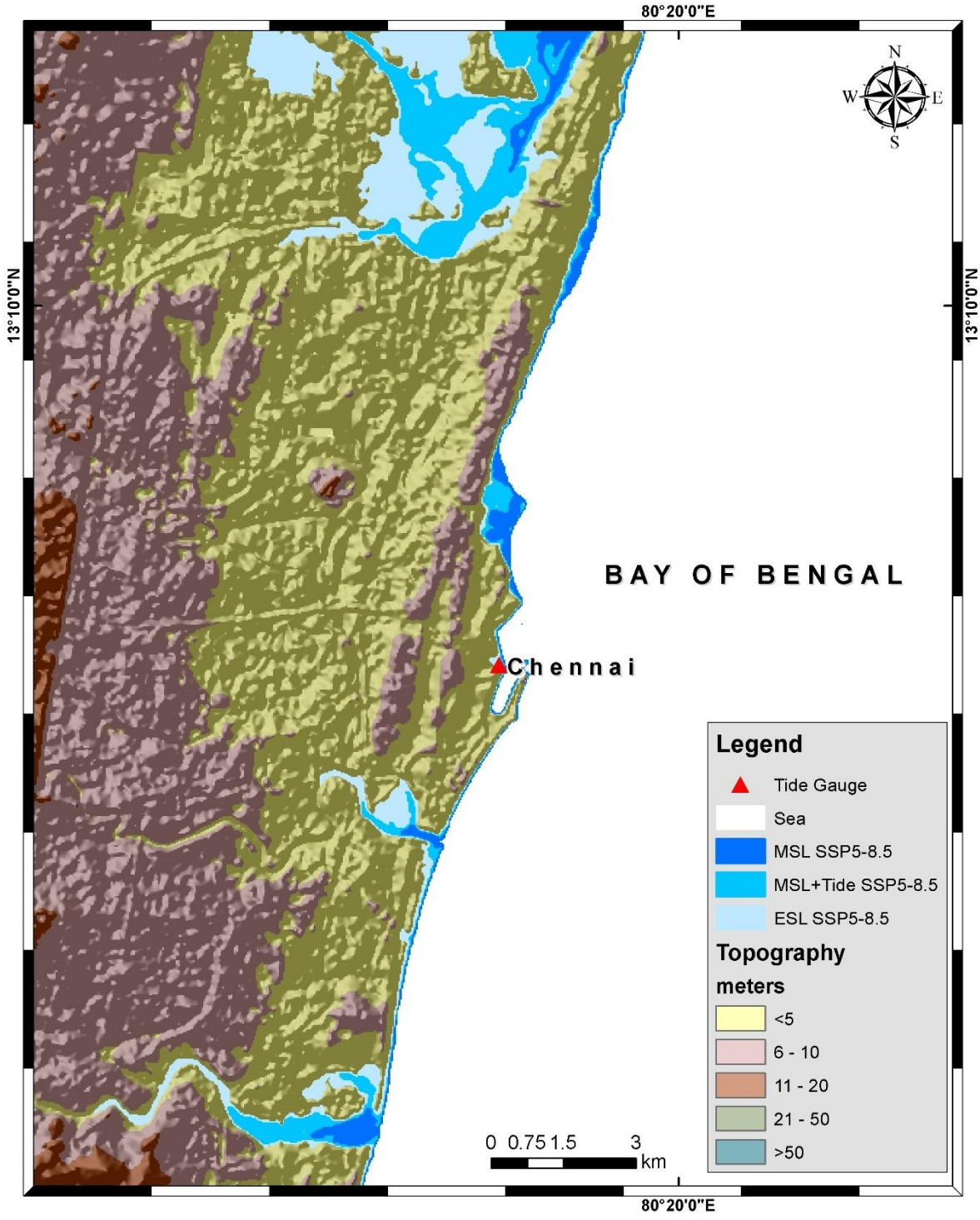
80°20'0"E
13°10'0"N
N
W
E
S
BAY OF BENGAL
Chennai
Legend
Tide Gauge
Sea
MSL SSP5-8.5
MSL+Tide SSP5-8.5
ESL SSP5-8.5
Topography
meters
<5
6 - 10
11 - 20
21 - 50
>50
0 0.75 1.5 3
km
80°20'0"E

7. Vishakhapatnam (Andhra Pradesh)

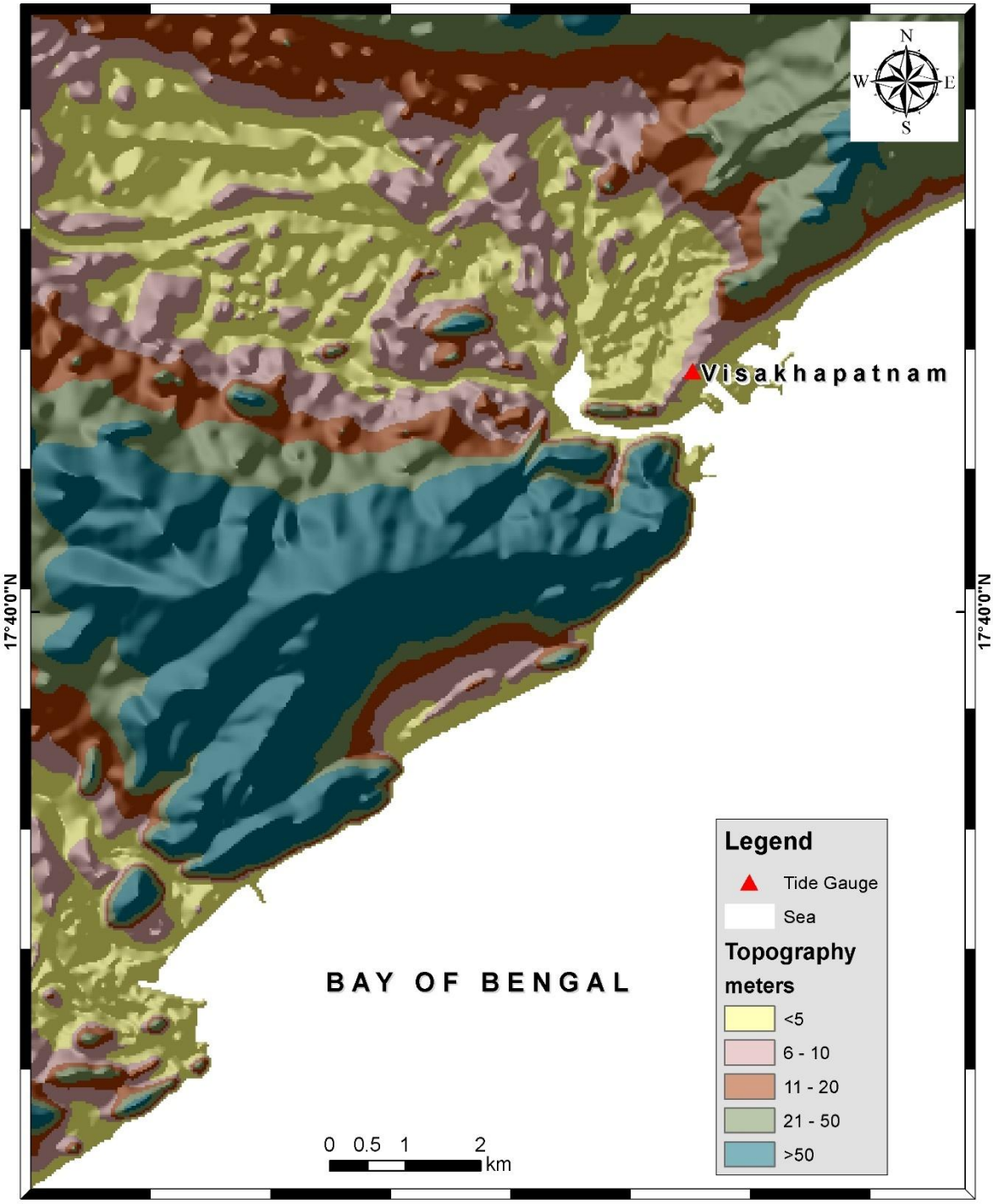

Basemap

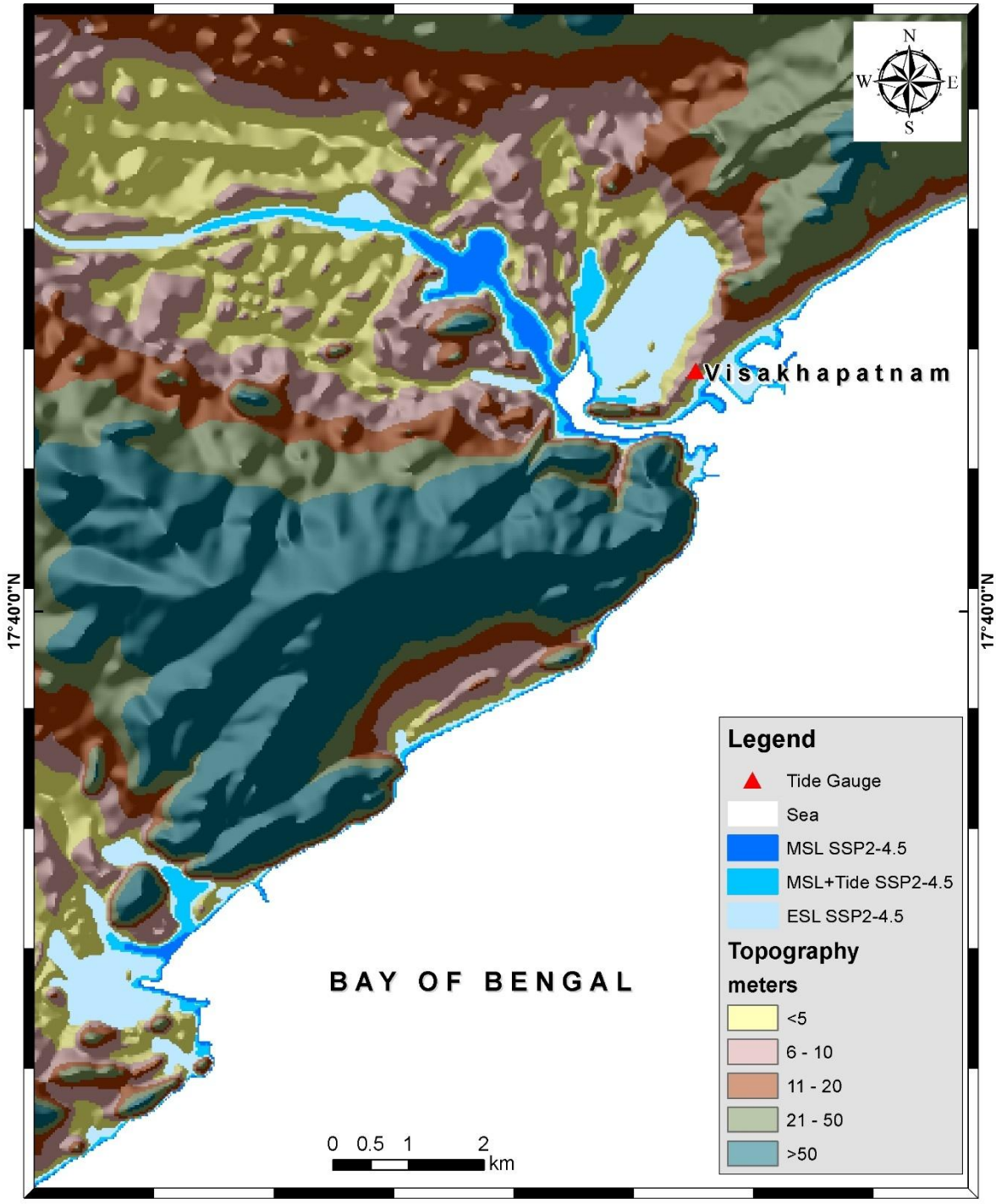
N
W
E
S
Visakhapatnam
17°40'0"N
17°40'0"N
BAY OF BENGAL
0 0.5 1 2
km
Legend
Tide Gauge
Sea
MSL SSP2-4.5
MSL+Tide SSP2-4.5
ESL SSP2-4.5
Topography
meters
<5
6 - 10
11 - 20
21 - 50
>50

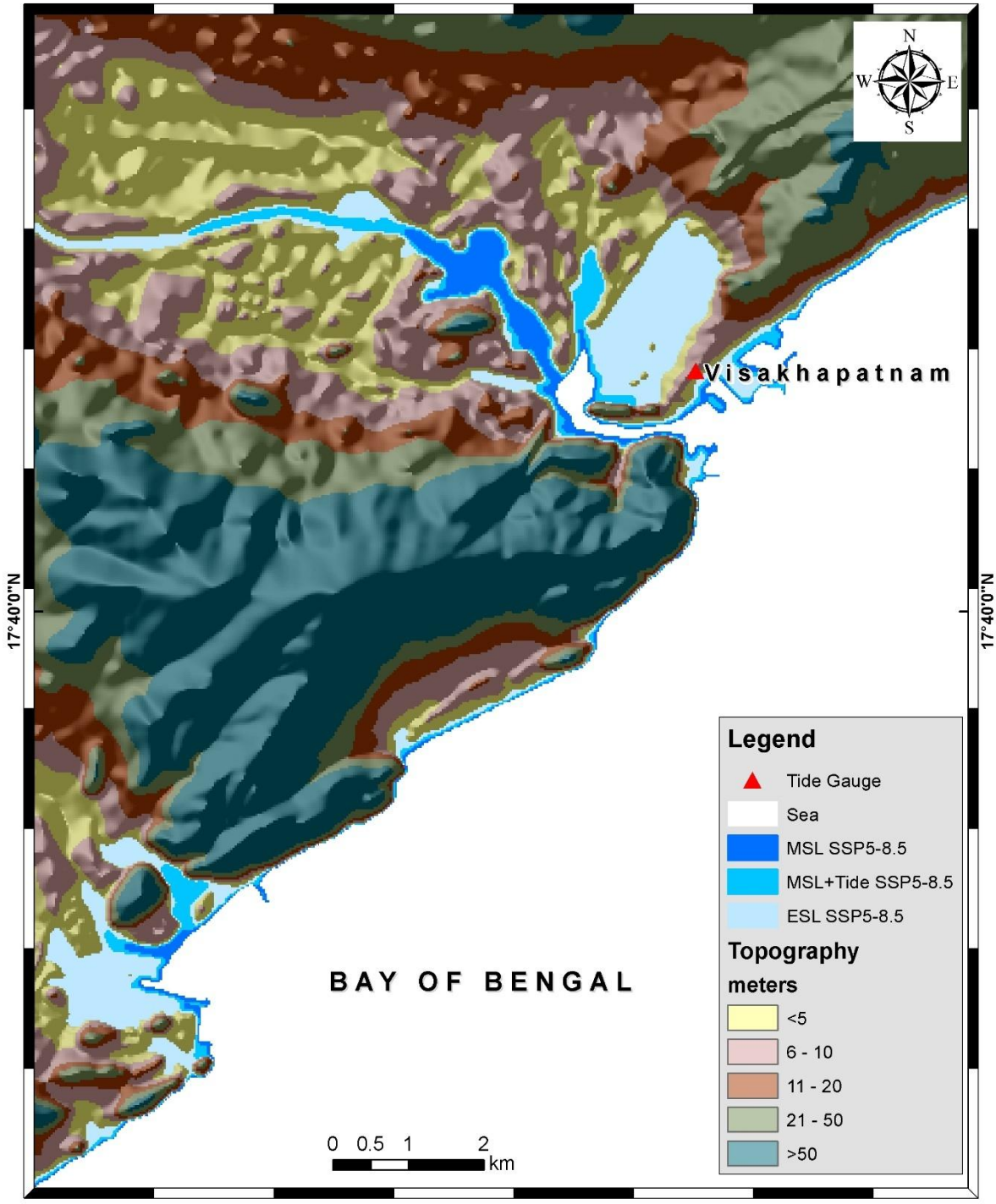
N
W
E
S
Visakhapatnam
17°40'0"N
17°40'0"N
BAY OF BENGAL
0 0.5 1 2
km
Legend
Tide Gauge
Sea
MSL SSP5-8.5
MSL+Tide SSP5-8.5
ESL SSP5-8.5
Topography
meters
<5
6 - 10
11 - 20
21 - 50
>50

8. Paradip (Odisha)

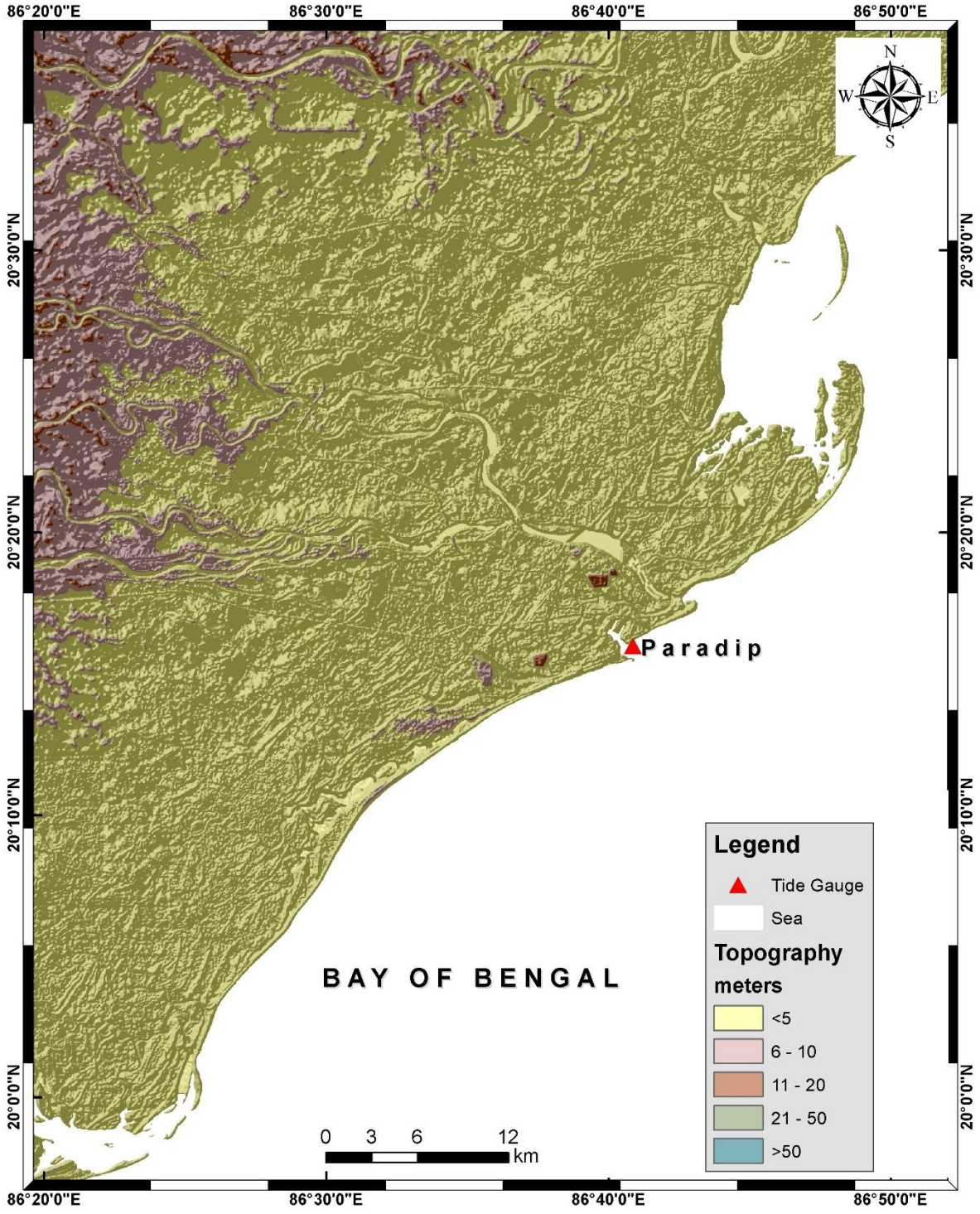

Basemap

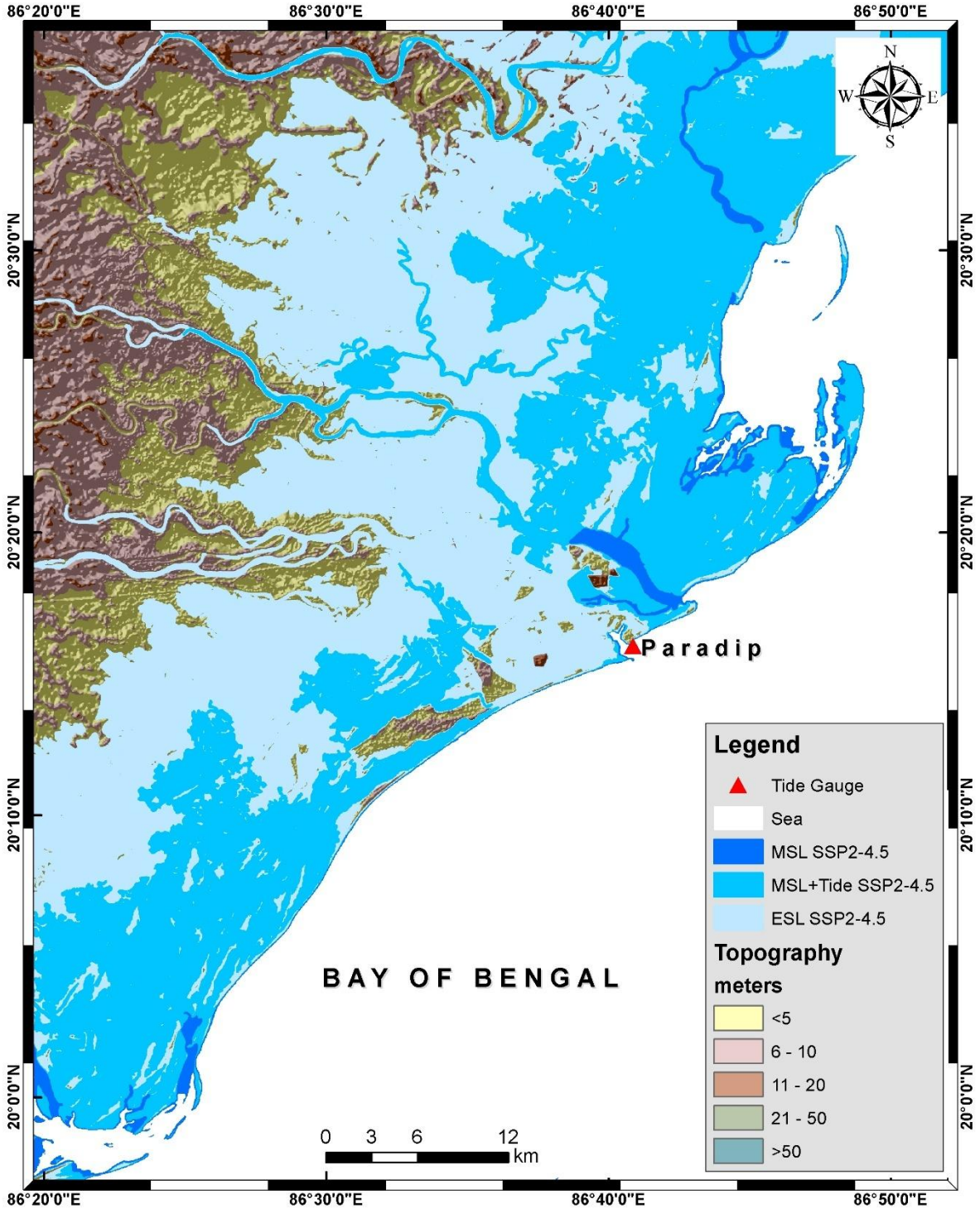
86°20'0"E
86°30'0"E
86°40'0"E
86°50'0"E
20°30'0"N
20°20'0"N
20°10'0"N
20°0'0"N
N
W
E
S
Paradip
BAY OF BENGAL
Legend
Tide Gauge
Sea
MSL SSP2-4.5
MSL+Tide SSP2-4.5
ESL SSP2-4.5
Topography
meters
<5
6 - 10
11 - 20
21 - 50
>50
0 3 6 12
km

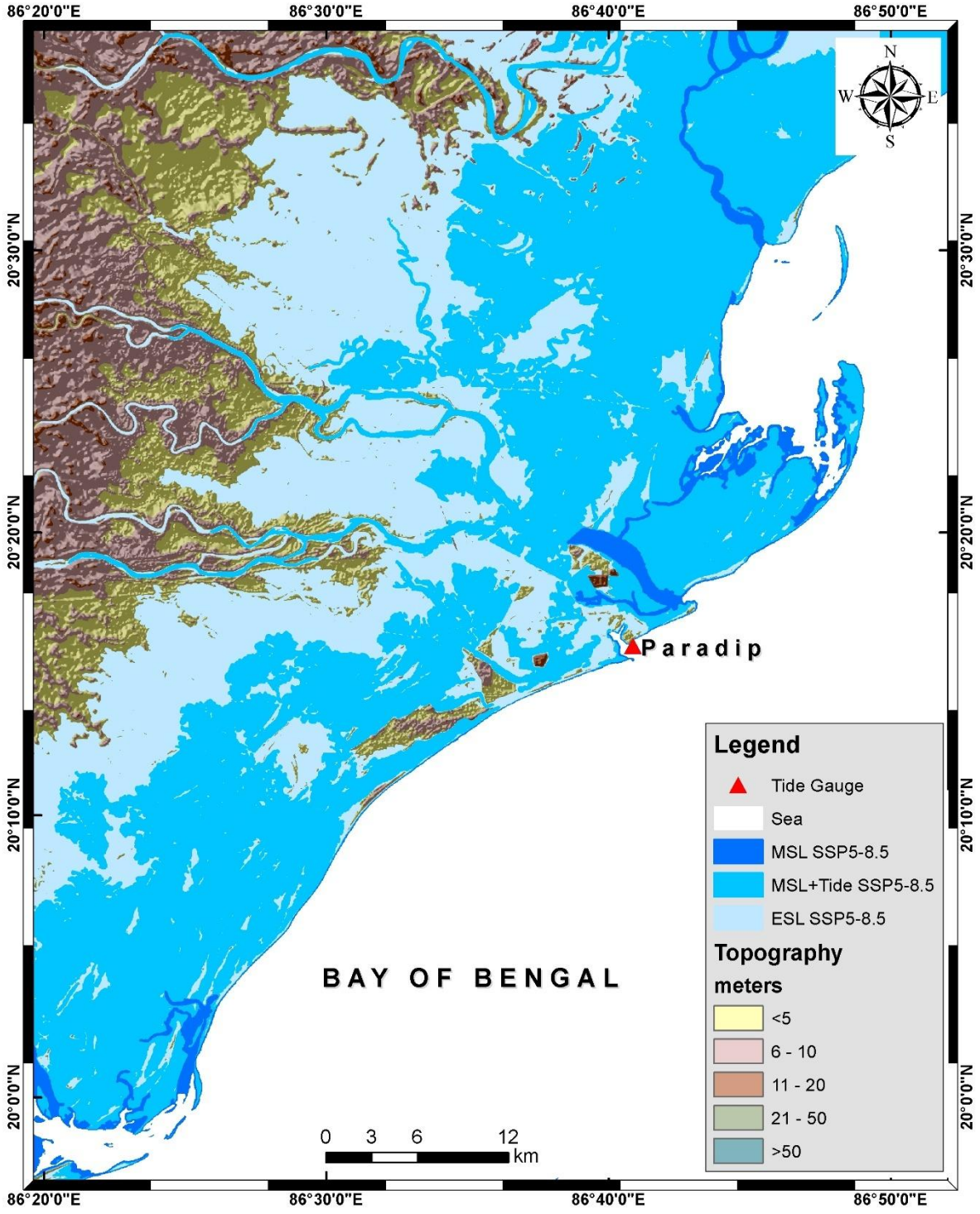
86°20'0"E
86°30'0"E
86°40'0"E
86°50'0"E
20°30'0"N
20°20'0"N
20°10'0"N
20°0'0"N
N
W
E
S
Paradip
BAY OF BENGAL
0 3 6 12
km
Legend
Tide Gauge
Sea
MSL SSP5-8.5
MSL+Tide SSP5-8.5
ESL SSP5-8.5
Topography
meters
<5
6 - 10
11 - 20
21 - 50
>50

9. Diamond Harbour (West Bengal)

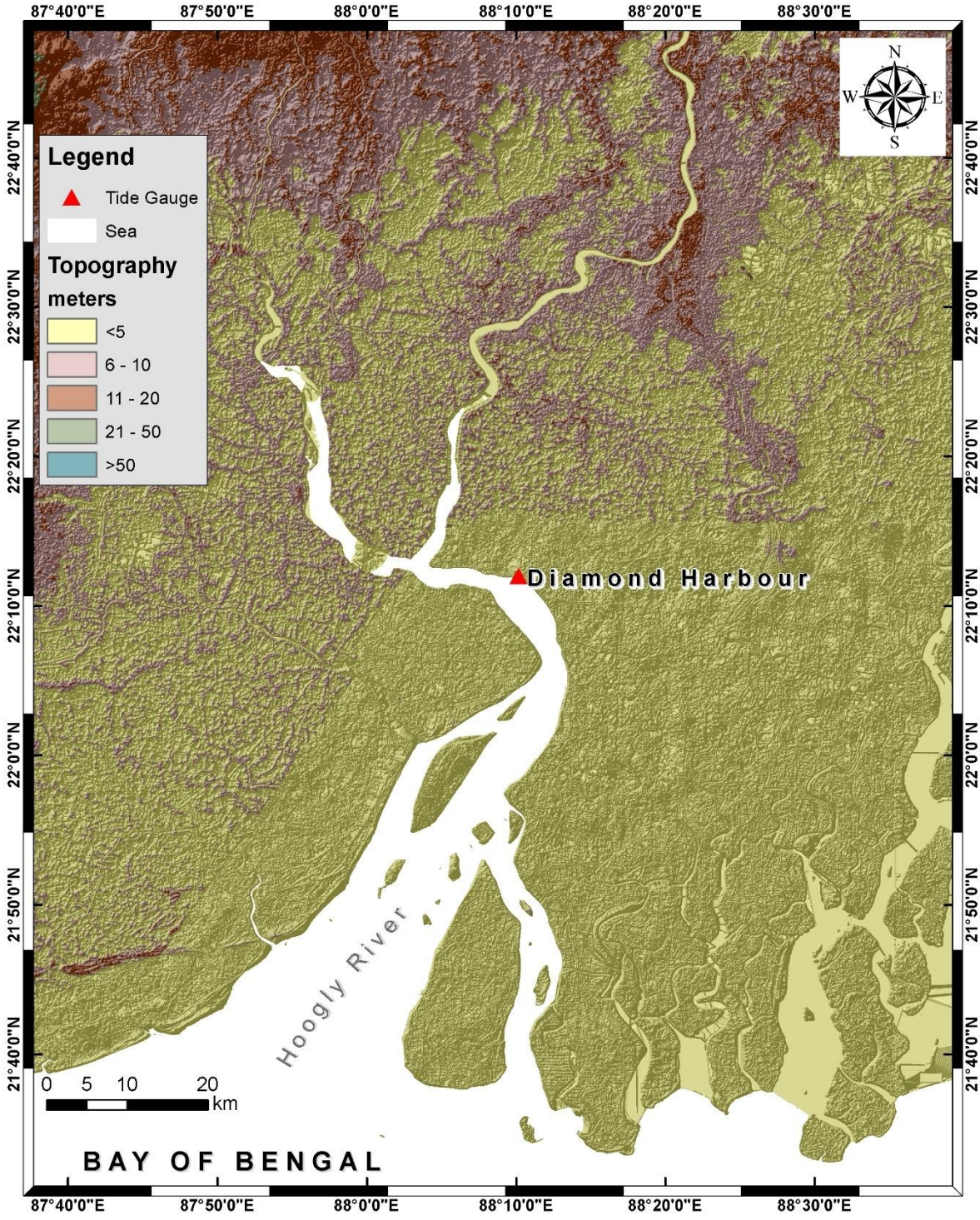

Basemap

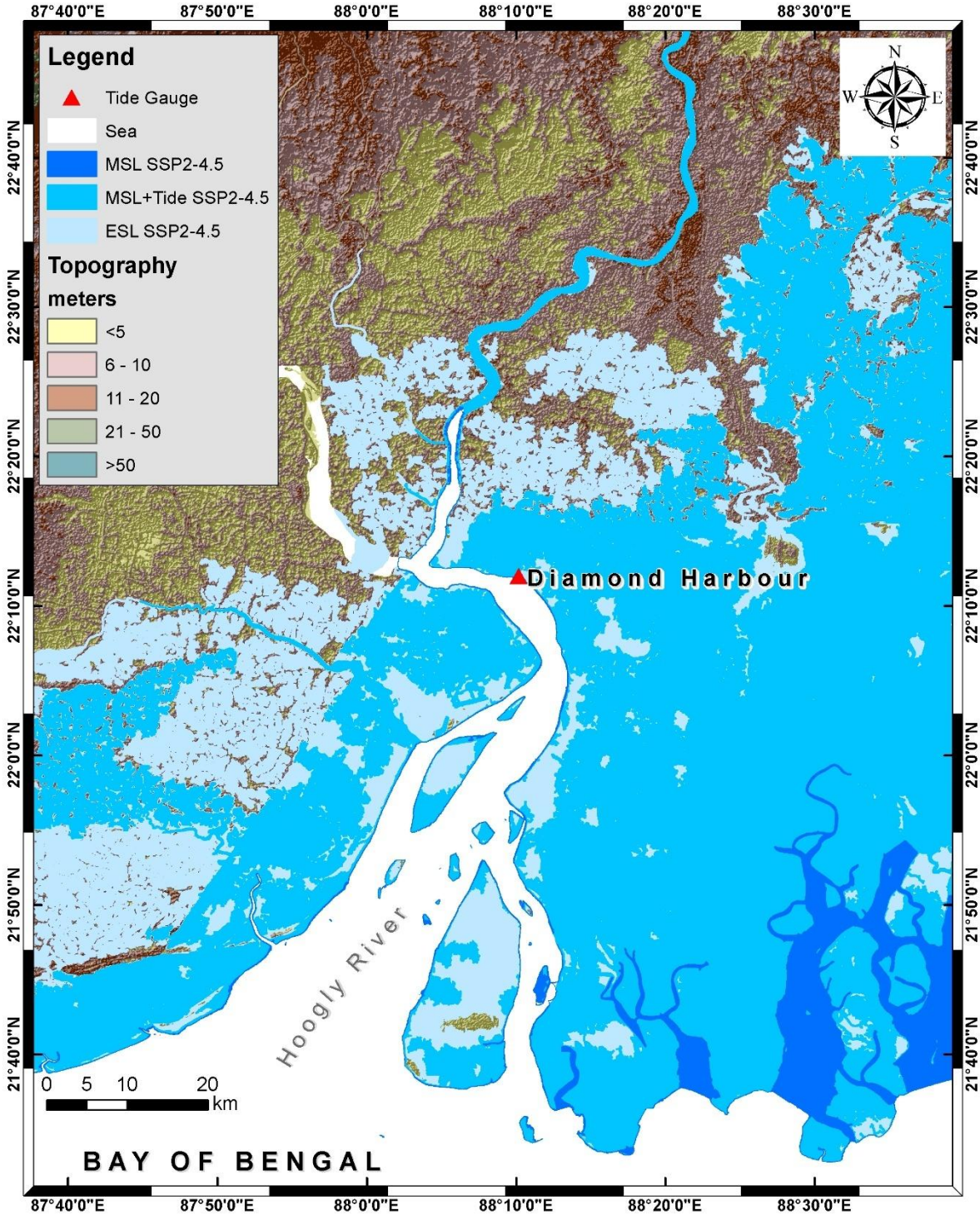
Legend
Tide Gauge
Sea
MSL SSP2-4.5
MSL+Tide SSP2-4.5
ESL SSP2-4.5
Topography
meters
<5
6 - 10
11 - 20
21 - 50
>50
N
W
E
S
Diamond Harbour
Hoogly River
0 5 10 20
km
BAY OF BENGAL
87°40'0"E
87°50'0"E
88°0'0"E
88°10'0"E
88°20'0"E
88°30'0"E
22°40'0"N
22°30'0"N
22°20'0"N
22°10'0"N
22°0'0"N
21°50'0"N
21°40'0"N

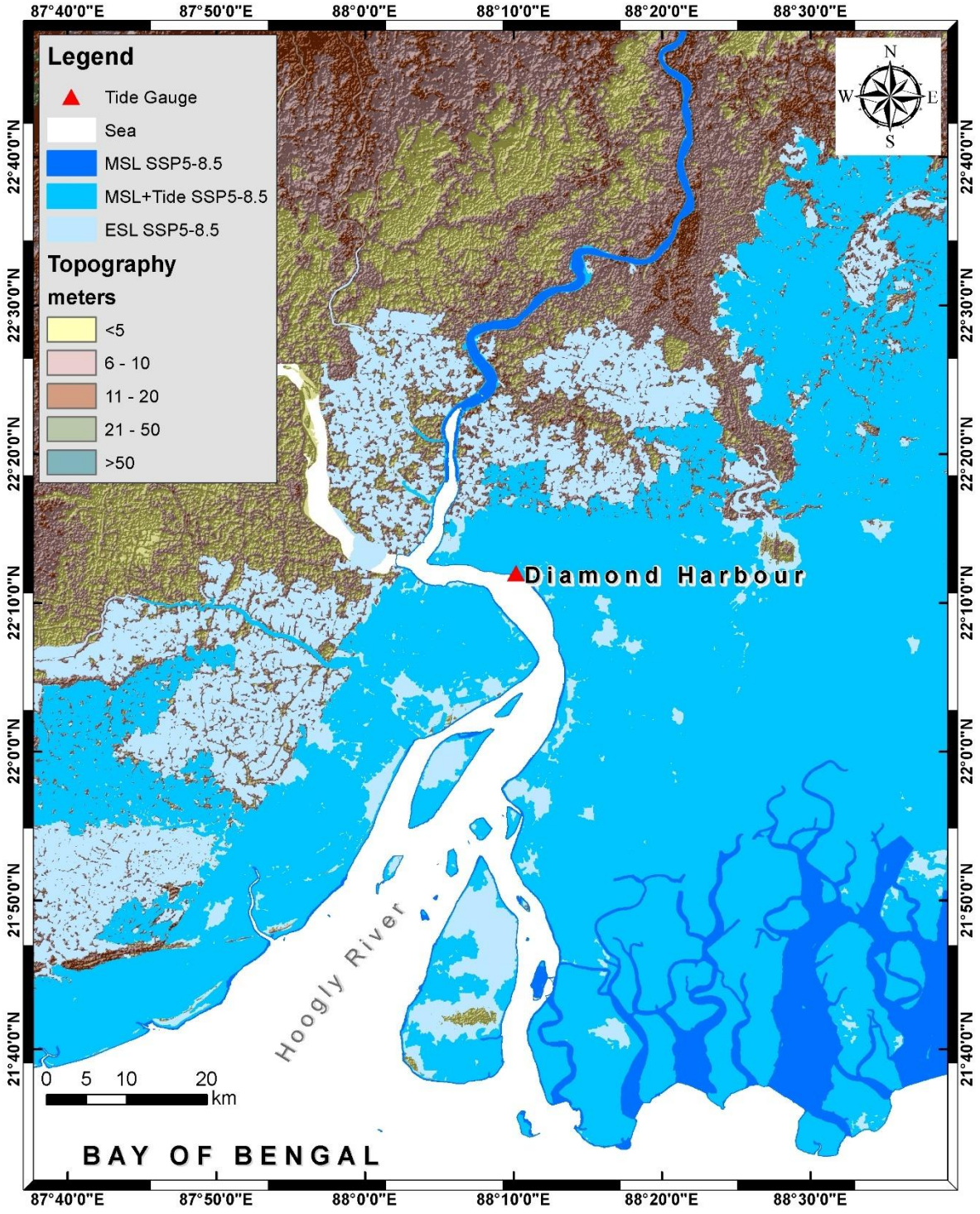
Legend
Tide Gauge
Sea
MSL SSP5-8.5
MSL+Tide SSP5-8.5
ESL SSP5-8.5
Topography
meters
<5
6 - 10
11 - 20
21 - 50
>50
N
W
E
S
Diamond Harbour
Hoogly River
0 5 10 20
km
BAY OF BENGAL
87°40'0"E
87°50'0"E
88°0'0"E
88°10'0"E
88°20'0"E
88°30'0"E
22°40'0"N
22°30'0"N
22°20'0"N
22°10'0"N
22°0'0"N
21°50'0"N
21°40'0"N

10. Minicoy (Lakshadweep)

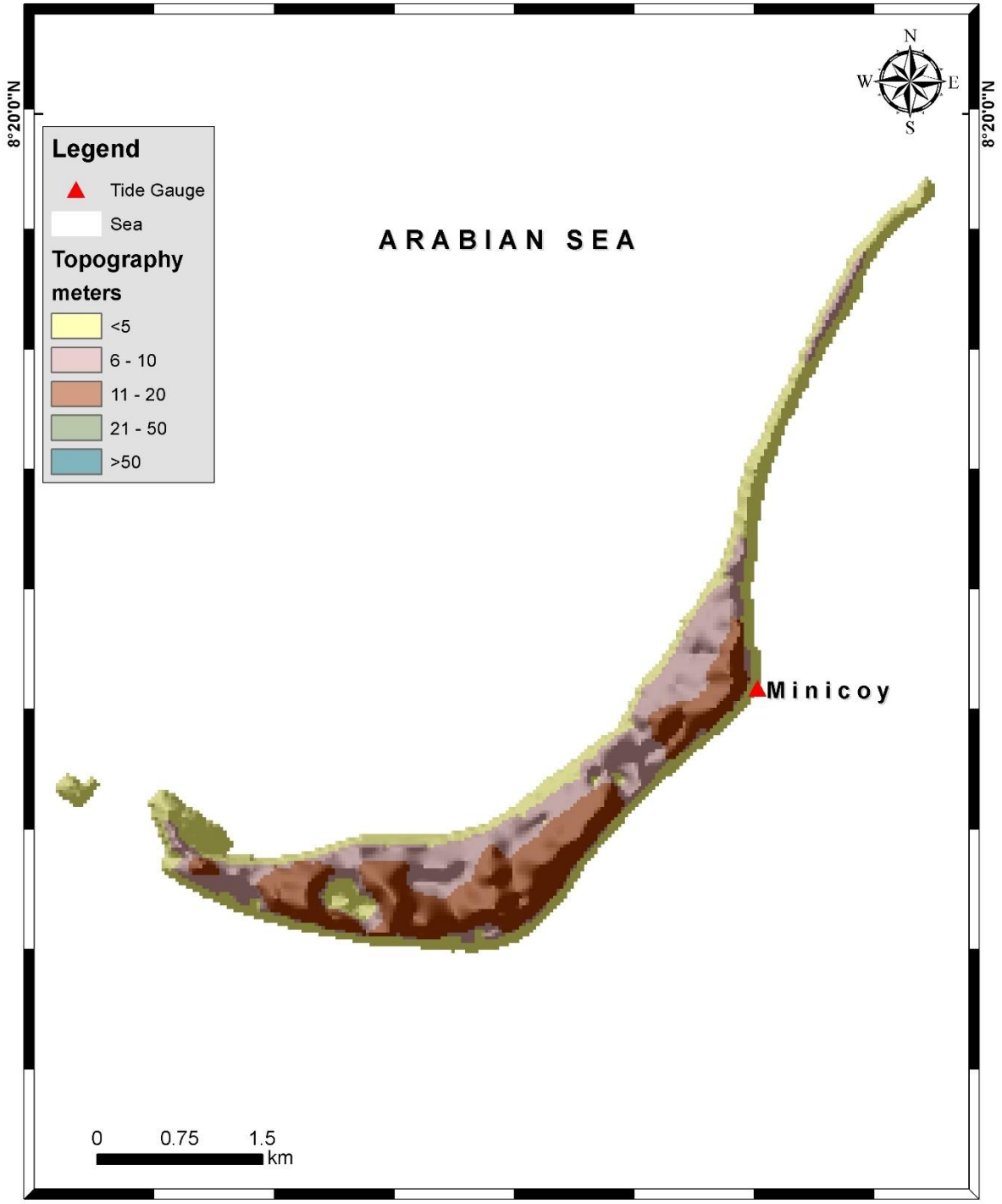

Basemap

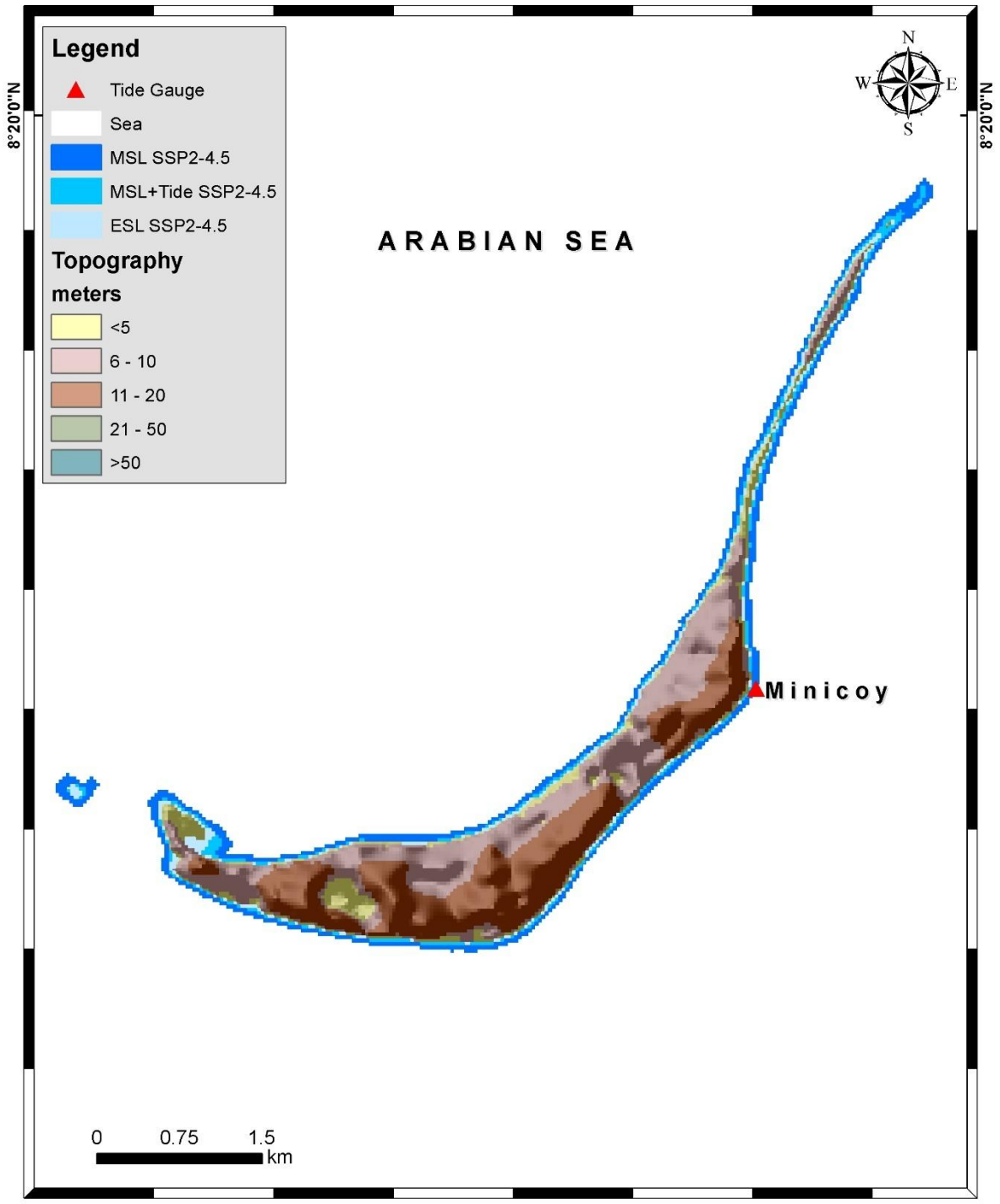
Legend
Tide Gauge
Sea
MSL SSP2-4.5
MSL+Tide SSP2-4.5
ESL SSP2-4.5
Topography
meters
<5
6 - 10
11 - 20
21 - 50
>50
N
W
E
S
8°20'0"N
8°20'0"N
ARABIAN SEA
Minicoy
0
0.75
1.5
km

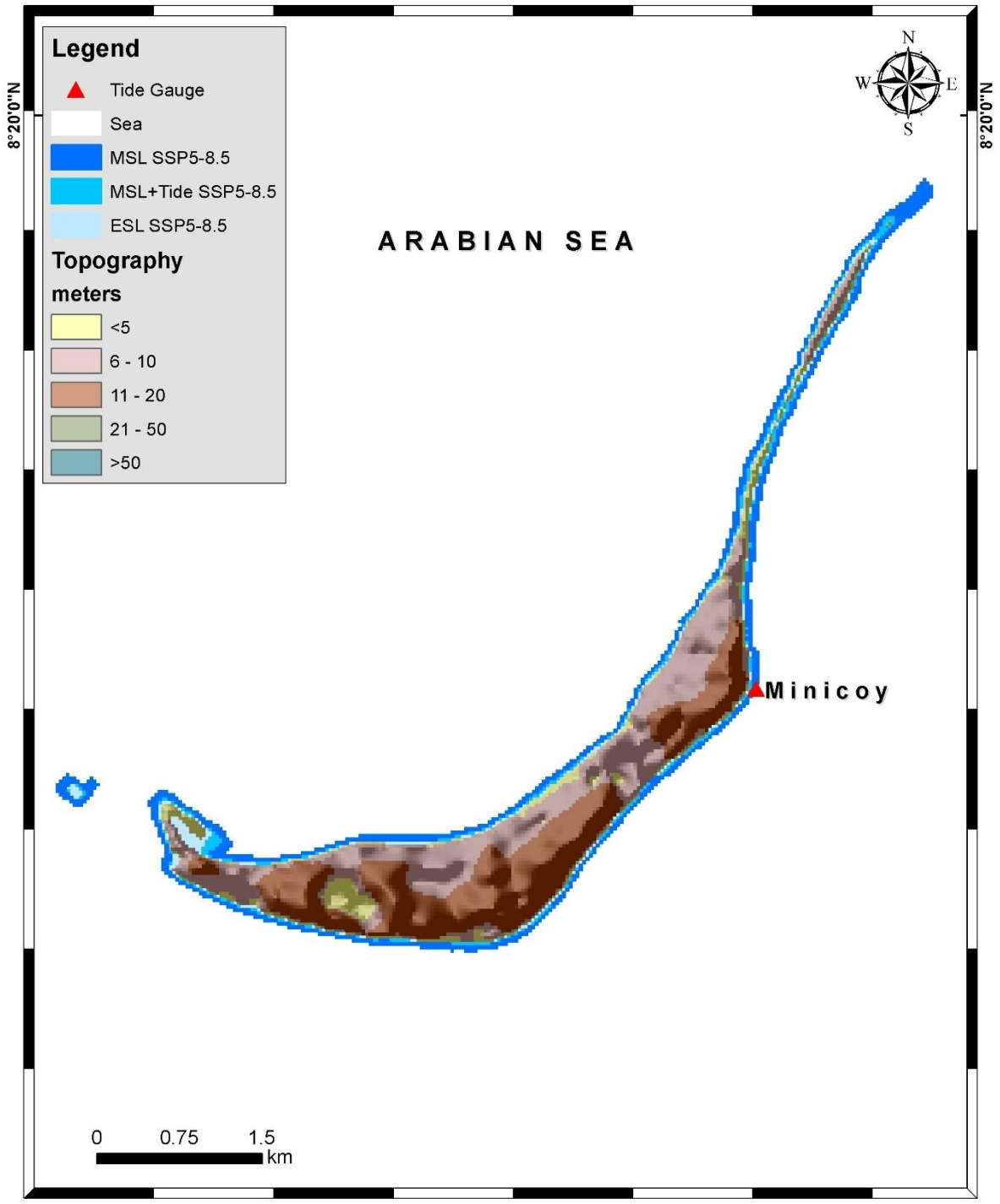
Legend
Tide Gauge
Sea
MSL SSP5-8.5
MSL+Tide SSP5-8.5
ESL SSP5-8.5
Topography
meters
<5
6 - 10
11 - 20
21 - 50
>50
N
W
E
S
8°20'0"N
8°20'0"N
ARABIAN SEA
Minicoy
0
0.75
1.5
km

11. Port Blair (Andaman Nicobar)

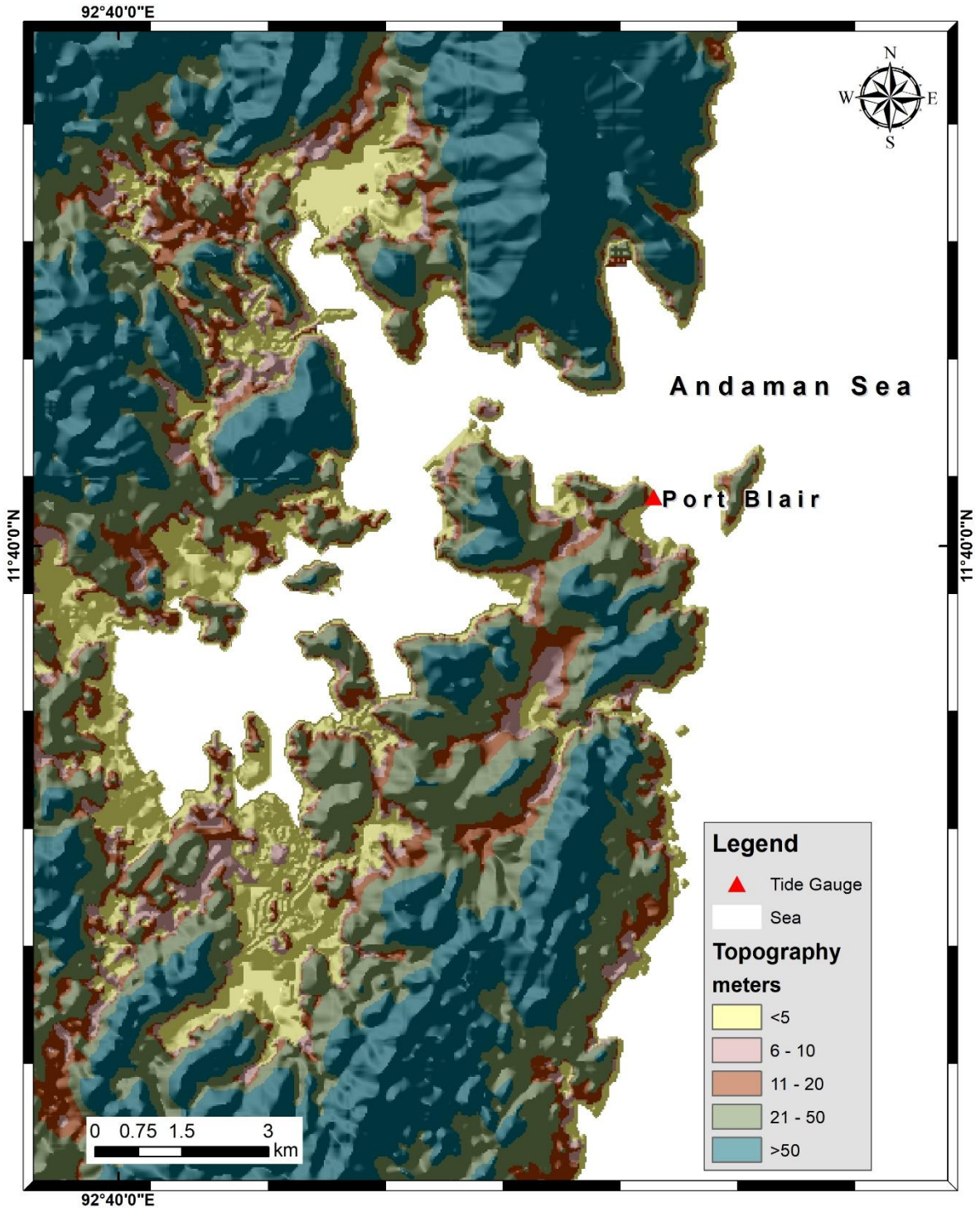

Basemap

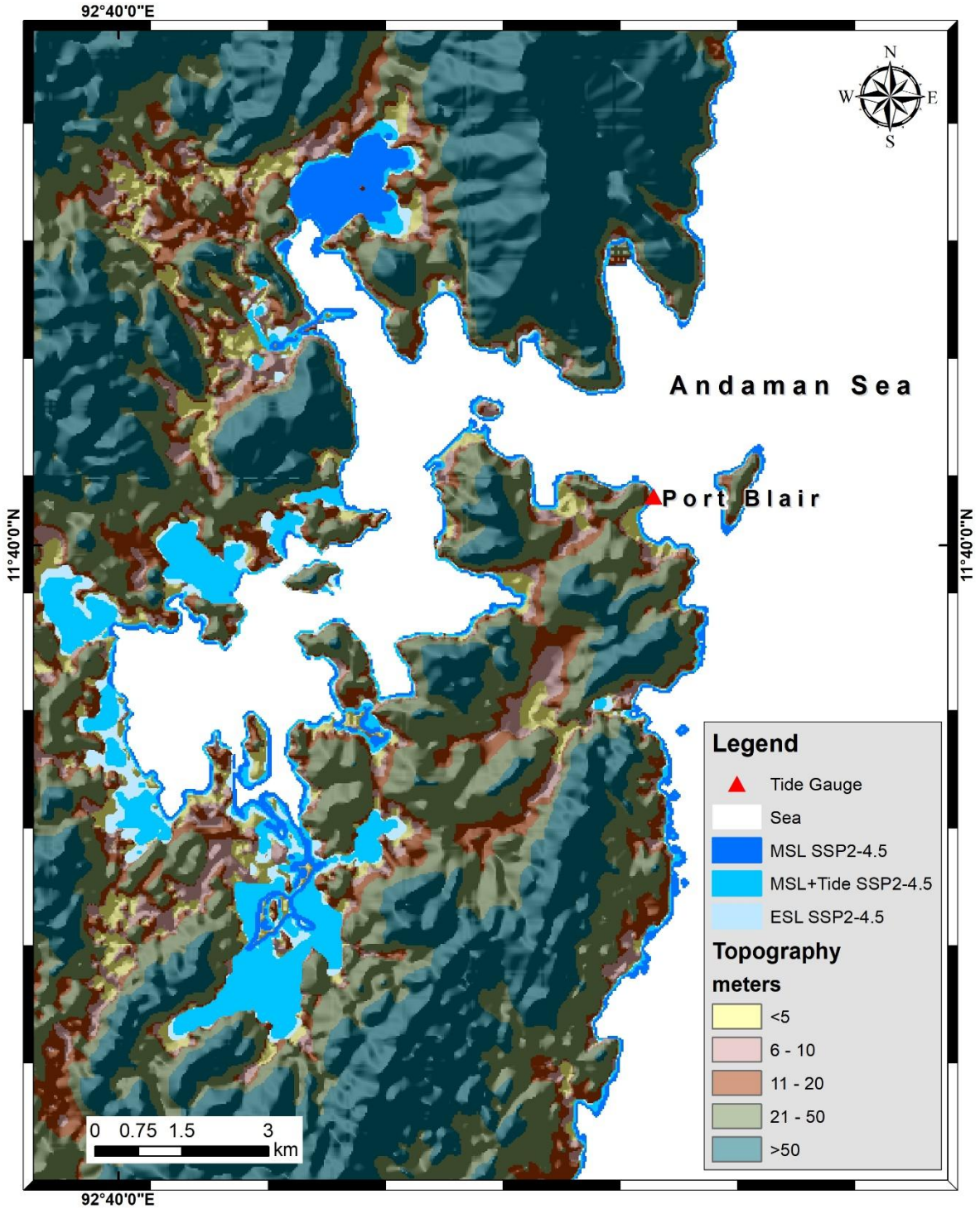
92°40'0"E
N
W
E
S
Andaman Sea
Port Blair
11°40'0"N
11°40'0"N
Legend
Tide Gauge
Sea
MSL SSP2-4.5
MSL+Tide SSP2-4.5
ESL SSP2-4.5
Topography
meters
<5
6 - 10
11 - 20
21 - 50
>50
0 0.75 1.5 3
km
92°40'0"E

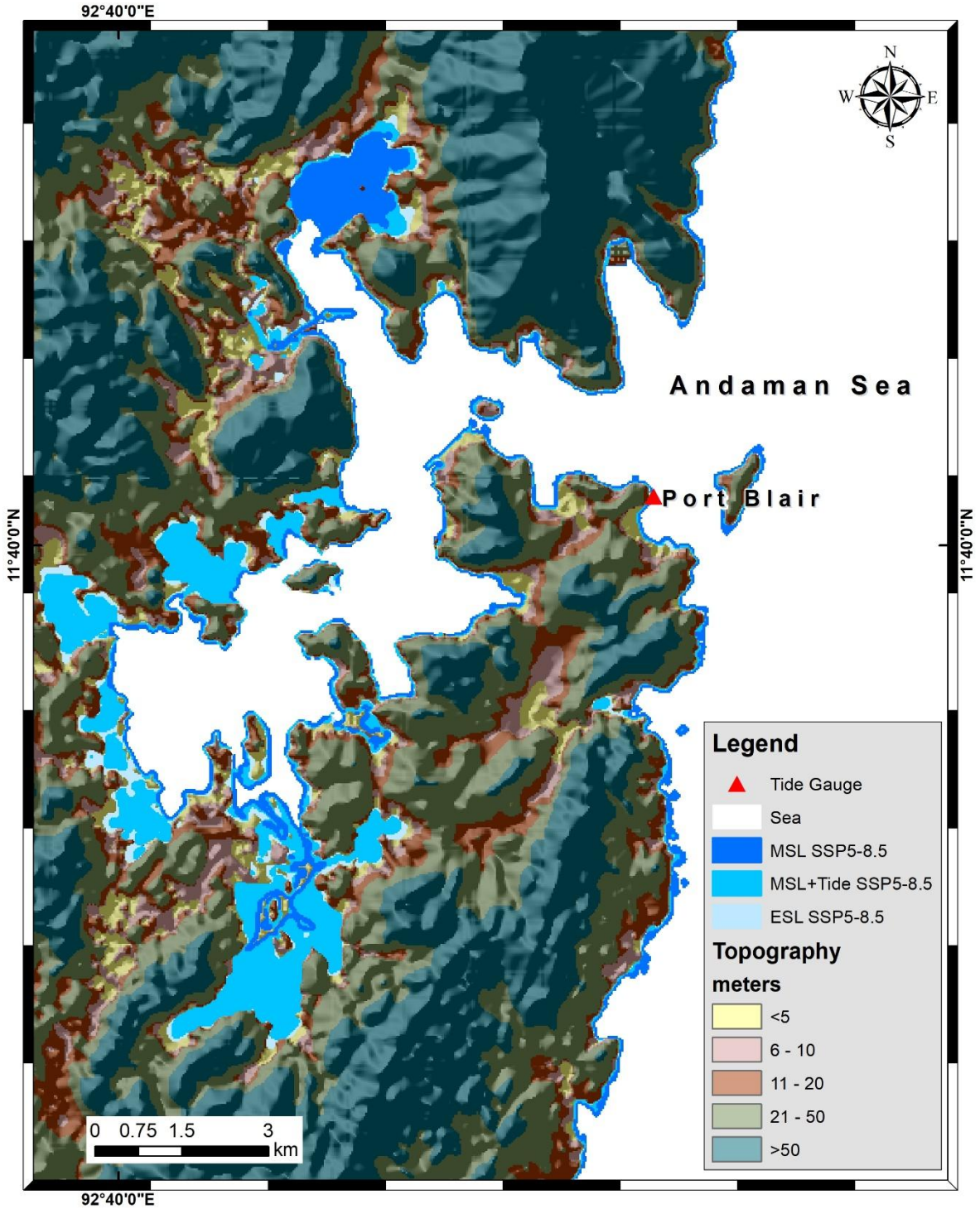
92°40'0"E
N
W
E
S
Andaman Sea
Port Blair
11°40'0"N
11°40'0"N
Legend
Tide Gauge
Sea
MSL SSP5-8.5
MSL+Tide SSP5-8.5
ESL SSP5-8.5
Topography
meters
<5
6 - 10
11 - 20
21 - 50
>50
0 0.75 1.5 3
km
92°40'0"E

References

Antony, C., Unnikrishnan A.S., Observed characteristics of tide-surge interaction along the east coast of India and the head of Bay of Bengal*, Estuarine, Coastal and Shelf Science*, 131, 6-11, ISSN 0272-7714, (2013). https://doi.org/10.1016/j.ecss.2013.08.004

Antony, C., Unnikrishnan A S & Woodworth, P., Evolution of extreme high waters along the east coast of India and at the head of the Bay of Bengal. *Global and Planetary Change.* 140, 59-67 (2016). https://doi.org/10.1016/j.gloplacha.2016.03.008

Bhatia, K., G. Vecchi, H. Murakami, S. Underwood, and J. Kossi, Projected Response of Tropical Cyclone Intensity and Intensification in a Global Climate Model. *J. Climate*, **31**, 8281–8303, (2018). https://doi.org/10.1175/JCLI-D-17-0898.1

Church JA, Clark PU, Cazenave A, Gregory JM, Jevrejeva S, et al., Sea level change *Climate Change 2013: The Physical Science Basis. Contribution of Working Group I to the Fifth Assessment Report of the Intergovernmental Panel on Climate Change*, Cambridge University Press (2013).

Deshpande, M., Singh, V.K., Ganadhi, M.K. et al. Changing status of tropical cyclones over the north Indian Ocean, *Clim Dyn,* 57, 3545–3567 (2021). https://doi.org/10.1007/s00382-021-05880-z

Fox-Kemper B, Hewitt HT, Xiao C, Aðalgeirsdóttir G, Drijfhout SS, et al., Ocean, cryosphere and sea level change *Climate Change 2021: The Physical Science Basis Contribution of Working Group I to the Sixth Assessment Report of the Intergovernmental Panel on Climate Change,* Cambridge University Press (2021).

Gan Zhang et al. Tropical cyclone motion in a changing climate. *Sci. Adv.* 6, eaaz7610 (2020). https://doi.org/10.1126/sciadv.aaz7610

Harrison BJ, Daron JD, Palmer MD, Weeks JH, Future sea-level rise projections for tide gauge locations in South Asia, *Environ. Res. Commun*, 3, (2021). https://doi.org/10.1088/2515-7620/ac2e6e

Hermans THJ, Gregory JM, Palmer MD, Ringer MA, Katsman CA, et al., Projecting global mean sea-level change using CMIP6 models, *Geophys Res Lett.* 48, (2021). https://doi.org/10.1029/2020GL092064

IPCC, 2023: Summary for Policymakers. In: *Climate Change 2023: Synthesis Report.* Contribution of Working Groups I, II and III to the Sixth Assessment Report of the Intergovernmental Panel on Climate Change [Core Writing Team, H. Lee and J. Romero (eds.)]. IPCC, Geneva, Switzerland, pp. 1-34, DOI: 10.59327/IPCC/AR6-9789291691647.001.

Jevrejeva S., Williams J., Vousdoukas M.I. & Jackson L P, Future Sea level rise dominates changes in worst case extreme sea levels along the global coastline by 2100, *Environ. Res. Lett.*, 18, (2023). https://doi.org/10.1088/1748-9326/acb504

Kossin, J. P., Emanuel, K. A., & Camargo, S. J., Past and Projected Changes in Western North Pacific Tropical Cyclone Exposure. *Journal of Climate*, 29(16), 5725-5739 (2016). https://doi.org/10.1175/JCLI-D-16-0076.1

Kossin, J. P., Knapp, K. R., Olander, T. L. & Velden, C. S., Global increase in major tropical cyclone exceedance probability over the past 40 years. *Proc. Natl. Acad. Sci.* U.S.A. 117, 11975–11980 (2020).

Kopp, R. E., Garner, G. G., Hermans, T. H. J., Jha, S., Kumar, P., Reedy, A., Slangen, A. B. A., Turilli, M., Edwards, T. L., Gregory, J. M., Koubbe, G., Levermann, A., Merzky, A., Nowicki, S., Palmer, M. D., and Smith, C.: The Framework for Assessing Changes To Sea-level (FACTS) v1.0: a platform for

characterising parametric and structural uncertainty in future global, relative, and extreme sea-level change, *Geosci. Model Dev.*, 16, 7461–7489, (2023) https://doi.org/10.5194/gmd-16-7461-2023

Knutson, T., Camargo, S.J., Chan, J.C.L., et al., Tropical cyclones and climate change assessment: Part2: projected response to anthropogenic warming. *Bull. Am. Meteorol. Soc.* 101, E303–E322, (2020) https://doi.org/10.1175/BAMS-D-18-0189.1

Knutson, T. R., Sirutis, J. J., Zhao, M., Tuleya, R. E., Bender, M., Vecchi, G. A., Villarini, G., & Chavas, D., Global Projections of Intense Tropical Cyclone Activity for the Late Twenty-First Century from Dynamical Downscaling of CMIP5/RCP4.5 Scenarios. *Journal of Climate*, 28(18), 7203-7224, (2015). https://doi.org/10.1175/JCLI-D-15-0129.1

Knutson, T. R., Chung, M. V., Vecchi, G., Sun, J., Hsieh, T.-L. & Smith, A. J. P. Climate change is probably increasing the intensity of tropical cyclones. In: *Critical Issues in Climate Change Science*, C. Le Quéré, P. Liss & P. Forster (eds), (2021). https://doi.org/10.5281/zenodo.4570334 .

Lowe, J.A., P.L. Woodworth, T. Knutson, R.E. McDonald, K. McInnes, K. Woth, H. Von Storch, J. Wolf, V. Swail, N. Bernier, S. Gulev, K. Horsburgh, A.S. Unnikrishnan, J. Hunter, and R. Weisse. Past and future changes in extreme sea levels and waves. In *Understanding Sea-Level Rise and Variability* (Chap. 11), *ed.* J.A. Church, P.L. Woodworth, T. Aarup, and W.S. Wilson. London: Wiley-Blackwell (2010).

Mitra, A., Sanil Kumar, V. & Jena, B., Tidal characteristics in the Gulf of Khambhat, northern Arabian Sea – based on observation and global tidal model data, *Oceanologia*. 62, (2020) https://doi.org/10.1016/j.oceano.2020.05.002

Muis, S., Verlaan, M., Winsemius, H. et al., A global reanalysis of storm surges and extreme sea levels. Nat Commun 7, 11969, (2016) https://doi.org/10.1038/ncomms11969

Murty, P. L. N. & Siva Srinivas, K., Future projections of storm surges and associated coastal inundation along the east coast of India. *J. Water Clim. Change*. 14 (5), 1413–1432, (2023) https://doi.org/10.2166/wcc.2023.358

Nayak, S., Srinivasa Kumar, T., Mahendra, R.S., Mohanty, PC., Rao, E.P.R., Joseph, S. and Nair, T.M.B. Coastal Multi-Hazard Vulnerability Atlas. INCOIS-OSAR-CGAM-CMV-2022-03, INCOIS, Ministry of Earth Sciences, Hyderabad, India, (2022).

Nicholls R. J., & Cazenave, A. Sea-Level Rise and Its Impact on Coastal Zones, *Science* 328,1517-1520 (2010). https://doi.org/10.1126/science.1185782

Nicholls, R.J., Lincke, D., Hinkel, J. et al. A global analysis of subsidence, relative sea-level change and coastal flood exposure. *Nat. Clim. Chang.* 11, 338–342 (2021). https://doi.org/10.1038/s41558-021-00993-z

Palmer M et al., Exploring the drivers of global and local sea-level change over the 21st century and beyond. *Earth's Future,* 8, e2019EF001413, (2020). https://doi.org/10.1029/2019EF001413

Palmer, M. D., & Weeks, J. H. The need for multi-century projections of sea level rise. *Earth's Future*, 12, e2023EF004403, (2024). https://doi.org/10.1029/2023EF004403

Pugh, D. & Woodworth, P.L. Sea-Level Science: Understanding Tides, Surges, Tsunamis and Mean Sea-Level Changes, *Cambridge University Press*, (2014).

Roxy, M. K., Ritika, K., Terray, P., & Masson, S., The Curious Case of Indian Ocean Warming. *Journal of Climate*, 27(22), 8501-8509 (2014). https://doi.org/10.1175/JCLI-D-14-00471.1

Ramakrishnan, R., Remya, P.G., Mandal, A. et al., Wave induced coastal flooding along the southwest coast of India during tropical cyclone Tauktae. *Sci Rep* 12, 19966 (2022). https://doi.org/10.1038/s41598-022-24557-z

Sindhu, B. & Unnikrishnan A S, Return period estimates of extreme sea level along the east coast of India from numerical simulations. *Natural Hazards*. 61 (2011).

Sindhu, B., & Unnikrishnan, A. S. Characteristics of Tides in the Bay of Bengal. *Marine Geodesy*, *36*(4), 377–407, (2013).

Singh, V. & Koll, R., A review of ocean-atmosphere interactions during tropical cyclones in the north Indian Ocean. *Earth-Science Reviews*. 226, 103967, (2022) https://doi.org/10.1016/j.earscirev.2022.103967

Sreeraj P, Swapna P, Krishnan R, Nidheesh AG, Sandeep N, Extreme sea level rise along the Indian Ocean coastline: observations and 21st century projections, *Environ. Res. Lett.* 17 (2022) https://doi.org/10.1088/1748-9326/ac97f5

Tinker, J., Palmer, M.D., Copsey, D. et al., Dynamical downscaling of unforced interannual sea-level variability in the Northwest European shelf seas, *Clim Dyn* 55, 2207–2236 (2020) https://doi.org/10.1007/s00382-020-05378-0

Testut, L., & Unnikrishnan, A. S., Improving modeling of tides on the continental shelf off the west coast of India. J Coast Res 32(1):105–115, (2016).

Unnikrishnan, A. S. & Shankar, D., Are sea-level-rise trends along the coasts of the north Indian Ocean consistent with global estimates? *Glob. Planet. Change* 57 301–7 (2007).

Unnikrishnan, A. S., Nidheesh, A. G., & Lengaigne, M., Sea-level-rise trends off the Indian coasts during the last two decades *Curr. Sci.* 108 966–70 (2015).

Unnikrishnan, A.S., Sundar, D., & Blackman, D., Analysis of extreme sea level along the east coast of India. *Journal of Geophysical Research,* 109, C06023 (2004).

Unnikrishnan, A.S. & Antony, C., Changes in Extreme Sea-Level in the North Indian Ocean. In: Unnikrishnan, A., Tangang, F., Durrheim, R.J. (eds) Extreme Natural Events. Springer, Singapore, (2022). https://doi.org/10.1007/978-981-19-2511-5_10

Vousdoukas, M.I., Mentaschi, L., Voukouvalas, E. et al., Global probabilistic projections of extreme sea levels show intensification of coastal flood hazard., *Nat Commun* **9**, 2360, (2018). https://doi.org/10.1038/s41467-018-04692-w

Woodworth, P.L., & Blackman, D.L., Evidence for Systematic Changes in Extreme High Waters since the Mid-1970s, *J. Clim.,* 17(6), (2004).

Weeks, J.H., Fung, F., Harrison, B.J., Palmer, M.D., The evolution of UK sea-level projections, *Environ. Res. Commun.,* 5(3), 2001, (2023).